Development of Antibacterial Functionalized Textiles with ZnO

Auteur : Gonzalez Vargas, Cristina
Promoteur(s) : Lambert, Stéphanie
Faculté : Faculté des Sciences appliquées
Diplôme : Master : ingénieur civil en chimie et science des matériaux, à finalité spécialisée en Advanced Materials - Innovative Recycling
Année académique : 2023-2024
URI/URL : http://hdl.handle.net/2268.2/19542

UNIVERSITE DE LIEGE
FACULTE DES SCIENCES APPLIQUEES

Development of Antibacterial Functionalized Textiles with ZnO

GONZÁLEZ, Cristina
S225155

Thesis presented for obtaining the Master's degree in
Civil Engineer in Chemistry and Materials Science, with a Specialization in Advanced Materials - Innovative Recycling

Supervisor:
LAMBERT, Stéphanie

Advisor:
Farcy, Antoine

Acknowledgements

I would like to extend my gratitude to several individuals and groups who have played an instrumental role in the successful completion of my master's thesis in chemical engineering. First and foremost, I am thankful to my advisor, Antoine Farcy, whose dedicated guidance and support proved to be invaluable throughout the entire laboratory work phase. Antoine's expertise, patience, and commitment truly enriched my research journey. I am equally indebted to my supervisor, Professor Stephanie Lambert, for her profound insights, astute guidance, and continuous encouragement that helped shape the direction of my research. I would also like to acknowledge the NCE research group committee for their weekly meetings, where their thoughtful discussions and constructive feedback provided me with invaluable perspectives on refining and advancing my experimental approach. Collectively, the contributions of Antoine Farcy, Professor Stephanie Lambert, and the NCE research group committee have been pivotal in shaping the outcome of this thesis, and I am truly fortunate to have had their support throughout this journey.

ABSTRACT

With the continuous rise in consumption and contamination of water due to industrial and domestic activities, the development of viable, sustainable, and innovative solutions for water treatment has become increasingly important. At the same time, there has been an increased interest in nanomaterials for applications in various fields. Zinc oxide nanoparticles (ZnO NPs) have become a highly attractive material across various industries due to its wide array of properties which include high chemical and thermal stability, UV protection, thermal conductivity, unique piezoelectric, optical, and luminescent properties, as well as self-cleaning photocatalytic and antibacterial activities. Because of this, the functionalization of textiles with ZnO NPs has viable applications in a variety of fields including water treatment. The project to which the work of this thesis is associated, has the goal of developing a functionalized textile, composed of nylon 6 coated in ZnO NPs, that enables the antibacterial treatment of continuously flowing process water in dark conditions. To that end, the objectives of this thesis are to conduct a series of experiments to determine the conditions at which an optimal ZnO NP coating is achieved on the nylon textile, by employing dip coating, while ensuring that the resulting functionalized textile exhibits antibacterial properties in the dark. Several experiments were conducted, evaluating the effects of operating conditions, ZnO synthesis methods, ZnO NP suspension concentrations and suface activation processes for the nylon: acid activation using HCl and Acetic Acid, basic activation using NaOH and physical activation using UVC irradiation. Characterization techniques, such as XRD, TEM, SEM, EDX and FTIR, were carried out with the aim of confirming the nature of the material of the coating achieved on the nylon and evaluating the effects of the activation processes on the nylon's molecular structure. The degradation of Nitro Blue Tetrazolium from the contact with the functionalized nylon samples was tested to confirm the presence of the ROS formation mechanism to which the ZnO NP's antibacterial activity is attributed. It was concluded that the most favorable conditions for achieving an optimal functionalization of nylon 6 for antibacterial activity in the dark, by dip coating, were the use of polyol synthesized ZnO NPs at 30 g/L and application of acid surface activation on the nylon, using HCl at low concentrations. Mechanisms were proposed to explain the adherence of ZnO NPs to the nylon textile based on the formation of hydrogen bonds and dipole-dipole bonds between the ZnO NPs and the oxygen and hydrogen atoms from the amide group of the nylon molecules. It was proposed that the acid activation of the nylon surface promoted a hydrolysis of the amide group which led to the formation of carboxyl and amine groups, which in turn resulted in an increase of the potential bonding sites for the ZnO NPs, ultimately achieving a better coating result.

CONTENTS

INDEX OF FIGURES

INDEX OF TABLES

1. INTRODUCTION

1.1. Wastewater Treatments

Water is an integral part of all processes on planet Earth, a compound without which life itself cannot exist. Water is also essential for the development and operation of most industrial processes; it plays several important roles such as dilution, heat exchange, washing, steam (and therefore energy) generation, and it is used as a raw material for several products. (Center for Disease Control, 2016), (USGS, 2018).

With the constantly increasing consumption and contamination of water from human activities, the need for the conservation of this essential resource and its correct treatment has become a priority across all industries. However, water treatment remains a challenging endeavor, given that the nature of the activities carried out differs from industry to industry and process to process. There is no true “cure all” for industrial water treatment across the board. This means that, even though there is a great variety of available technologies to address specific water treatment needs, there is a constant need for innovation, to develop solutions of water treatment that will allow specific objectives to be met, while at the same time minimizing the costs that the implementation of these solutions might entail.

This great amount and variety of available water treatment technologies include those aimed at water disinfection (antibacterial treatment). Methods for water disinfection include physical technologies such as filtration, reverse osmosis and UV irradiation, chemical methods such as the use of acids or chlorine compounds, and even biological methods, with the use of enzymes (Collivignarelli *et al*., 2017). Among the variety of chemical methods for antibacterial water treatment, the advanced oxidation processes (AOPs) can be found.

AOPs were originally proposed in the 1980s and were defined by the use of hydroxyl (·OH), and later sulfate ($\cdot SO_4^-$) radicals, as strong oxidizing agents. These oxidants were strong enough to degrade recalcitrant contaminants (both organic and inorganic) into smaller, less harmful compounds (Deng & Zhao, 2015), (Ameta, 2018). More recently, a bigger emphasis has been given to reactive oxygen species (ROS) as oxidants generated through AOPs. ROS include both free radicals: hydroxyl (·OH), superoxide ($\cdot O_2^-$), peroxyl ($\cdot RO_2$), and hydroperoxyl ($\cdot HO_2$) and non-free radicals: hydrogen peroxide (H_2O_2), hydroxide ions (OH^-) and ozone (O_3), among others (Dong *et al*., 2022).

AOPs are a favorable alternative to other chemical water treatment methods given that it is considered a “greener” approach, since it leads to the generation of less harmful products through

degradation of contaminants. These oxidative processes can be triggered through a variety of mechanisms, including Fenton-like processes (Fenton, Photo-Fenton, Electro-Fenton), ozonation, ultrasonication and (photo)catalysis (Ameta & Ameta, 2018), (Verma & Haritash, 2020). Nanostructured materials are necessary for increasing the kinetics and selectivities of these processes (Kurian, 2021).

1.2. Antibacterial Activity of Zinc Oxide Nanoparticles

Over the past decades, the field of nanomaterials has attracted increasing interest due to the wide variety of scientific and industrial applications that can be addressed with the use of this technology. These materials are characterized by having dimensions smaller than 100 nm, as well as having unique chemical, mechanical, electrical, and thermal properties that allow them to be used for a myriad of applications (Stankovic *et al*., 2013). Among these materials, ZnO has stood out due to its unique and versatile chemical and physical properties (Shamhari *et al*., 2018), (Matei *et al*., 2014).

ZnO's wide variety of properties include a high chemical and thermal stability, UV protection, thermal conductivity, unique piezoelectric, optical, electronic, photonic and luminescent properties (Verbic *et al*., 2019). It also displays self-cleaning photocatalytic and antibacterial activities, while still being safe, non-toxic and biocompatible with human cells. The material also has the advantages of being low cost, being able to be synthesized in a relatively simple manner, from a wide range of methods and precursors, which in turn lead to a great variety of morphologies and sizes, each of which has a different effect on the compound's properties (Babayevska *et al*., 2022). Considering this, zinc oxide nanoparticles (ZnO NPs) present an attractive material for antibacterial treatment applications; they are known to have effective antibacterial properties, due to various mechanisms, including the formation of ROS (Fiedot-Tobola *et al*., 2018).

Generally speaking, there are three main mechanisms that have been suggested in the literature to explain the ZnO NPs' antibacterial activities throughout the past couple of decades. However, there is still some discussion as to which of these is dominant (Sirelkhatim *et al.,* 2015). These mechanisms are:

1.2.1. Internalization of the ZnO NPs into the cell

This mechanism is determined mainly due to the particle size and morphology of the ZnO NPs. The thickness of the cell walls of gram-positive bacteria is around 20-80 nm while for gram-negative bacteria it is between 7-8 nm thick. ZnO NPs can reportedly be synthesized to a size as small as < 10 nm, allowing them to pass through the cell wall into the bacteria. Once inside the bacteria, the ZnO NPs can disrupt its activity, having a toxic effect (Sirelkhatim *et al*., 2015).

Studies have been conducted regarding the antibacterial effects of ZnO NPs upon contact with the bacteria's cell walls. Those studies claim that the cell walls of the bacteria being tested presented damage upon being in contact with the ZnO NPs suspensions used, this in turn resulted in a higher permeability of the cell wall which allowed for a higher number of nanoparticles to get into the cell and cause even more damage. From these studies, it was concluded that this antibacterial activity increases with smaller particle sizes of the ZnO and higher concentration of the particles (Brayner *et al*., 2006), (Zhang *et al*., 2006).

1.2.2. The release of zinc ions (Zn^{2+})

The release of zinc ions (Zn^{2+}) into the medium containing bacteria is also one of the most defended mechanisms regarding the antibacterial activity of ZnO NPs. It is known that the presence of Zn^{2+} has a significant role in inhibiting active transport in the cell and disrupting amino acid metabolism activities and enzymatic systems (Sirelkhatim *et al*., 2015). Several studies have stated that even at low concentrations, Zn^{2+} ions released by the ZnO NPs show a successful antibacterial activity (Sirelkhatim *et al*., 2015), (Kasetmets *et al*., 2009).

1.2.3. Generation of Reactive Oxygen Species (ROS)

As was stated earlier, the use of AOPs and the generation of ROS have been proposed as effective methods for antibacterial treatments. ROS are a group of reactive molecules and free radicals composed of oxygen, that have a high reactivity and oxidizing properties which are credited with being the reason for the toxicity of ROS to bacteria (Sirelkhatim *et al*., 2015). In particular, the ROS generated by the interaction between ZnO with water are the superoxide anion ($\cdot O_2^-$), hydrogen peroxide (H_2O_2), hydroperoxyl radical ($\cdot HO_2$) and hydroxide anion (OH^-) (Raghupathi *et al.,* 2011).

The generation of ROS from ZnO has initially been established as being a photocatalytic process, triggered by the exposure of the ZnO NPs to UV light. ZnO is a semiconductor with a wide band gap near the UV-spectral region (3.37 eV) and a high electron mobility, which is the reason for the compound's photocatalytic properties (Parihar *et al*., 2018), (Verbic *et al*., 2019).

The proposed reactions for the generation of ROS from ZnO when exposed to light are as follows (Sirelkhatim *et al*., 2015):

$$ZnO + h\nu \rightarrow e^- + h^+, \quad (1)$$

$$h^+ + H_2O \rightarrow \cdot OH + H^+, \quad (2)$$

$$e^- + O_2 \rightarrow \cdot O_2^- \,, \quad (3)$$

$$\cdot O_2^- + H^+ \rightarrow HO_2^{\cdot} \,, \quad (4)$$

$$HO_2^{\cdot} + H^+ + e^- \rightarrow H_2O_2 \quad (5)$$

It has been noted however, that it is difficult to pin-point the exact antibacterial mechanism from ZnO NPs that might be taking place at any given moment, as seemingly contradictory information has been seen during the evaluation of ZnO NPs' antibacterial activity. For instance, even though a high antibacterial activity is inversely related to particle size, in given tests, similar antibacterial activity was observed between ZnO NPs suspensions with small particle size and suspensions that presented aggregation of the nanoparticles, at the same concentrations (Adams *et al*., 2006).

Another example of these seeming contradictions is the fact that, while it is clear that the presence of light is a significant factor for the formation of ROS with ZnO, since it is a photocatalytic process, antibacterial activity from ZnO NPs has still been observed to happen in experiments conducted under dark conditions. Various mechanisms have been proposed to be responsible for these antibacterial activities, including the formation of ROS, even without the presence of light.

On the first hand, Adams *et al* reported in their study "Comparative eco-toxicity of nanoscale TiO_2, SiO_2, and ZnO water suspensions" (2006) the fact that even in dark conditions there was evidence of bacterial growth inhibition in the experiments conducted. However, they claim that UV light is essential for the generation of ROS and propose that therefore there must be another (yet unknown) mechanism for this antibacterial activity, though they fail to offer a hypothesis as to what mechanism this might be. Later, in 2009, Hirota *et al.* conducted a study on the "Preparation of zinc oxide ceramics with a sustainable antibacterial activity under dark conditions", in which they state that through the use of electron spin resonance spectroscopy (ESR) and chemical photoluminescence analyses, they were able to identify the generation of ROS, specifically superoxide ions ($\cdot O_2^-$). They claim that this generation of ROS in the dark happened repeatedly, specifically for hydrothermally treated ZnO, allowing it to have a sustainable antibacterial activity.

This explanation for the ZnO NPs' antibacterial behavior in dark conditions is supported by Prasanna and Vijayaraghavan who claim that ROS are still significantly produced in the dark when using ZnO. According to them, the ROS generation in the dark occurs mainly due to the interactions of water with superoxide ions ($\cdot O_2^-$), which are readily available due to surface defects of the ZnO NPs (Prasanna & Vijayaraghavan, 2015). On the other hand, Joe *et al.* disputed this claim in their paper "Antibacterial mechanism of ZnO nanoparticles under dark conditions" stating that insufficient direct microscopic observation of ROS production from ZnO nanoparticles has been performed in order to

confirm these claims. Instead, they propose that the main mechanism for the antibacterial activity of the ZnO NPs in the dark should be attributed to the release of Zn^{2+}. Specifically, it should be attributed to the increased release of Zn^{2+} ions caused by the local dissolution within the bacteria's cytoplasm of the ZnO NPs that have attached to the bacteria (Joe *et al*., 2016).

Additionally, it has been generally proposed that both the size and morphology of the ZnO NPs have a key role on the performance of the different properties presented by the nanoparticles. ZnO NPs have been known to present several morphologies such as spheres, rods, hexagons, flowers, rings, helixes, among many others (Wang, 2004). Many studies have been conducted focusing on the effects of the morphology of ZnO NPs on the antibacterial activity of the compound and there appears to be a consensus in the claim that the spherical and the rod-like morphologies are the two most favorable morphologies for the NPs, in terms of an effective antibacterial behavior (Verbic *et al*., 2019), (Da Silva *et al*., 2023).

1.3. Synthesis Methods for ZnO NPs.

In terms of the synthesis methods for ZnO NPs, they include chemical pathways such as chemical precipitation, sol-gel methods (solvothermal and hydrothermal methods), mechanochemical synthesis and ultrasonic synthesis. There are also organic synthesis pathways, which use natural reactants for the ZnO production. ZnO produced metallurgically from metallic zinc is also possible though less common. All these methods can result in different morphologies of the ZnO NPs, as well as different properties depending on the chosen pathway, the conditions under which they are carried out, the precursors and reactants used, among other factors (Verbic *et al*., 2019), (Droepenu *et al*., 2020).

Generally speaking, synthesis methods for nanomaterials can be classified according to the approach in which the nanomaterial is synthesized or according to the method. In terms of the approach, there are two main categories: the top-down approach and the bottom-up approaches. The top-down approaches consist of starting off with a bulk material which is broken down to produce the nanostructured material; methods like mechanical milling, etching, sputtering and laser ablation employ this approach (Baig *et al.,* 2021). On the other hand, the bottom-up approach consists of building nanostructures up from basic atomic or molecular building blocks using chemical or physical forces (Picraux, 2023). Synthesis methods such as solvothermal and hydrothermal, sol-gel methods, chemical vapor deposition, the colloidal method and laser pyrolysis, are all routes that employ the bottom-up approach (Baig *et al*., 2021).

The classification of the synthesis routes for nanomaterials can also be done through types of methods, which include physical methods: mechanical milling, sputtering, laser ablation or laser pyrolysis, among others; chemical methods: solvothermal and hydrothermal, sol-gel methods, chemical vapor deposition among others; and green synthesis methods which are characterized for the use of biological agents, such as plants and fungi, as precursors or reagents in the synthesis process (Goutam *et al*., 2019).

Sol-gel methods are some of the most commonly utilized synthesis routes, specifically for creating metal oxide nanoparticles. Essentially, it is a chemical process in which a solution or colloidal suspension from a precursor (sol) is transformed into a solid network structure (a gel). Sol-gel methods themselves are divided into two distinct categories. The first are the aqueous methods, which use hydrolysis to convert precursors such as inorganic metal salts or metal alkoxides into inorganic solids. On the other hand, there are the non-aqueous methods, which use organic solvents for the formation of the sol and convert the precursors (such as inorganic metal salts, metal alkoxides or metal acetates, among others) through thermal decomposition (Baig *et al*., 2021), (Droepenu *et al*., 2021), (Kadam *et al*., 2022).

Once the hydrolysis or chemical decomposition of the precursor is done, the synthesis via sol-gel method continues with a condensation step, which results in the increased viscosity of the mixture because porous polymeric structures are formed. This step advances into gelation and then into aging, which lead to changes in the porosity of the structures formed. Subsequently, the water or organic solvent is removed from the gel through drying and the gel is then calcined to obtain the corresponding metallic oxide NPs (Baig *et al*., 2021), (Droepenu *et al*., 2021).

There are several advantages associated with the implementation of sol-gel synthesis routes. The resulting nanomaterial is homogeneous, which allows for a relatively good control of particle size and shape which, as said before, lead advantages in a wide variety of applications. The method also leads to a good rate of thermal stability of the NPs and good flexibility in terms of crystal formation. The methods themselves are relatively inexpensive, given the fact that the needed set up is affordable and the process takes place at relatively low temperatures. Conversely, factors like the nature and the concentration of the precursor, the pH, the hydrolysis rate, temperature, condensation and aging time, all have an effect on the final product and need to be closely controlled. This is predominantly true for aqueous sol-gel methods and tends to be overcome when applying the non-aqueous methods (Baig *et al*., 2021), (Droepenu *et al*., 2021). Polyol synthesis is one of these sol-gel methods, which is characterized by the use of glycol solvents. It has been stated in the literature that polyol solvents, such as diethylene glycol (DEG), act as good stabilizing agents when it comes

to particle growth and agglomeration, ensuring the desired results of small particle size and high dispersion (Alves *et al*., 2018).

Alternatively, two other commonly employed synthesis routes are the solvothermal and the hydrothermal route. Both routes involve the synthesis of NPs through heterogeneous reactions, in non-aqueous and aqueous media respectively. The methods are usually carried out in closed systems, at relatively high pressures and temperatures (even close to the critical point of water or the boiling point of the solvent in the medium). These methods have the advantage of being able to produce and have control over a great variety of morphologies of the nanostructures (Baig *et al*., 2021).

1.4. Functionalization of Textiles with ZnO NPs

Textile functionalization consists of modifying a certain textile, to impart on its properties which enhance its function. With the advance of technology and the evolving demands and needs of consumers, the demand for a wider variety of functions in textiles has grown over the years. In the book “Textiles for Functional Applications” (2021), Singh proposed 9 categories for functional textiles according to their desired response towards certain stimuli and/or functions. These categories are biological, chemical, durability, electronic, fire and temperature, mechanical, performance, water, and special features. For example, Singh lists under the biological category that the desired functions and response towards stimuli include antibacterial activity, deodorizing, and foul odor scavenging (Somkuwar, 2021).

Functionalized textiles can be classified in a different way, under two main categories based on the nature of the textile’s functionalization process. On one hand, there is the functionalization of the textile through the modification of the fibers by adding dope additives to modify the fiber forming polymers which are then used in the manufacturing of the textiles. The other category corresponds to textiles that have been functionalized by modifying the textile’s surfaces with the use of biomaterials, resins and finishes (Somkuwar, 2021).

Given the wide range of properties and applications attributed to ZnO NPs, the use of this material to provide textiles with these properties has been growing in recent years. This has led to a myriad of combinations with regards to the development of functionalized textiles with ZnO NPs. There are a great number of variables that can be combined, including the nature of the textile, the desired functionality, the pathway used for the synthesis of the ZnO NPs, the technique employed for the functionalization of the textile among many others. **Table 1** compiles a few examples of studies that

have been carried out on the functionalization of various textiles using ZnO NPs for the purpose of providing the textile with the function of antibacterial activity.

Table 1: Some examples of the factors involved in textile functionalization with ZnO coating found in the literature

Textile Substrate	ZnO NPs Synthesis	Coating Methods	Additional Treatment	Intended Functionalization	Authors
Polyamide 6 PET PP	Unspecified	Hydrothermal deposition	Hexamethylenetetramine	Antibacterial Activity	Fiedot-Tobola et al (2018)
Polyamide 6	Unspecified	Spray coating	Modified siloxane (APESP)	Enhancing washing durability	Song et al (2022)
Polyester	Sol-gel (NaOH + Urea as reactants)	Dip coating	N/A	Antibacterial activity	Amani et al. (2018)
Polyester	Sol-gel	Dip coating + shaking	NaOH UVC irradiation	Photocatalytic activity	Sudrajat and Babel (2016)
Polyester	Purchased (Sigma-Aldrich)	Dip coating	NaOH	Antibacterial and self-cleaning activities	Nourbakhsh et al., (2018)
Polyamide 6,6	N/A	Enzyme Immobilization	HCl	Self-cleaning properties	Damle et al., (2018)

Fiedot-Tobola *et al* (2018) carried out a study in which the objective was to compare the effectiveness and durability of the desired textile functionalization, which was antibacterial activity. The textiles they chose to compare were polyamide 6 (PA 6 or nylon 6), polyethylene terephthalate (PET) and polypropylene (PP), three commonly used polymeric textiles. The method through which the ZnO NPs were synthesized is not specified in this study. However, it is explained that the textiles were submerged in a colloidal suspension of ZnO NPs, which were spherical and had an average radius of 6 nm. The aim was for the NPs that adhered to the textiles' surfaces to act as crystallization nuclei to induce the crystallization of the NPs into ZnO microrods through hydrothermal deposition. The measured average length of the resulting microrods varied from around 3 to 6 µm, depending on the observed textile (Fiedot-Tobola *et al*., 2018).

Several methods, including scanning electron microscopy (SEM), X-ray diffraction (XRD), Fourier transform infrared spectroscopy (FTIR), differential scanning calorimetry (DSC) and the liquid absorption capacity (LAC) were used to characterize both the original textiles, previous to the functionalization, and the resulting ZnO coated textiles. One objective was to determine the textile's properties which influence the functionalization process. Another objective of these characterizations was to confirm that the resulting coating on the textiles was in fact ZnO microrods. The weight gain of each of the textiles was measured in order to determine the amount of ZnO that was deposited on each one. The results were the following: PA: 6.3 ± 0.2 mg, PET: 5.1 ± 0.1 mg and PP: 3.9 ± 0.1 mg. The resulting antibacterial activity of the functionalized textiles was tested following the ISO

20645:2004 standard “Textile fabrics -Determination of antibacterial activity. Agar diffusion plate test” (Fiedot-Tobola *et al.,* 2018).

Among the conclusions presented in Fiedot-Tobola ’s study, is the claim that both the surface roughness and wettability of the polymeric textiles have a direct effect on the effectiveness of the deposition of the ZnO. A balance needs to be struck between both characteristics, having a higher wettability and a lower roughness to achieve the highest deposition. The highest deposition of ZnO in this study was achieved on the PA textile. A significant antibacterial activity was observed across all textiles, which was identified to be related to ROS generation, and specially against gram-negative bacteria, PA also displayed the highest antibacterial activity (Fiedot-Tobola *et al.*, 2018).

Another example is that of the study conducted by Amani *et al.*: “Synthesis of applicable hydrogel corn silk/ZnO nanocomposites on polyester fabric with antimicrobial properties and low cytotoxicity” (2018). In this case, they employed a dip-coating technique to endow a polyester textile with antibacterial activity function. An in-situ sol-gel synthesis method was carried out using zinc acetate as a precursor to the ZnO NPs. Additionally, they employed the use of corn silk in the reaction to create a hydrogel in which to dip the polyester fabric to carry out its functionalization. Characterization techniques such as SEM, energy-dispersive X-ray spectroscopy (EDX), XRD, and FTIR were used to determine the composition of the resulting hydrogel, confirming it was made of corn silk and contained ZnO. They claim that the textiles that were functionalized using the corn silk/ZnO hydrogel displayed better self-cleaning and antibacterial properties, when comparing their results with those obtained in studies that employed ZnO NPs without the corn silk doping. Their proposed explanation for this finding was the fact that the synthesis of the ZnO NPs along with the corn silk resulted in a lower band gap in the material, which enhanced its photocatalytic properties. They claim that the governing mechanism for the ZnO’s antibacterial properties is the generation of ROS. However, they don’t appear to have carried out tests to validate this claim. Additionally, they determined the effectiveness of the coating process by calculating the percentage in weight increase of the coated textiles vs the un-coated ones (Amani *et al.*, 2018).

Among others, *Amani et al;* compared their findings to those from Noubakhsh ’s study: “Zinc oxide nanoparticles coating on polyester fabric functionalized through alkali treatment” (2018). This study focused on the effects that alkali surface treatment of polyester had on the wettability of the textile and therefore on the effectiveness of the adherence of the ZnO NPs; The dip-coating is used to functionalize the textile. They mention that alkaline hydrolysis of polyester is a method that is widely used in the industry for this very purpose of increasing wettability. In this study, they also compare the effectiveness of a coating process in which the polyester textile is pretreated with sodium hydroxide (NaOH) and subsequently coated and a process in which both the treatment and the

coating are carried out simultaneously, concluding that the former is more effective. The desired functionalities for the textile in this case are self-cleaning and antibacterial properties. However, in this case, they focus on the formation of Zn^{2+} ions as the main mechanism for the material's antibacterial activities. Additionally, they conduct a textile laundering test according to the AATCC 124-1996 standard test method to determine the durability of the adherence of the ZnO NPs on the textile (Nourbakhsh *et al.*, 2018).

A further example includes that of Song *et al.* (2022), which employed a process of spray-coating on the textile with an additional treatment of modified siloxane to improve the adherence. In this work, they sought to enhance the washing durability of the coating on the textile, rather than focusing on a specific desired functionalization. Similarly to Noubakhsh *et al.* (2018), Sudrajat and Babel (2016) used pretreatment of a polyester textile with NaOH as a means to increase the adherence of the ZnO NPs, which in this case were synthesized through a sol-gel method. The coating was done through dip-coating and the desired functionalization was photocatalytic activity. In contrast, Damle *et al.* (2018) carried out a study on textile functionalization of polyamide 6,6, through enzyme mobilization, to provide the textile, similarly to the previously mentioned studies, with self-cleaning properties. In this case, they employed a textile surface acid pretreatment, using HCl.

1.5. The DAF3D Project

The work pertaining to this thesis is related to an ongoing European CORNET project entitled "Development of Antibacterial Functionalized Textiles by 3D Printing" (DAF3D) developed by the Nanomaterials, Catalysts, Electrochemistry (NCE) research group in the Department of Chemical Engineering at the University of Liège. The aim of this project is to "develop an innovative and sustainable 3-D printed filter based on antibacterial functionalized textiles with ZnO for industrial water disinfection" (Farcy *et al.*, 2022). The project is divided into different work steps: (i) testing and optimizing different synthesis pathways by which the ZnO NPs reach their optimum antibacterial activity, (ii) coating of the commercial nylon-based textile, and (iii) coating of filters prepared by 3D printing.

Step (i) of the project focused on two sol-gel synthesis methods, namely a modified polyol method which used zinc acetate as the precursor and DEG as the solvent. On the other hand, the optimization of the pepti synthesis pathway for ZnO NPs was mainly based on the work of Shamhari *et al.* "Synthesis and Characterization of Zinc Oxide Nanoparticles with Small Particle Size Distribution" (2018). In their work, Shamhari *et al.* claim that this synthesis method allows for a comparatively faster process that other known synthesis methods and that it results in ZnO NPs that have a smaller particle size (< 10 nm), a more uniform shape and a higher dispersion (Shamhari *et*

al., 2018). In turn, Shamhari *et al.* partly based their research on the work of Matei *et al.*, who claim that this type of synthesis has the advantage of being easy to perform under controlled conditions. Furthermore, depending on the reaction conditions, the resulting morphologies of the ZnO NPs can be changed (Matei *et al.*, 2014). They also based their research on the work of Bai *et al.*, who claimed that this type of synthesis method results in an enhanced dispersion of the ZnO NPs (Bai *et al*., 2014).

For step (ii), the DAF3D project, the group NCE has partnered with ACE, a Belgian company dedicated to the manufacture of films and laminates with broad medical applications (ACE Films, 2023). Like any other industries, the manufacturing of films and laminates uses a substantial amount of water for its processes. Specifically, ACE's process includes a step in which the formed film exits the extruder at 250 ºC onto a pressure roller; water is circulated in a closed loop in order to cool down that pressure roller and once the heat exchange is done, the water is found at 40 ºC. Given that they have the water in a closed loop, they need the water to be clean and free of bacteria, to be able to reuse it. Among their water treatment methods, they use monofilament filter bags made from nylon 6 textile. These specific filter bags are manufactured and supplied by the company Eaton.

The aim is to turn those nylon monofilament filter bags into antibacterial filters through the coating of ZnO on the textile. The use of ZnO NPs is of particular interest to this project given proven antibacterial activity of ZnO NPs under dark conditions, since, once again, the filters will be located inside a closed system. One of the DAF3D project's hypotheses is that fixing these NPs on a stable surface, such as the nylon textile, and achieving a good adherence, will lead to an efficient antibacterial functionalized textile, with a prolonged active lifespan.

1.6. Objectives of Master Thesis

The specific stage of the project that pertains to this thesis (step (ii)) consists in determining whether suspensions made from ZnO NPs, which have been synthesized through the previously developed methods from stage (i) (pepti and polyol pathways), can be used for developing antibacterial functionalized textiles through coating, specifically employing a dip-coating technique.

The objective involves the development of an antibacterial water treatment, by creating functionalized textiles to be used in water filters, to disinfect the water that is being used in a closed-loop cooling system. Since the antibacterial water treatment is meant to act in a continuous manner within that same closed-loop system, the disinfection must be able to take place in the dark. This solution should also be viable in terms of scalability, ease of implementation and affordability. Additionally to what has been mentioned on the antibacterial properties of ZnO NPs, even under

dark conditions, ZnO has also proven advantageous in the development of functionalized textiles for several different applications, including conferring the textiles with antibacterial and photocatalytic properties (Verbic *et al.*, 2019).

Hence, the aim is to determine the procedure and conditions with which the best ZnO NP coating results are achieved. This means finding the conditions with which the highest possible amount of ZnO NPs can be attached to the nylon textile, even after being exposed to running water, while maintaining a satisfactory antibacterial activity.

The development of this thesis consisted in carrying out a series of experiments in which the dip-coating technique was used to coat the previously described nylon monofilament textile with the ZnO NP suspensions. The experiments were conducted with varying conditions and parameters, including the use of chemical and physical surface activation techniques, with the aim of determining the effects that each of those parameters had on the effectiveness of the coating. The effectiveness of the coating was mainly assessed through measurements of the changes in the weight of each nylon sample before coating, after coating and after a wash. Both the polyol and the pepti synthesized ZnO NPs suspensions were used in the development of these experiments and their performance was compared as part of the assessments.

Once the coating experiments were done, a series of characterization techniques were applied to the resulting ZnO NPs functionalized nylon samples. These characterization techniques included X-ray diffraction (XRD), transmission electron microscopy (TEM), scanning electron microscopy (SEM) and backscattered electrons (BSE), as well as energy dispersive X-ray spectroscopy (EDX) and fourier transform infrared spectroscopy (FTIR). These techniques were applied with the aim of validating that the coating achieved on the nylon substrate corresponded to ZnO NPs, as well as analyzing the characteristics of the coatings that were achieved. An additional objective was to identify the effects that some of the conditions of the experiments, such as the use of chemicals, had on the nylon's surface and how that might relate to the results of the coating experiments.

Finally, tests were performed in order to determine the effectiveness of the ROS generation of the resulting functionalized textiles, in dark conditions. As was mentioned earlier, AOPs have been found to be highly effective in the degradation of organic compounds due to the presence of the highly oxidative ROS that are generated (Ameta *et al.*, 2018), this includes the degradation of dyes such as methylene blue (MB) and nitroblue tetrazolium (NBT). Because of this, these compounds have been widely used to evaluate the activity and presence of ROS in specific scenarios (Prasanna & Rajagopalan, 2016), (Wolski *et al.*, 2019).

The following thesis report is divided into four main chapters dedicated to the methodology applied for each of the stages of the experimental and characterization work, the presentation of the results obtained, the discussion of the observations drawn from the results and the conclusions.

2. METHODOLOGY

Given that the general aim of this thesis is to develop antibacterial functionalized textiles for industrial application by coating nylon with ZnO NPs, a series of experiments, characterizations and tests were performed to determine the most effective method for achieving the desired results.

The textile used to do the coating experiments was the nylon 6 monofilament textile, which the filter bags used by the industrial partners are made of. These nylon monofilaments, which have a thickness of < 125 μm, are woven into a specific pattern and the intersections between the monofilaments are fusion-welded (EATON, 2016). The picture of the nylon monofilament bag is shown in **Figure 1**.

Figure 1: Nylon Monofilament filter bag by Eaton, taken from the SENTINEL® and SNAP-RING® monofilament filter bag for surface filtration Datasheet (EATON, 2016)

Considering the goal of the project, the outcomes of the experiments carried out need to comply with the following criteria:

1. The ZnO NPs should coat the substrate thoroughly and efficiently, and this coat should remain on the textile even after it is exposed to a continuously running water flow.

2. The coating process should be scalable at an industrial level. Industrially, the coating should be done at the end of the filters' manufacturing process, to prevent other steps from affecting the coating or vice versa. This means the substrate will not be a flat nylon surface during the coating process but a 3-dimensional structure (as it is shown in **Figure 1**). For this reason, surface coating processes such as spray-coating or bar-coating were rejected as options, and it was determined that the methodology that was to be tested in the development of this thesis was **dip-coating.** Dip-coating is a technique that will allow thorough contact between

the suspension of the ZnO NPs and the entirety of the textile from the filter, even at an industrial scale.

3. Since the application of the filters seeks to reduce the presence of bacteria in industrial wastewaters, in order to treat it and reuse it, the antibacterial activity of the ZnO coated nylon has to work under dark conditions, as it would inside a pipe.

The general methodology of the experiments carried out for this thesis consisted in preparing the ZnO NP suspensions as needed, using the previously mentioned synthesis pathways and using the dip-coater to submerge pieces of nylon textile within the suspensions. Different experiments were carried out changing parameters such as dipping time, textile surface pre-treatment, and suspension concentrations. The nylon pieces were weighed before and after the dipping process (once dried) in order to determine the added mass. The pieces were then washed under water, dried and weighed again, in order to determine any loss of mass that could be attributed to the washing away of the ZnO coat.

Next, several samples were characterized using TEM, SEM, BSE, EDX, XRD and FTIR, in order to determine any changes done to the nylon textile and to confirm that the resulting added weight of each piece was in fact the adhesion of ZnO NPs. Finally, NBT degradation tests were conducted to determine whether the ZnO NPs from the functionalized nylon textiles had the capacity for ROS formation in dark conditions, as this is the ultimate goal of the project.

2.1. ZnO Synthesis Processes

As was mentioned during the introduction section (section 1.3), there is an extensive number of known methods that can be used to synthesize ZnO NPs. Each of these lead to different results in terms of the compound's nanostructures and its performance with regards to its different properties. As a result of the work that has been previously carried out by the team NCE, it has been determined that the sol-gel synthesis pathways (pepti and polyol) yield ZnO NPs which present highly favorable characteristics for the intended purpose (industrially scalable synthesis processes and efficient antibacterial activity under dark conditions).

The suspensions are made by mixing the synthesized ZnO NPs in absolute ethanol at the desired concentrations. No changes to these synthesis pathways were made during the development of these experiments, as this did not fall within the scope of the stage of the DAF3D project that pertains to this thesis.

The following are the methods implemented for the two chosen synthesis pathways:

a. Pepti pathway:

5.9 g of zinc acetate dihydrate ($Zn(CH_3COO)_2 \cdot 2H_2O$) was dissolved in 250 mL of industrial grade ethanol (99%) in a 1000 mL Erlenmeyer flask. The solution was placed in an oil bath and heated up to 80-90 ºC while stirring, to assist with the dissolution process. Once completely dissolved, the temperature was lowered until it reached 60 ºC. At the same time, 4.5 g of potassium hydroxide (KOH) was dissolved at room temperature in 130 mL of industrial grade ethanol. Once the KOH was dissolved, this solution was also placed in an oil bath to heat up to 60 ºC.

Once the two solutions reached approximately the same temperature, the KOH solution was added very slowly to the zinc acetate dihydrate solution. The resulting solution was maintained at 60 ºC and with constant stirring for 6 h in order to ensure the completion of the nanoparticles' formation.

After 6 h, the nanoparticles were recovered from the solution by pouring it into flacons and separating them via centrifuge at 12.500 rpm for 15 min. The leftover liquid was discarded while the nanoparticles remained at the bottom of the flacons. These were then washed using clean industrial grade ethanol (at 99%), in order to remove the leftover KOH and spent ethanol. The clean ethanol was added and the nanoparticles were thoroughly mixed using an ultrasonic bath and a vortex mixer as needed. The flacons were placed again in the centrifuge to separate the nanoparticles once more and the process was repeated. A total of two washes with ethanol were done.

The resulting washed ZnO nanoparticles could now be used to create the suspension. This suspension was done by either directly adding absolute ethanol to the recovered nanoparticle sludge to reach a concentration of 10 g/L or the ZnO nanoparticles were dried at 100 ºC overnight and then mixed in absolute ethanol to reach 10 g/L. This 10 g/L concentration was previously determined by the team NCE, to be the highest concentration that could be reached while maintaining a relatively good stability, after being placed in an ultrasonic bath overnight.

b. Polyol Pathway:

Similar to the pepti synthesis method, the polyol method used zinc acetate dihydrate as the precursor for the ZnO NPs. This method consists of dissolving zinc acetate dihydrate in diethylene glycol (DEG) at high temperatures as follows:

16.302 g of $Zn(CH_3COO)_2 \cdot 2H_2O$ were dissolved in 200 mL (223.2 g) of DEG. The mixture was set in an oil bath and heated up to 140 ºC with constant stirring until completely dissolved. Once dissolved, the solution was further heated up to 180 ºC and kept at that temperature for 2 additional

h. The solution was then poured into flacons and centrifuged at 12.500 rpm for 15 min to recover the ZnO NPs; the remaining DEG was discarded. The nanoparticles were then washed by adding industrial grade ethanol (99%) to the drained flacons, thoroughly mixing the nanoparticles and the ethanol using an ultrasonic bath and a vortex mixer as needed. The washed nanoparticles were then separated from the spent ethanol via centrifuge. This process was repeated two more times, for a total of three washes. Once again, similarly to the pepti method, the ZnO NPs suspension was made either by mixing the absolute ethanol directly with the resulting sludge or by drying the nanoparticles overnight at 100 ºC and then mixing them into the absolute ethanol. The concentration used for the polyol synthesized ZnO NPs suspension was equal to 30 g/L.

2.2. Dip-Coating Experiments

In terms of the dip-coating process of the nylon textile with the ZnO NPs, a total of 8 sets of experiments were carried out, with at least 50 individual experiments conducted altogether. The experiments included changing certain operating parameters of the dip-coater, changing the concentrations of the ZnO suspensions, and carrying out different methods to alter or activate the nylon surface in order to promote further interactions with the ZnO NPs. As each of the sets of experiments was developed, the approach of the subsequent experiments was determined based on the results that were being observed. All of the experiments were carried out in triplicate.

The dip-coating process works by attaching the substrate to one of the clamps of the dip-coater, placing the suspension in a flask below the clamp and setting the required parameters for the motor to move as desired. The dip-coater has a simple set up and a limited amount of control parameters which allows for a relatively good control in terms of the reproducibility of the experiments.

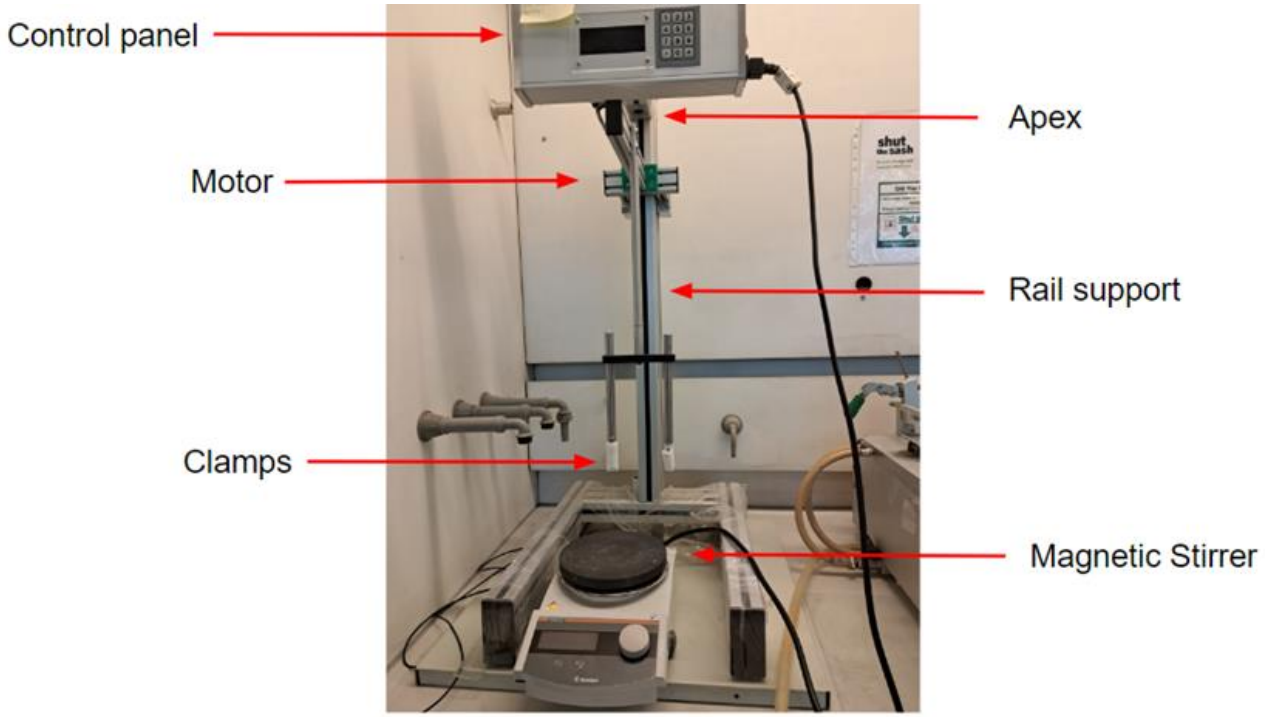

Figure 2: Set-up for the dip-coater.

Table 2: Dip-coater Control Parameters

Dip-coater Control Parameters			
Parameter type	**Parameter**	**Unit**	**Description**
Speed	Speed Down Distance	mm/min	The speed at which the motor moves downwards along the rail from the offset position.
	Speed Up Distance		The speed at which the motor moves upwards along the rail from the set dipping position to the set offset position.
Time	Time dip	min	The amount of time that the motor remains at the dip position = the amount of time the substrate remains submerged in the suspension
	Time up		The amount of time that the motor remains at the offset position between each dip iteration

Iterations	Iterations	#	The number of iterations a set **cycle** is repeated

A cycle in the dip-coater consists of the motor traveling along the rail from the offset position at the given speeds to a “distance” position, then to a “dip” position, remaining during the set “Time Dip”, then traveling back up to the “distance” position and the offset position, remaining at the offset position during the set “Time Up”. Finally, traveling upwards to the apex of the rail and back down again to the offset position.

A **general procedure** was followed for each of the experiments that was carried out:

1. The nylon textile was cut in pieces of around 3 x 3 cm^2.

2. The pieces were placed in a flash and a washing agent was added. The flask was then placed inside an ultrasonic bath for 15 min. This was done to clean the nylon surface and ensure that any contaminant was removed before doing the coating.

3. The pieces were removed from the washing agent and placed in individual plastic petri dishes.

4. The petri dishes then placed inside a drying oven for 15 min at 60 ºC (even though the melting point of nylon 6 is between 240 °C and 265 ºC, its glass transition temperature goes up to 60 ºC, which is why the nylon pieces were not dried at higher temperatures (Perkin Elmer, 2019)).

5. Once dry, each nylon piece was weighed. This weight was recorded as the **initial weight.**

6. The nylon pieces were clamped individually to the dip-coater and dipped into the ZnO NPs suspension, using the specified parameters for each experiment.

7. Once the dip-coating was completed, the nylon piece was removed from the dip-coater and placed back in the petri dish.

8. The petri dishes were once again placed inside a drying oven for 15 min at 60 ºC.

9. Once dried, each nylon piece was weighed again. This weight was recorded as the **post-coating weight.**

10. The nylon pieces were then placed under a constant flow of running water for 10 s.

11. The pieces were placed back in the petri dishes and inside the 60 ºC drying oven once again, overnight to ensure that all the water molecules evaporated for the surface.

12. The pieces were weighed once more and the weight was recorded as the **post-wash weight.**

The equation (7) shows the calculations that were done in order to obtain the added weight from the ZnO NPs coating after the dip-coating process. The equation (8) represents the final added weight corresponding to the added coat weight after the nylon textile was washed.

$$\underline{W}_{Added\ post\ coat\ (mg)} = \underline{W}_{Post-coating\ (mg)} - \underline{W}_{Initial\ (mg)} \quad (7)$$

$$\underline{W}_{Total\ Added\ \ (mg)} = \underline{W}_{Post-wash\ (mg)} - \underline{W}_{Initial\ (mg)} \quad (8)$$

Unless it is specified otherwise in the description of each experiment, the general procedure presented above was followed in every experiment conducted. The nylon pieces were always handled with pliers to avoid contamination of the surface and to prevent the ZnO coating from being removed due to contact friction with the fingers.

Due to qualitative observations made on the precipitation of the suspensions of the ZnO NPs, it was determined that these should be placed on magnetic stirrers for the duration of the coating process. This was done so that the ZnO NPs remained suspended and dispersed homogeneously in the solvent to ensure an equal contact between the entirety of the nylon textile pieces and the ZnO NPs. The magnets used for the stirring were relatively small and the speed set for the rotation was adjusted (between 250 - 300 rpm) to be fast enough to ensure the homogeneity of the suspension while avoiding the formation of a vortex. Additionally, enough volume of the suspension was placed in the flask so that the dip-coater's clamps were able to be lowered at a dip distance enough to submerge the nylon pieces completely, while also preventing the nylon from touching the stirring magnet.

The following sections are the descriptions for each of the 8 dip coating experimental sets that were carried out.

2.2.1. Optimization of the Dipping Times (Set A)

The goal of this first set of experiments was to determine the time required for the nylon to be submerged in the ZnO suspension in order to achieve a good coat. The general procedure explained previously was followed, using industrial grade ethanol (99%) as the washing agent. This set of experiments was carried out using only the pepti suspension at 10 g/L concentration.

Table 3: Set of parameters for the dip-coater during optimization of the dipping times experiments.

Parameter		**Experiment 1A**	**Experiment 2A**
Speed Up (mm/min)	Distance	300	300
	Dip	300	300
Speed Down (mm/min)	Distance	300	300
	Dip	300	300
Time Dip (min)		3	10
Time Up (min)		5	5
Total Dip Time (min)		9	30
Total Experiment Time (min)		24	45
Iterations (#)		3	3

In **Table 3**, all the parameters regarding the speed at which the motor of the dip-coater travels are set at the same value; the speed is maintained the same throughout the entire movement of the motor. This is done to minimize the variables involved in this first experiment.

The times were determined based on preliminary experiments, in which the substrate was dipped in the suspensions for 1 min, 10 min and 2 h; these preliminary experiments did not follow the steps laid out in the **general procedure** (page 27), like the dimensions of the nylon pieces and the initial washing of the nylon, but they served as a starting point to determine the times established in **Table 2**.

2.2.2. Determination of the Washing Agent (Set B)

During the first set of experiments, the washing agent used to clean the nylon before the coating process was industrial grade ethanol (99%). This solvent was selected primarily due to the fact that the ZnO suspension is composed of absolute ethanol, meaning that any residual ethanol from the washing process will have no adverse interaction with the ZnO suspension, this allowed for further control of the variables during the first experiment. For the second set of experiments, different

washing agents were tested, to determine whether different washing agents used to clean the substrate before the dip-coating had any effect on the amount of ZnO NPs that would ultimately adhere to the nylon.

The parameters that were set on the dip-coater for these experiments were the same ones used for más atrás (**Table 2**), meaning 10 min of submersion and 5 min at the offset position during 3 iterations. Given that ethanol was already used as a washing agent, this serves as the first experiment for experimental set B. The other two washing agents that were used were acetone and a two-step process with RBS detergent followed by acetone. In the case of the two-step process, the substrate was first submerged in the RBS detergent and placed in the ultrasonic bath for 15 min, then rinsed with water and immediately submerged in acetone and placed once again in the ultrasonic bath for another 15 min before being dried and continuing with the general procedure.

2.2.3. Determination of Speed Up Setting (Set C)

During the setup of the first set of experiments (**Set A** (paragraph **2.2.1**)**, Table 3)** it was determined that the speed down parameters should be slow in order to prevent the substrate from possibly unclamping when it came into contact with the ZnO suspensions. Still, it was determined that the speed down was a variable that had no real impact on the coating capacity of the experiments, which is why it was increased for the rest of the experiments to 2000 mm/min, to increase the overall speed of the process.

However, the speed up parameter was considered to be relevant to the experiment goals, by having a substrate submerged in a suspension of NPs and pulling it out. The interactions between the suspension that remained in the flask and the NPs attached to the nylon might cause some of the NPs to be pulled back to the suspension rather than remain attached to the substrate. Different speeds for taking the substrate out of the suspensions might cause the surface tension of the suspension to break easier and reduce the effects that these interactions might have on the final coating results.

Once again, the general procedure remained the same, this time using ethanol as the washing agent when applying the coat with the pepti suspension at 10 g/L and acetone as the washing agent when applying the coat with the polyol suspension at 30 g/L. The three values for the speed up setting that were evaluated during this experimental set were 300 mm/min, 2000 mm/min and 6000 mm/min.

2.2.4. S**Variation of the concentrations for the Pepti Synthesized ZnO NPs Suspension (10 g/L vs 5 g/L) (Set D)**

As it was mentioned previously, due to qualitative observations on the settling behavior of the different ZnO NPs suspensions, it was determined that the suspensions should be constantly stirred to ensure the homogeneity of the suspensions. From these qualitative observations, it was seen that the pepti ZnO suspension at 10 g/L tended to precipitate faster than the 30 g/L polyol ZnO suspension. Additionally, the added weight results from the previous experiments indicated higher values of added weight when the 30 g/L suspension was used. Due to these observations, it was determined that the following set of experiments would be to test the performance of the nylon coating process by the pepti suspension at 10 g/L vs 5 g/L, in order to evaluate the effect of the concentration and the dispersion of the ZnO NPs in the suspension on the resulting added weight of the substrate.

This set of experiments once again followed the steps of the general procedure, using ethanol as the washing agent, the time parameters configurations from **Set A -** Optimization of the Dipping Times (Set **A)** (**Table 3**) and using a 2000 mm/min Speed Up setting, based on the results observed from the previous experiments (**Set C**) (paragraph **2.2.3**)

2.2.5. Double and Triple Coatings (Set E)

After having conducted several sets of experiments and observing the behavior of the measured changes in the weight of the substrate (the difference between the initial weights, the post coating weights and the post wash weights), it was proposed that doubling the coating process for each of the tested concentrations, using the previously optimized procedures. These further coatings could increase the amount of ZnO NPs that would adhere to the substrate.

The experiments were done in the following manner: double coat using pepti 5 g/L, pepti 10 g/L and polyol 30 g/L and triple coat using pepti at 5 g/L. The general procedure was followed all the way steps 1-12 described in page 27, once the coated substrates were dried and weighed post-wash, they were re-coated following the steps 6-12 of the general procedure (page 27). This was done once more for a third coat with the pepti 5 g/L suspension. The resulting data would include the initial, post-coating and post-wash weights for each of the added coats, plus the total final added weight. The hypothesis behind this set of experiments was that once washed and dried, the ZnO NPs that had failed to make full contact with the nylon surface and therefore would have weaker interactions with it, would be washed away leaving space for new nanoparticles to fill in the gaps.

2.2.6. Basic and Acid Surface Pretreatment of the Nylon 6 (Set F)

Experimental sets realized in previous paragraphs (2.2.1 to 2.2.5) mainly dealt with the operating parameters of the dipping process and the conditions for the general dip coating procedure. From the experimental **Set F**, the attention was shifted towards the substrate. Hypotheses were stated regarding a possible chemical activation of the nylon 6 surface, using either a base or an acid solution. The objective of activating the surface of the substrate, with the aid of acid or basic chemicals is to alter the structure of the surface to achieve a better adherence of the ZnO NPs to the substrate. There are reports of the use of NaOH and different acids as additional treatment methods in the functionalization of polymeric textiles using ZnO NPs (Verbic *et al.*, 2019). Additionally, the use of HCl is mentioned in the literature as pretreatment for the immobilization of other molecules on nylon 6 specifically (Damle *et al.*, 2018). This would lead to believe that the experimentation with a basic or an acid pretreatment of the nylon is a promising route to explore.

For the development of this set of experiments, the general procedure was the same as presented in page 27, But, in step 2, rather than using ethanol or acetone as the washing agent, a basic or acidic solution was used. A key difference here was that once the nylon pieces were taken out of the acid or base of choice, they were thoroughly washed with demineralized water before drying and weighing for the first time. This was done to prevent as much as possible an excess of protons or hydroxide ions, resulting from the chemical bath, and which could interact with the ZnO suspension. Since the substrates were washed with demineralized water, they were placed in the drying oven overnight to ensure they were dried before taking down the initial weight.

Table 4 shows the different chemicals used for these surface activation experiments of nylon 6 and their respective concentrations:

Table 4: List of acid and basic chemicals used for the nylon 6 surface activation with their respective concentrations and the concentrations of the corresponding ZnO suspension used.

Chemical	Concentration	ZnO Suspension Concentration
NaOH	1% (0.25M)	Pepti 5 g/L Polyol 30 g/L
Acetic Acid	1% (0.17M)	Pepti 5 g/L Polyol 30 g/L
Acetic Acid	0.5 M	Pepti 5 g/L Pepti 10 g/L Polyol 30 g/L

Acetic Acid	1 M	Pepti 10 g/L Polyol 30 g/L
HCl	0.1 M	Pepti 5 g/L Polyol 30 g/L
HCl	0.25 M	Pepti 5 g/L Pepti 10 g/L Polyol 30 g/L
HCl	0.5 M	Pepti 10 g/L Polyol 30 g/L
HCl	1 M	Pepti 5 g/L Polyol 30 g/L

During the development of the entire experimental **Set F** (paragraph **2.2.6**), the configuration of times and iterations was set as 10 x 5 x 3, the same as what had been established in the experimental **Set A** (paragraph **2.2.1**), and the speed up setting was 2000 mm/min.

2.2.7. Double and Triple Coatings with Acid Surface Pretreatment (Set G)

After finishing the experiments regarding the chemical activation of the nylon surface, the premises of experimental **Set E** (the double and triple coating experiments, paragraph **2.2.5**) and experimental **Set F** (Acid and Basic nylon surface pretreatment, paragraph **2.2.6**) were combined. The same procedure as in experimental **Set E** (paragraph **2.2.5**) was followed, but replacing the washing agent (either ethanol or acetone) with the acids that had yielded promising results in experimental **Set F** (paragraph **2.2.6**). Based on results from previous experiments, experimental **Set G** was carried out using only the pepti synthesized ZnO NPs suspension at a 5 g/L concentration and the acids used were: Acetic Acid at 0.5 M and HCl at 0.25 M.

2.2.8. UVC Nylon Surface Activation (Set H)

To finalize, a set of experiments was performed to test the effects of UVC light as a means of physical activation of the surface of the substrate. This set of experiments was done using the pepti suspension at 10 g/L and the polyol suspension at 30 g/L. In this case, the substrates were washed, dried, and weighed following steps 1 - 5 of the general procedure (page 27), using ethanol and acetone as washing agents as per the procedure in experimental **Set C** (paragraph **2.2.3**). Once the nylon pieces were weighed, they were placed inside glass petri dishes and placed under direct UVC light for a duration of 1, 20 or 60 min. Then, the general procedure was continued through steps 6 – 12 (page 27).

The complete list of experiments organized by each experimental set can be found in **Table A - 1** in the annexes.

2.3. Characterization techniques

Several characterization techniques were employed during the development of this thesis, mainly with the aim of verifying that the weight gained by each of the nylon pieces during the dip-coating experiments corresponded to an adhered layer of ZnO NPs. Transmission electron microscopy (TEM) and X-ray diffraction (XRD) were used to characterize the ZnO NPs resulting from the different synthesis pathways (pepti and polyol) and evaluate their particle size and level of dispersion, as well as to confirm their chemical composition. Scanning electron microscope (SEM) imaging was used to identify the visible differences between the blank substrate and the substrates that had been coated by the different types of suspensions and through the different experiments. Backscattered electrons (BSE) and energy-dispersive X-ray spectroscopy (EDX) were used to verify that the observed layers adhered to the nylon surface were actually composed of zinc and oxygen atoms. Finally, Fourier transform infrared spectroscopy (FTIR) was used on un-coated nylon pieces that had been pre-treated with a base, an acid or under UVC previously described in paragraphs **2.2.6** to **2.2.8.** FTIR allows discerning the effects that these pretreatments may have had on the chemical structure of the nylon textile.

TEM, SEM and BSE are imaging techniques. TEM consists of the use of an accelerated beam of electrons which is transmitted through particularly thin specimens; the interactions between the electrons and the specimen enables the observation of information such as the morphology and structure of the sample (Fields, 2019). TEM was specifically used to analyze the synthesized ZnO NPs in powder form, to draw conclusions on the particles' morphology, size, and dispersion. Similarly, SEM is a technique that uses a beam of electrons for the generation of images, rather than visible light (optical microscopy). In this case, the electrons do not go through the specimen but they interact with the specimen's surface. These interactions allow obtaining some information of the material's surface structure and defects (Ul-Hamid, 2018). BSE imaging is a type of SEM imaging that is created from electrons from the same beam but that have been reflected due to elastic interactions between the electron beam and the sample's atomic nuclei, because of this, BSE images are highly sensitive to atomic numbers. What results from this is a high contrast image, the higher the atomic number of a material, the brighter it will appear (ThermoFischer Scientific, 2022). Both techniques were used to analyze the surface of the coated nylon textiles, to compare them against a blank as well as to identify differences between the results of the different experiments.

EDX, XRD and FTIR techniques are used for the chemical characterization of samples. EDX works on the principle that whenever “core” electrons of an atom are forcibly ejected, it leaves a gap in an inner electron shell that higher energy electrons can then fill, in order to get the atom back from an excited state to a relaxed one. During this relaxation process, energy is released. According to Moseley’s Law (Talukdar, 2023), there is a direct correlation between the frequency of light from this released energy and the atomic number of an atom, making it possible to determine the elemental composition of an analyzed material through the measurement of these released light frequencies. EDX can work in conjunction with SEM, wherein the electron beam from SEM is used as an excitation source. (Gaston & Protter, 2022). In this case, EDX was used to characterize the coating adhered to the nylon pieces and confirmed that they were in fact made of ZnO NPs.

XRD is used to characterize the properties and crystalline structure of a material based on the principle that whenever an X-ray beam hits a specific crystalline structure at a specific angle (Bragg’s law, (Henry & Mogk, 2023)), the X-ray will be diffracted by the structure at the same angle or it will be interfered by that structure. The angles of diffraction of the X-rays and their intensity correspond specifically to a type of crystalline structure that can then be associated to a specific material (Vendatu, 2023). XRD was used to characterize the synthesized NPs in powder form, in order to confirm that the synthesized material was in fact crystallized ZnO NPs.

Finally, FTIR is a technique that is used to identify the molecular organization of a sample. It works on the principle that a molecule’s covalent bonds are able to selectively absorb radiation of different wavelengths, meaning that whenever infrared radiation (IR) is made to pass through a sample, some of the radiation will be absorbed and the radiation that passes through the sample is recorded. The absorbance of the radiation in turn, changes the vibrational energy in the bond. The type of vibration that is induced depends on the atoms in the bond. Since each molecule has a specific structure, they will produce specific spectra of the induced vibrations with respect to the absorbance of the IR, creating in essence a fingerprint of the molecule (Merck, 2022). In this work, this technique was used to analyze the effects that the different chemical and physical surface activation processes (paragraphs **2.2.6** to **2.2.8**) had on the nylon’s molecular structure.

2.4. Nitro Blue Tetrazolium Degradation Test in the Dark

Considering that the desired property for these functionalized textiles is the antibacterial activity in the dark, and the fact that one of the most proposed mechanisms that explain this activity with regards to ZnO NPs is the generation of ROS, even in dark, a basic test based on the degradation of Nitro Blue Tetrazolium (NBT) was conducted. NBT has specifically been used for the detection of superoxide ions ($\cdot O_2^-$) (Bielski *et al.*, 1980), (Prasanna & Rajagopalan, 2016). This is due to the

reaction of the degradation of the soluble NBT dye into an insoluble form, formazan, as shown below (**Figure 3**).

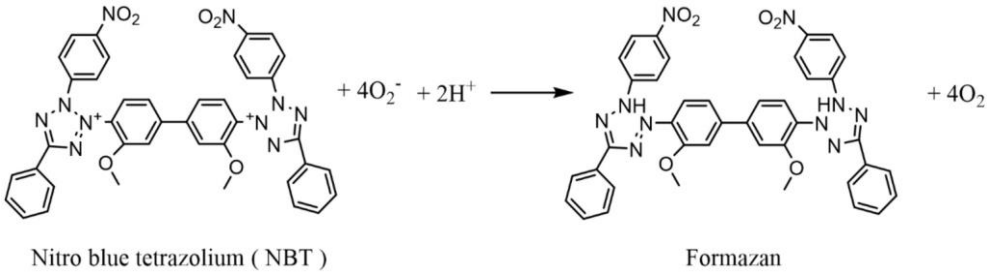

Figure 3: Reaction mechanism for the degradation of Nitro Blue Tetrazolium salt (NBT) into NBT-Formazan due to the reaction with a superoxide ion (Bakr & Rahaman, 2016).

Given that NBT is known to present a maximum level of absorbance light at 259 nm, UV-Visible light spectroscopy is used to detect its degradation (Prasanna & Rajagopalan, 2016).

Similar to the characterization step, specific samples from each of the experiments were chosen to measure their efficiency in NBT degradation, based on the obtained results regarding the added weight of the substrates, while looking for a diversity in the experiments represented.

The test was conducted by placing a blank nylon sample and each of the chosen coated samples in an individual test tube. A solution of NBT at 0.05 mM was used. For each respective sample, enough NBT solution was added in order to ensure a concentration of ZnO of 10 g/L in relation to the NBT solution. Given that the added weight for each of the nylon pieces varied, the amount of solution added was adjusted accordingly.

Once the correct amount of solution was added to each of the test tubes, a stirring magnet was added to each tube. All the test tubes were then placed on a magnetic stirrer inside a dark environment for 48 h. The absorbance was then measured for each of the resulting solutions and the blank to determine the degradation of the NBT after 48 h. In order to determine the proportion of degradation observed, the absorbance measurements for the peaks at 259 nm were compared.

3. RESULTS

The following section is dedicated to presenting the results obtained for each of the experimental sets described in the methodology section (paragraphs **2.2.1- 2.2.8**), as well as the results obtained from the various characterization techniques mentioned and the NBT degradation test. The results are presented in line with the sequence of events carried out in the methodology section.

3.1. Morphology of ZnO Samples.

During the experiments conducted in the first step of the DAF3D project, XRD measurements were carried out on each of the powders, to verify that what was synthesized through the described pathways **(section 2.1)** was in fact ZnO, as intended, as well as to identify specific characteristics of the synthesized NPs such as crystallite size and morphology.

Figure 4 shows the diffractograms which resulted from the XRD measurements for the ZnO NPs synthesized through the pepti pathway (shown in red) and the polyol pathway (shown in blue). The diffractograms for both types of synthesized NPs present three significant peaks at the angles that correspond to a typical ZnO XRD pattern (Rajan *et al*., 2023).

It can also be observed that the peaks for the polyol synthesized ZnO NPs crystallites are much higher (representing a higher intensity) and have a smaller width, than those shown in the diffractogram corresponding to the pepti synthesized ZnO NPs crystallites. These observations would suggest that the polyol crystallites exhibit a bigger size than that of the pepti crystallites (Rajan *et al*., 2023).

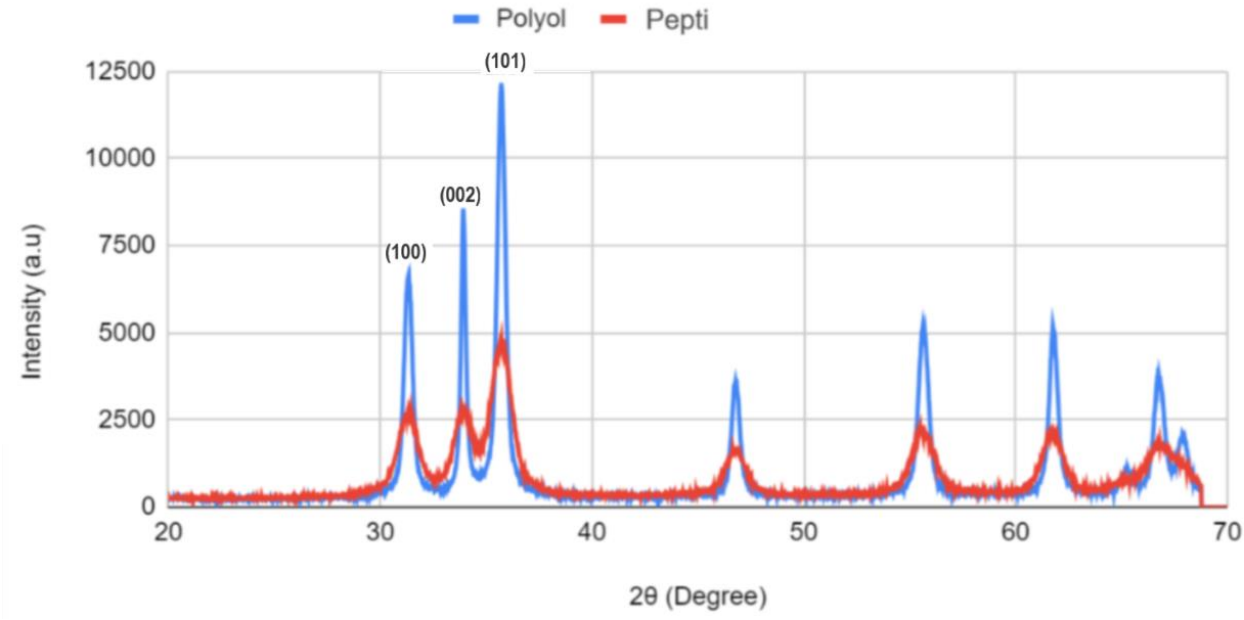

Figure 4: Diffractograms obtained for the ZnO NPs powders synthesized via the pepti and polyol pathways.

In conjunction with the XRD data on the ZnO NPs, TEM images were obtained for the ZnO NPs synthesized via the pepti and the polyol methods. This was done to have a second evaluation of the level of dispersion and sizes achieved for the ZnO NPs' crystallites, when being synthesized through each method. Using the Scherrer equation, as will be explained further in the discussion section, the crystallite size was calculated to be around 5 nm for the pepti synthesized particles and around 15 nm for the polyol particles.

In **Figure 5a**, the crystallites formed from the pepti synthesis present a high level of agglomeration, with most of the powder seen gathered on the lower left-hand corner of the image. On the other hand, the polyol ZnO crystallites take up the entirety of the space observed in the TEM image (**Figure 5b**), with a homogeneous distribution. However, at a first glance, it can be seen that the pepti synthesized crystallites have a relatively smaller size and more spherical shape, than the polyol ZnO NPs' crystallites, which generally appear to have a bigger size and a more elongated shape. These observations would be in line with what is displayed in the diffractograms in **Figure 4.**

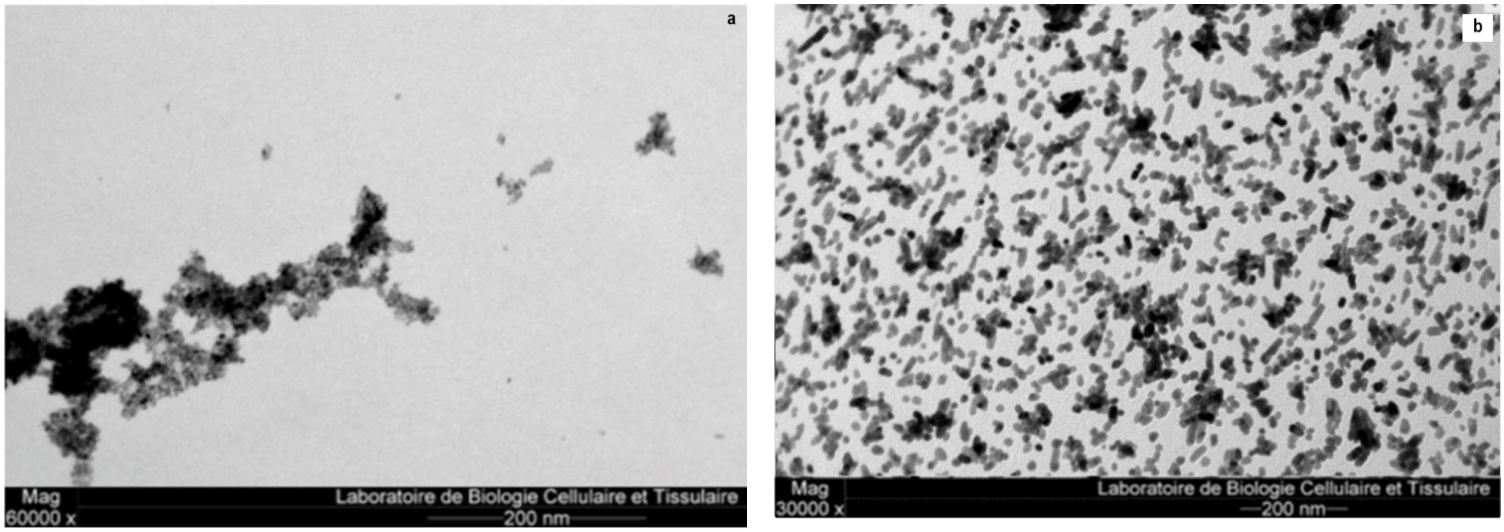

Figure 5a and 5b: TEM Images for the ZnO nanoparticles synthesized via **a)** the Pepti method and via **b)** the polyol method. (Farcy et al., 2023).

In addition to the TEM images and the XRD analysis conducted for the synthesized ZnO NPs, there were qualitative observations that could be made while working with the suspensions. **Figure 6** shows the photographs of the pepti 10 g/L and the polyol 30 g/L suspensions. While working daily with the suspensions, it could be seen that the polyol suspension remained dispersed in a stable manner for at least 24 h from the moment it was originally synthesized and created, once those 24 h passed, the solution started to precipitate slowly. The precipitated polyol suspension could be re-homogenized in an ultrasonic bath overnight but the timeframe in which this stability was maintained decreased significantly after that first precipitation. On the other hand, the pepti suspension only remained dispersed for a period between 3-6 h before it started to precipitate.

Figure 6: Photographs of the suspensions used in the experiments illustrating the qualitative analysis of the suspension's propensity to precipitate and agglomerate. a) Pepti 10 g/L after being left resting for around 6 h b) Polyol 30 g/L after being left resting for around 6 h

3.2. Amount of coated ZnO on textiles.

The added weight measurements were the focal point of the objectives established for this thesis. The desired result was to achieve a ZnO NPs coat on the nylon substrate that contained the highest amount of ZnO NPs coating possible, which is why the measurement of the added weight for the dip-coated substrate is essential. As was mentioned in the methodology, the nylon substrates were weighed initially with no added coat (once washed/pre-treated) and this was noted as the **initial weight.** The substrates were then weighed once the dip-coating process was done and having dried; this was noted as the **added weight post-coating**. Finally, the substrates were weighed after being rinsed under running water and dried overnight, this weight was noted as the **added weight post-wash.**

Both the post-coating and post-washing added weights were considered during the data processing of the results, as well as the standard deviations obtained in all the experimental triplicates. Calculations for the normalization of the data were done by dividing the total average added weight after washing (mg) by the initial average weight of the uncoated nylon pieces (g). The normalization of the data allows for all the values to be in comparable units, which in turn allows for more reliable conclusions to be drawn. The entirety of the results organized by experimental sets are presented in **Table A - 2** to **Table A - 11** and **Figure A - 1** to **Figure A - 16** in the annexes. Additionally, statistical significance analyses were done using various samples of the results achieved, by applying the t-student test, for two individual variables, with a sample size of 3 for each of the variables being tested and applying a significance level of a = 0.05. The results for these calculations are also included in the annexes, **Table A - 12.**

The following results show the performance of each of the experiments carried out, in terms of the normalized data (mg of ZnO / g of substrate). All the experiments are grouped by the specific ZnO NP suspensions used (Pepti 5 g/L, Pepti 10 g/L and Polyol 30 g/L) in order to allow for a common ground for the evaluation of the performance of each of the experiments conducted. The normalization of the data to a comparable unit (mg of ZnO added / g of substrate) and the grouping of each of the experiments to their respective suspension, allows for a valid comparison of the data and the determination of the optimum process for the goal.

The results for the first group of experiments presented in **Figure 7** correspond to those carried out using the pepti 5 g/L suspension, these include experimental **Set E** (paragraph **2.2.5**) - Double and Triple coats (shown in blue), **Set F** (paragraph **2.2.6**) - Basic and Acid Pretreatment (shown in green), and **Set G** (paragraph **2.2.7**) - Triple Coat + Acid Pretreatment (shown in red). In this graph, it can be observed that the total added weight achieved at the end of experimental **Set E** (paragraph **2.2.5**) (triple coat) and **Set G** (paragraph **2.2.8**) (using the HCl 0.25 M pretreatment) are significantly greater than the rest of the results achieved using the pepti 5 g/L suspension. On the other hand, it is clear that the lowest added weight achieved when using the pepti 5 g/L was during the experiment that employed the basic pretreatment of the substrate, using NaOH (0.25 M).

Additionally, certain patterns can be discerned from looking at the results displayed in **Figure 7**. From the results obtained for experimental **Set E** (paragraph **2.2.5**), it is observed that while applying several subsequent coats to the same substrate ultimately results in a high added weight achieved, the added weight of each individual coat lowers as the experiment progresses. It is observed that among the three coats, the first one achieved the highest added weight, followed by the second coat and the third coat achieved the lowest among the three. For the case of experimental **Set F** (paragraph **2.2.6**) (shown in green) a similar pattern emerges. When looking at the added weights achieved when applying the acid pretreatment of the substrate it can be seen that as the concentration of the acid increases, the added weight achieved through the coating decreases. This is true for both the acetic acid and the HCl pretreatment.

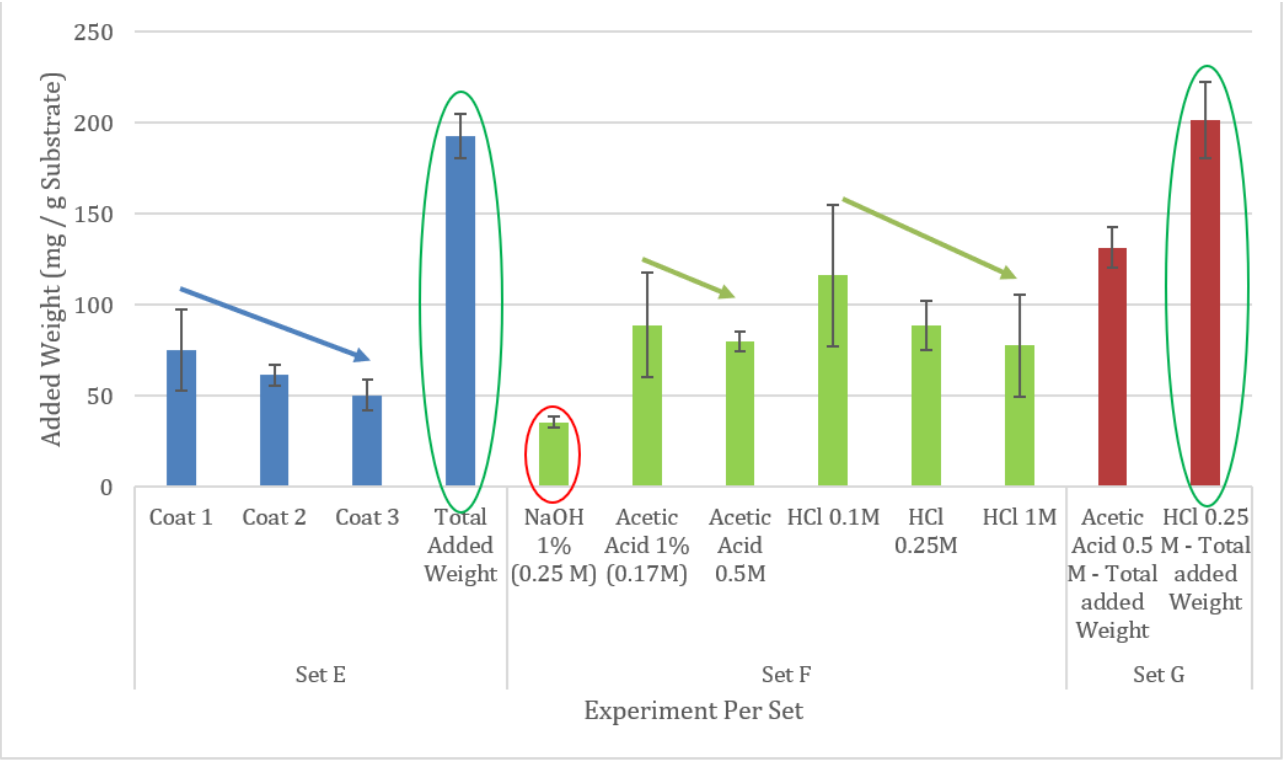

Figure 7: Comparison for the added weight achieved in each of the experiments conducted for the pepti 5 g/L ZnO NP suspension in terms of mg of ZnO / g of substrate.

Figure 8 displays the added weight results obtained for the experiments conducted using the pepti 10 g/L ZnO NP suspension, these experimental sets were: **Set B** (paragraph **2.2.2**) - Determination of the Washing Agent (shown in green), **Set C** (paragraph **2.2.3**) - Determination of the Speed Up Setting (shown in blue), **Set E** (paragraph **2.2.5**) - Double and Triple Coats (shown in red), **Set F** (paragraph **2.2.6**) - Acid and Basic Pretreatment (shown in purple), and **Set H** (paragraph **2.2.8**) - UVC Surface Activation (shown in light blue).

Similar to the results obtained for experimental **Set F** (paragraph **2.2.6**) when using the pepti 5 g/L suspension, it is observed that for both the acetic acid and the HCl, as the concentration of the acids increases, the achieved added weight in the experiments decreases. In the case of the experiments conducted using the pepti 10 g/L suspension, the acid pretreatment experiments appear to be the only experiments that display some kind of noticeable pattern. Additionally, it can be seen that the highest added weight measured was achieved with the HCl 0.25 M pretreatment experiment. Additionally, the results achieved with the acetic acid (0.5 M) pretreatment and the UVC 20 min surface activation, are fairly high. Finally, there doesn't appear to be a particularly noticeable difference among the lowest added weights achieved.

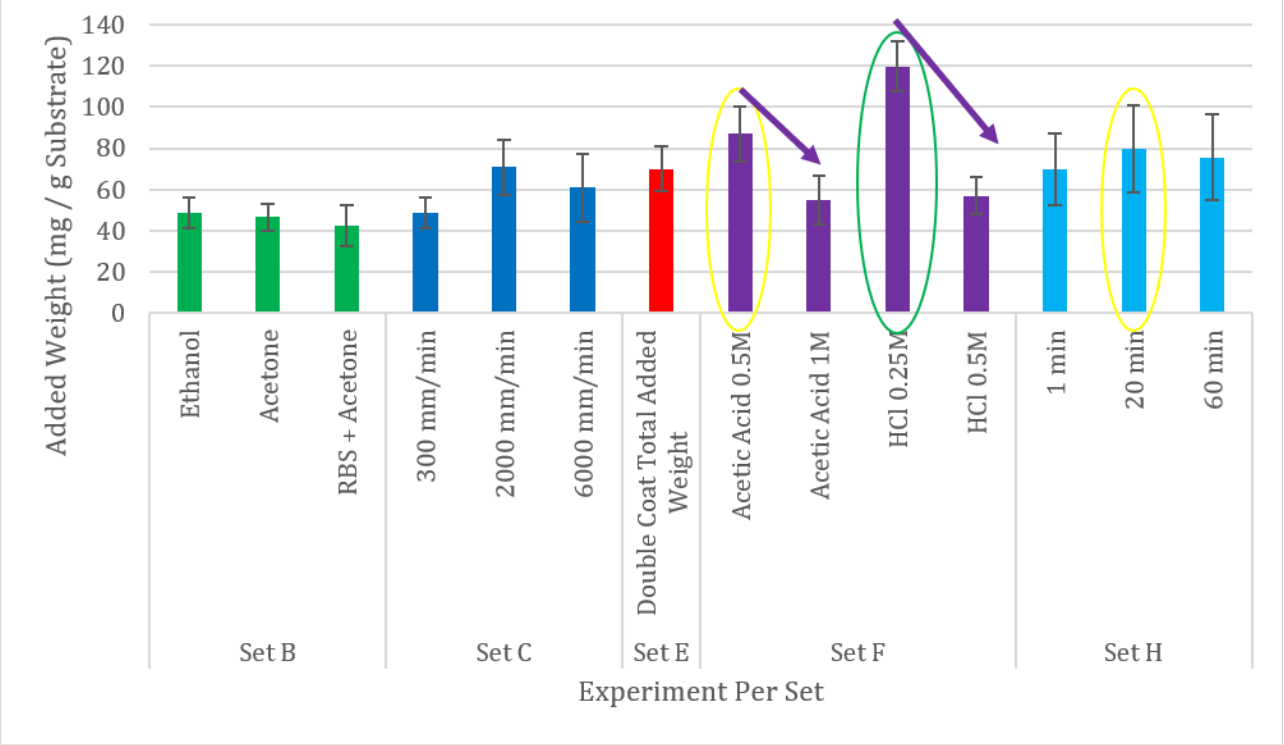

Figure 8: Comparison for the added weight achieved in each of the experiments conducted for the pepti 10 g/L ZnO NP suspension in terms of g of ZnO / g of substrate.

Finally, **Figure 9** shows the added weight results for the experiments carried out using the polyol 30 g/L suspension. In this case, the experiments conducted included: experimental **Set B** (paragraph **2.2.2**) - Determination of the washing agent (shown in green), **Set C** (paragraph **2.2.3**) - Determination of the Speed Up Setting (shown in red), **Set E** (paragraph **2.2.5**) - Double and Triple Coats (shown in light green), **Set F** (paragraph **2.2.6**) - Acid and Basic Pretreatment (shown in dark blue), **Set H** (paragraph **2.2.8**) - UVC Surface Activation (shown in light blue).

Once again, the same patterns and observations as those seen in the case of the pepti 5 g/L and pepti 10 g/L experiments emerge. Just as it was seen in the results for experimental **Set F** (paragraph **2.2.6**) with the other two suspensions, as the concentrations of the acids used to pretreat the substrate increase, the added weight of ZnO achieved, decreases. The two highest added weights achieved when using the polyol 30 g/L suspension correspond to the acid pretreatment experiments at the lowest concentrations (acetic acid 0.17 M and HCl 0.1 M), the same as with the pepti 10 g/L suspension, in this case with the HCl 0.1 M achieving the highest. Again, similar to the pepti 10 g/L, the UVC surface activation after 20 min achieved a notably high added weight and, equally to what was observed with the pepti 5 g/L experiments, the NaOH pretreatment experiment yielded a significantly low added weight.

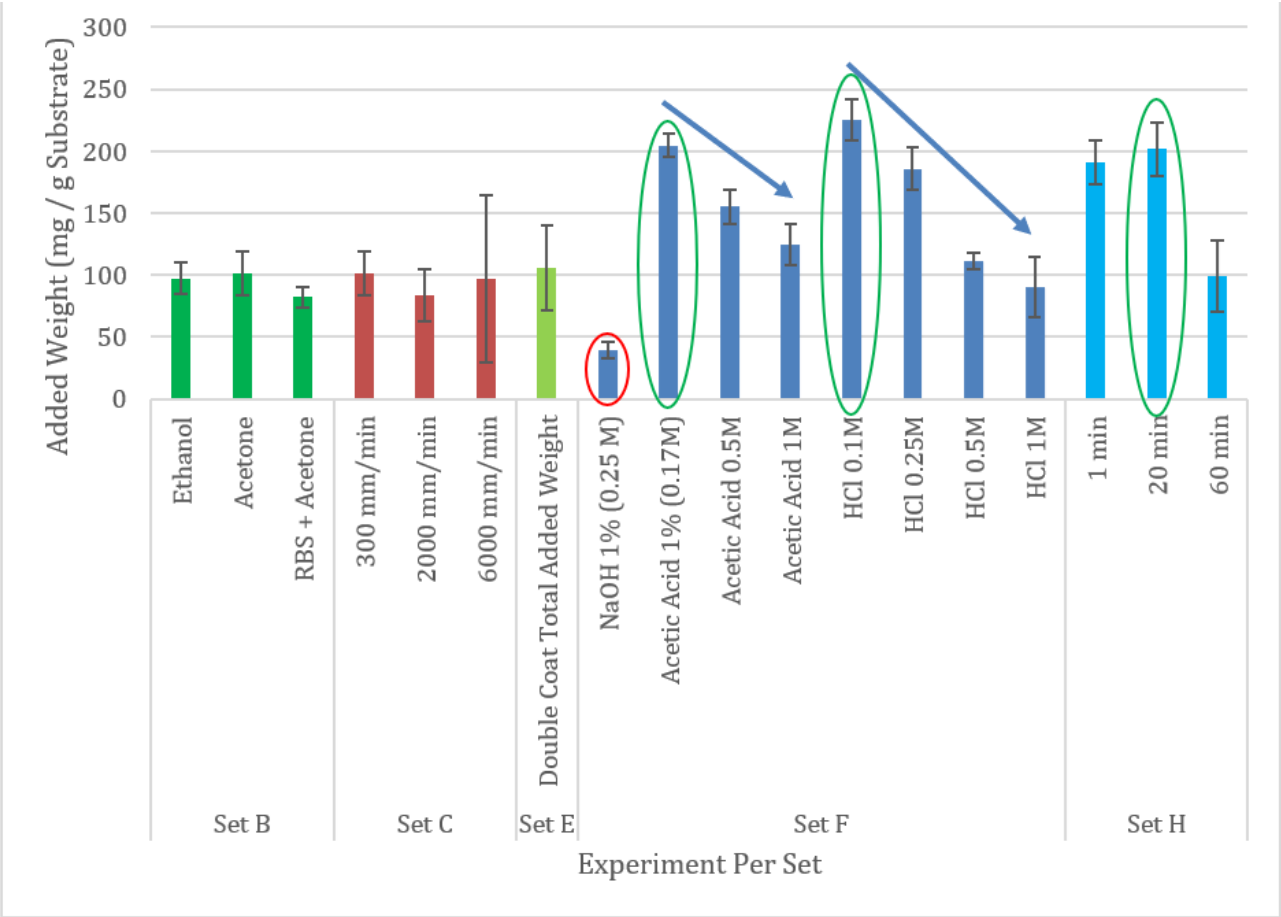

Figure 9: Comparison for the added weight of ZnO achieved in each of the experiments conducted for the polyol 30 g/L ZnO NP suspension in terms of mg of ZnO / g of substrate.

With regards to the standard deviations calculated for each of the experiments across all of the suspensions, there are no apparent patterns that can be observed.

After having collected the measured results for every set of experiments, normalizing the data and grouping it for a proper analysis, the maximum added weight of ZnO achieved out of all the experiments conducted for each of the three different ZnO suspensions was identified. This is shown in **Table 5.**

Table 5: Maximum added weight achieved for each of the ZnO NP suspensions with the respective experiment in which it was achieved.

	Maximum Added Weight Achieved per ZnO NP Suspension Type		
	Pepti 5 g/L	**Pepti 10 g/L**	**Polyol 30 g/L**
Most Successful Experiment	HCl 0.25 M Pretreatment + Triple Coat	HCl 0.25 M Pretreatment	HCl 0.1 M Pretreatment

Maximum Added Weight (mg)	14.37	6.29	17.1
Maximum Added Weight (mg/g substrate)	201.69	119.85	225.32
Standard Deviation (mg/g substrate)	27.79	11.93	16.76

3.3. SEM Imaging of the Coated Samples.

Representative samples of some of the experiments performed were selected to be characterized via SEM imaging. **Figure 10(a-i)** and **Figure 11(a-f)** display the images for each of the selected samples plus a blank sample of the nylon textile to use as a reference **(Figure 10a).** Specifically, **Figure 10(b-i)** display SEM images for samples from experimental **Set E** (paragraph **2.2.5**) - Double and Triple Coats, while **Figure 10(b-e)** show samples for experiments conducted using the pepti 5 g/L suspension in order of the increasing number of coats. **Figure 10(f-i)** show samples for experiments conducted using the polyol 30 g/L suspension at different levels of magnitude, starting with the single coat and followed by the double coat.

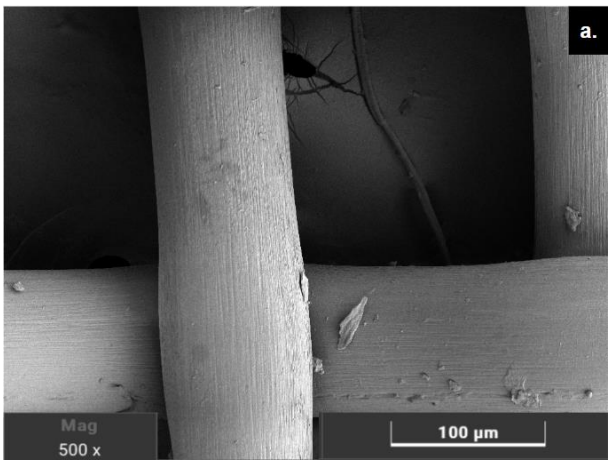

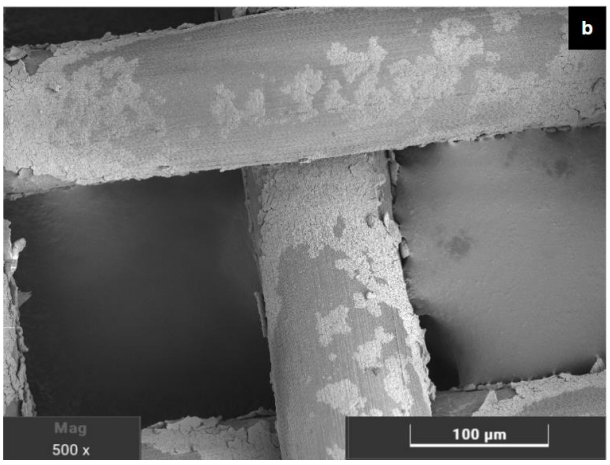

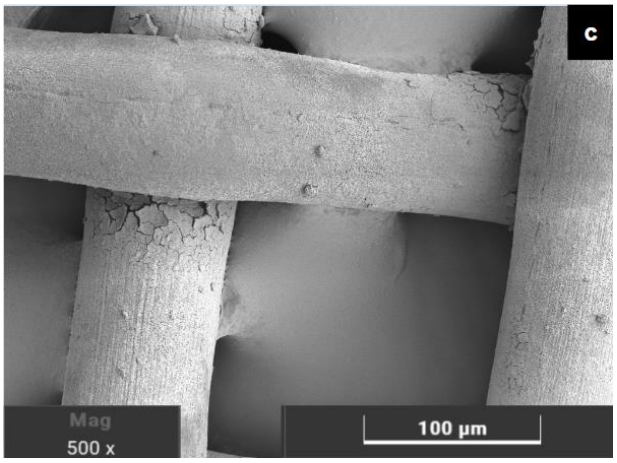
c
Mag
500 x
100 µm

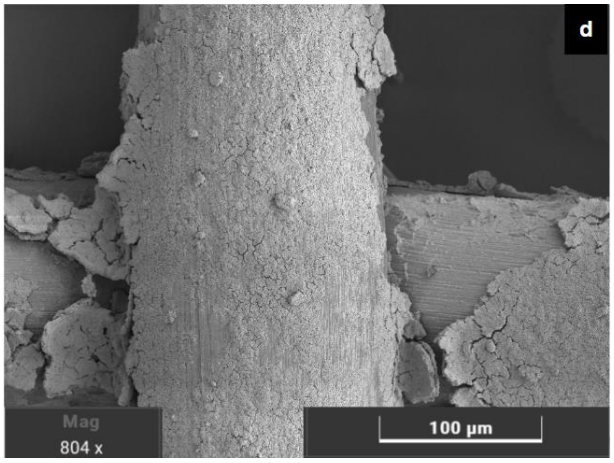
d
Mag
804 x
100 µm

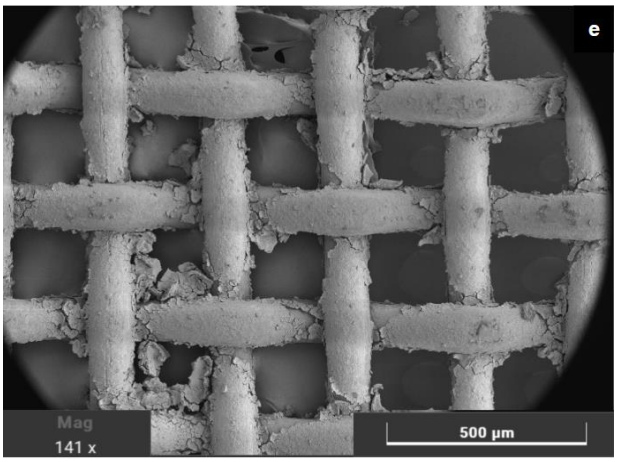
e
Mag
141 x
500 µm

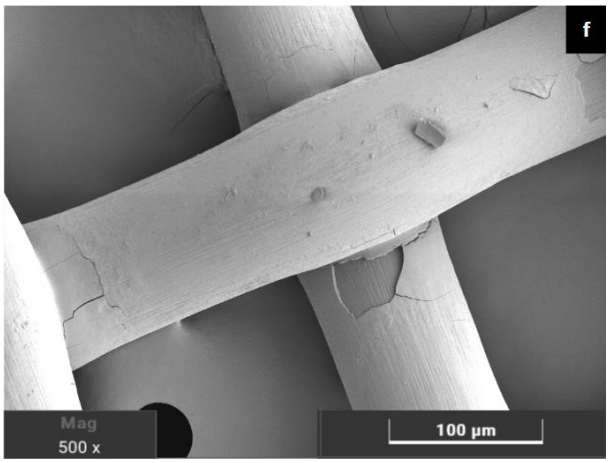
f
Mag
500 x
100 µm

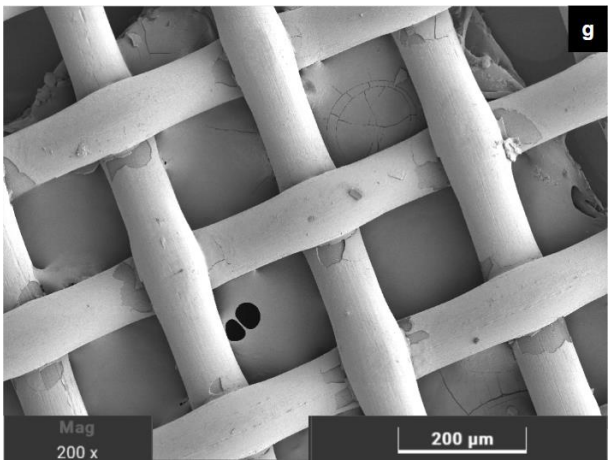
g
Mag
200 x
200 µm

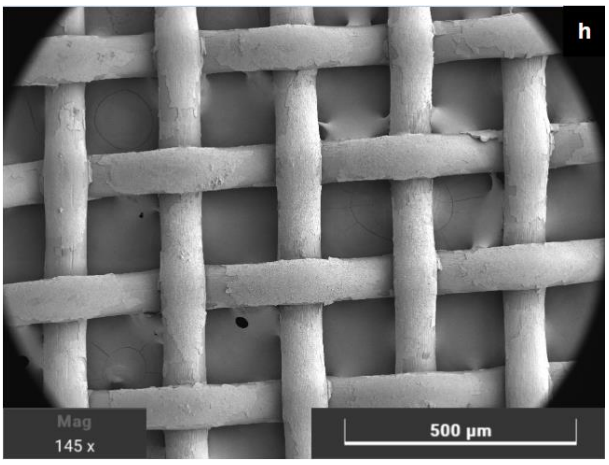
h
Mag
145 x
500 µm

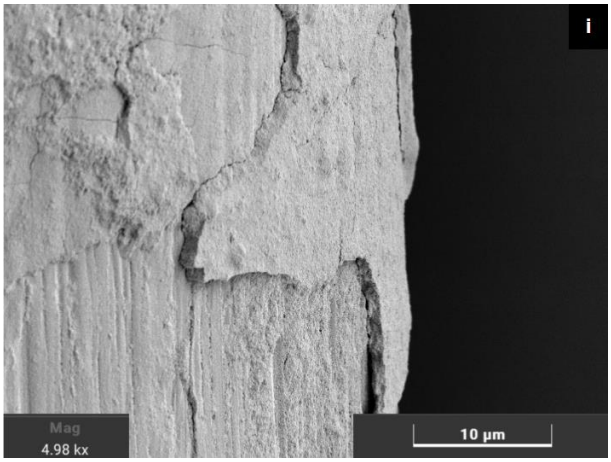

Figure 10: SEM images for selected samples from experimental **Set E (2.2.5). a)** Blank Substrate, **b)** Pepti 5 g/L - single coat, **c)** Pepti 5 g/L - double coat, **d)** Pepti 5 g/L - triple coat, experimental, **e)** Wide view of Pepti 5 g/L - triple coat, **f)** Polyol 30 g/L - single coat, **g)** Wide view Polyol 30 g/L – single coat **h)** Polyol 30 g/L double coat**, i)** Polyol 30 g/L double coat, Mag. 5K detail

On the other hand, **Figure 11(a-f)** show SEM images of selected samples from experimental **Set F** (paragraph **2.2.6**) - Acid and Basic Pretreatment and one sample corresponding to experimental **Set H** (paragraph **2.2.8**) - UVC surface activation. In this case, **Figure 11a** corresponds to HCl 0.1M acid pretreatment plus a pepti 10 g/L coating, **Figure 11b** and **11c** correspond to polyol 30 g/L coating and respective pretreatments with HCl 0.25 M and NaOH 0.25M. **Figure 11d, 11e** and **11f** show blank nylon pieces that have undergone Acetic Acid 0.5 M pretreatment, HCl 0.25 M pretreatment and UVC 20 min surface activation, respectively.

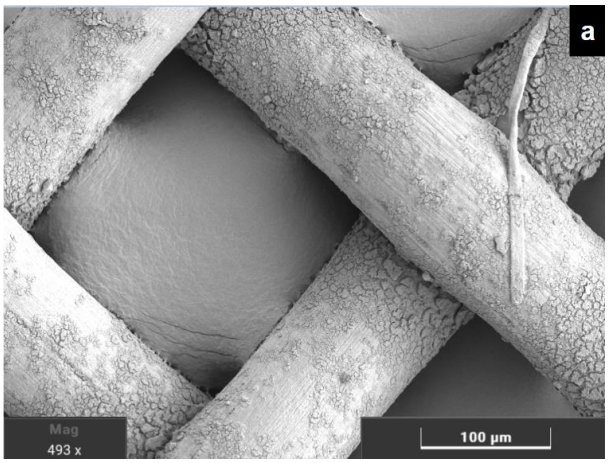

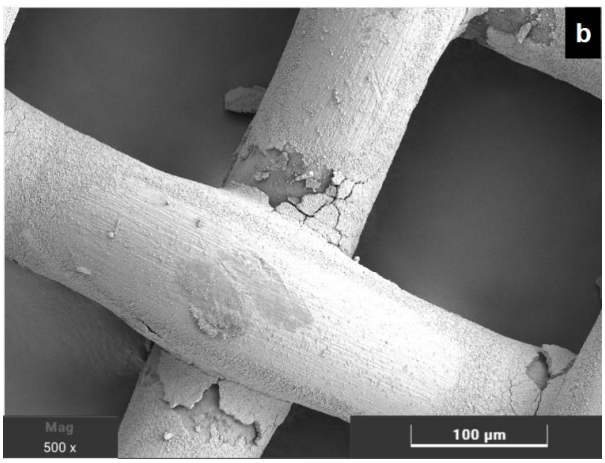

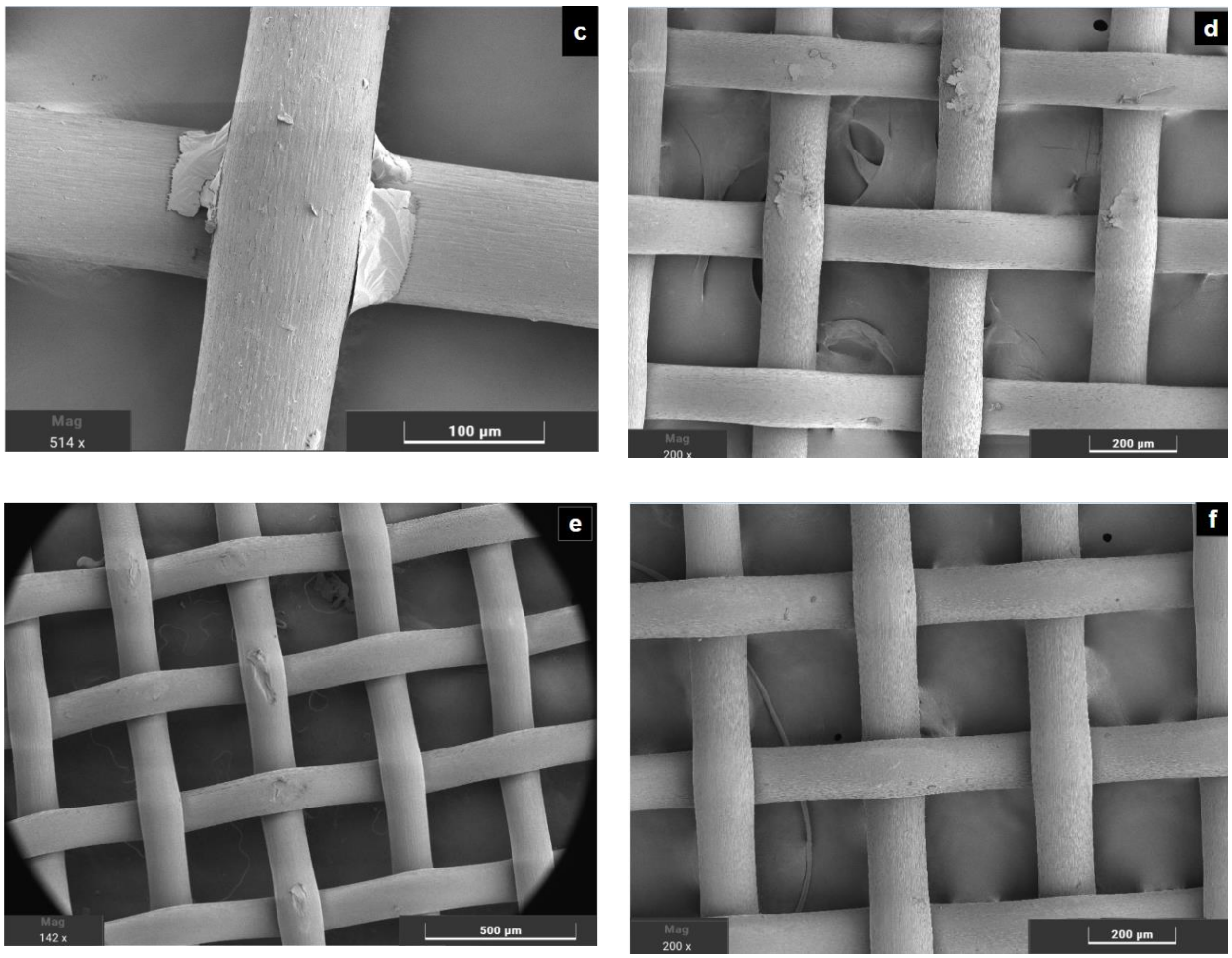

Figure 11: SEM images for selected samples from experimental **Set F** (**2.2.6**) and **Set G** (**2.2.7**). **a)** Pepti 10 g/L, HCl 0.1 M surface activation, **b)** Polyol 30 g/L, HCl 0.25 M surface activation, **c)** Polyol 30 g/L, NaOH 1% (0.25M) surface activation, **d)** Blank nylon after Acetic Acid 0.5 M surface activation, e) Blank nylon after HCl 0.25M surface activation, **f)** Blank nylon after UVC – 20 min surface activation.

3.4. Determination of the Composition of the Coated Samples.

Further characterization methods were performed on some of the samples, following the SEM imaging, in order to have confirmation that the substance that is being observed coating the substrate in **Figure 10(a-i) - Figure 11(a-f)** is in fact ZnO NPs, as is the goal of the project.

The image in **Figure 12a** is a close-up SE image of a blank sample of the uncoated nylon textile, as a base reference. The BSE images shown in **Figure 12b** and **Figure 12c** correspond to nylon samples coated by the pepti 5 g/L suspension (with a single coat and a triple coat respectively). Finally, **Figure 12d** shows a BSE image of a polyol 30 g/L single coat sample.

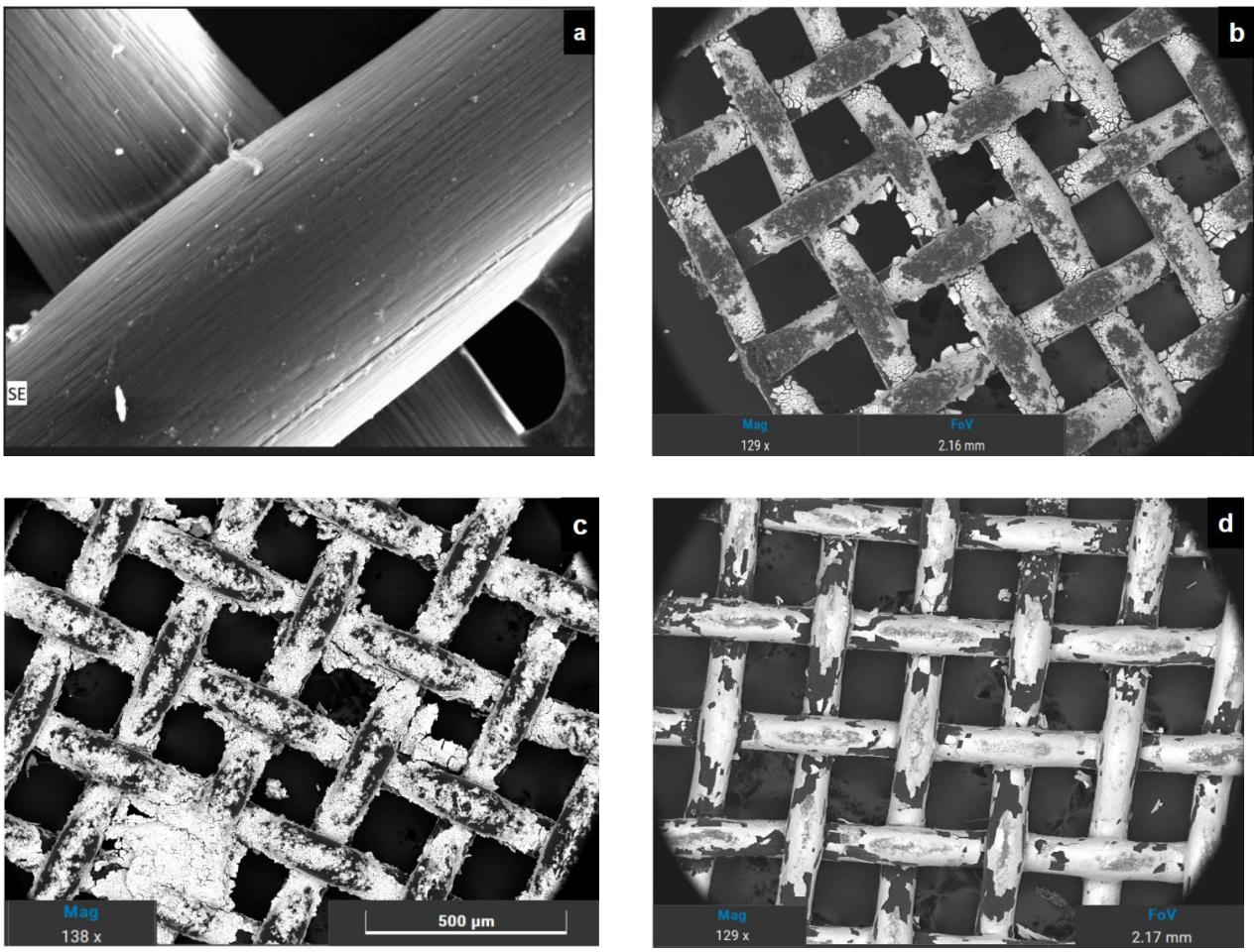

Figure 12: Backscattered and Secondary Electron images of the sampled nylon pieces: **a)** SE Image of a blank sample of the uncoated nylon**, b)** BSE image of the pepti 5g/L - Single Coat sample**, c)** BSE image of the pepti 5 g/L - Triple Coat sample, **d)** BSE image of the polyol 30 g/L – Single Coat sample

The EDX spectra corresponding to the SE and BSE images shown in **Figure 12a-d** are shown below in **Figure 13-Figure 15. Figure 13** shows the EDX spectrum obtained for the uncoated nylon textile, in which it can be seen that the material is mostly composed of carbon, with the presence of oxygen and nitrogen. This is consistent with the molecular composition of nylon 6 (polyamide). **Figure 14** shows the EDX for the sample of nylon triple coated with pepti 5 g/L suspension, without any previous surface pretreatment or activation of the textile. This EDX spectrum corresponds to the BSE image shown in **Figure 12c** and it is observed that there is a significant presence of zinc that was not observed in the blank nylon, as well as the presence of carbon and oxygen. Finally, **Figure 15** shows the EDX spectrum corresponding to the BSE image shown in **Figure 12d**, of a nylon piece coated by the polyol 30 g/L suspension, with a single coat and without any pretreatment or surface activation. Once again there are peaks that show a significant presence of carbon, oxygen and zinc, and nitrogen to a lesser extent.

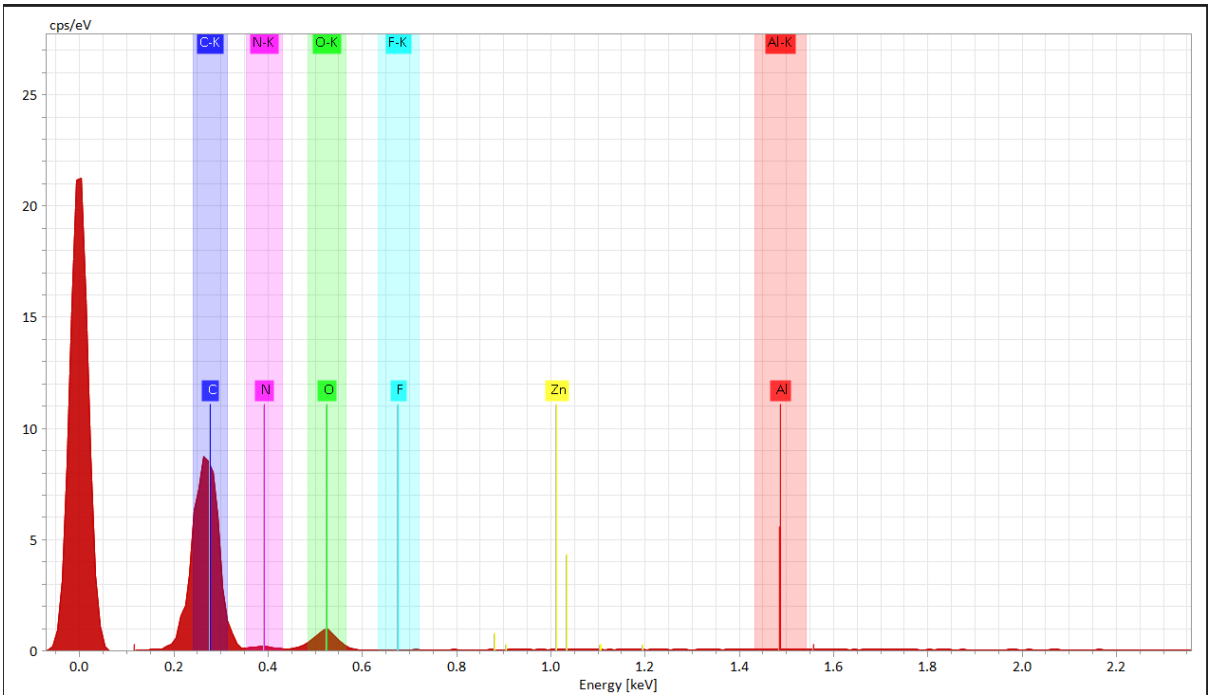

Figure 13: EDX spectrum for the uncoated nylon textile.

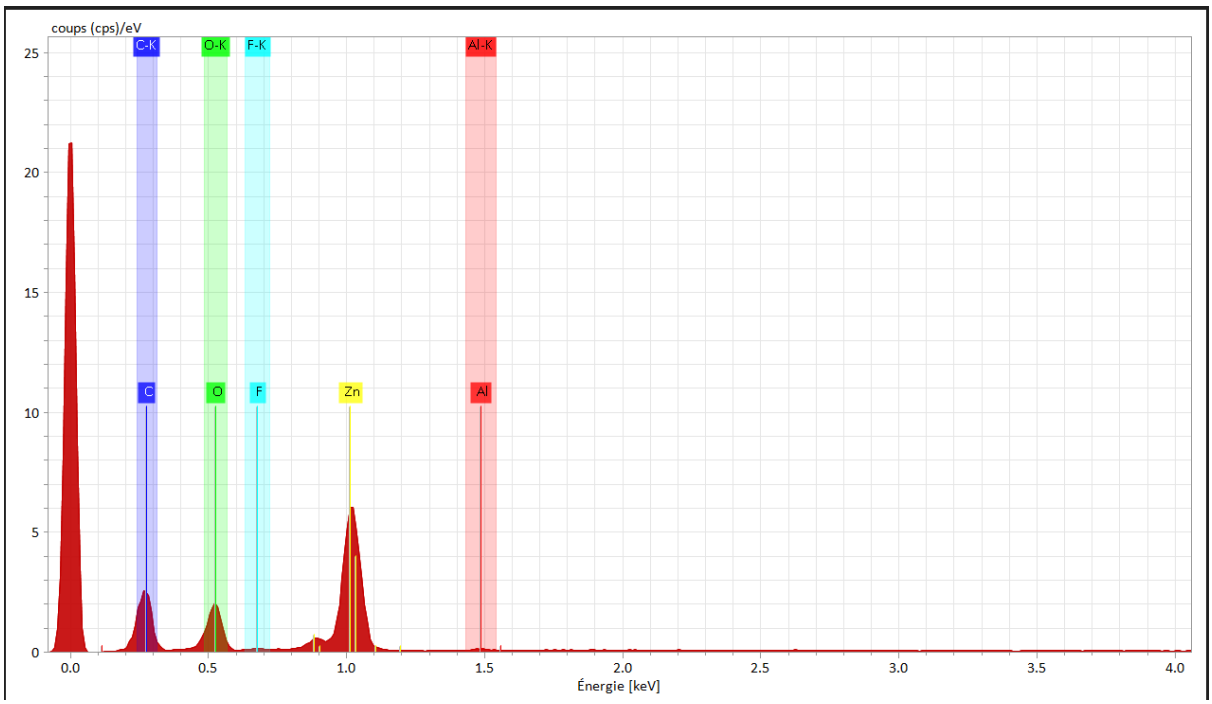

Figure 14: EDX Spectrum for the nylon piece coated by pepti 5 g/L - Triple coat. Without any previous surface activation of the textile.

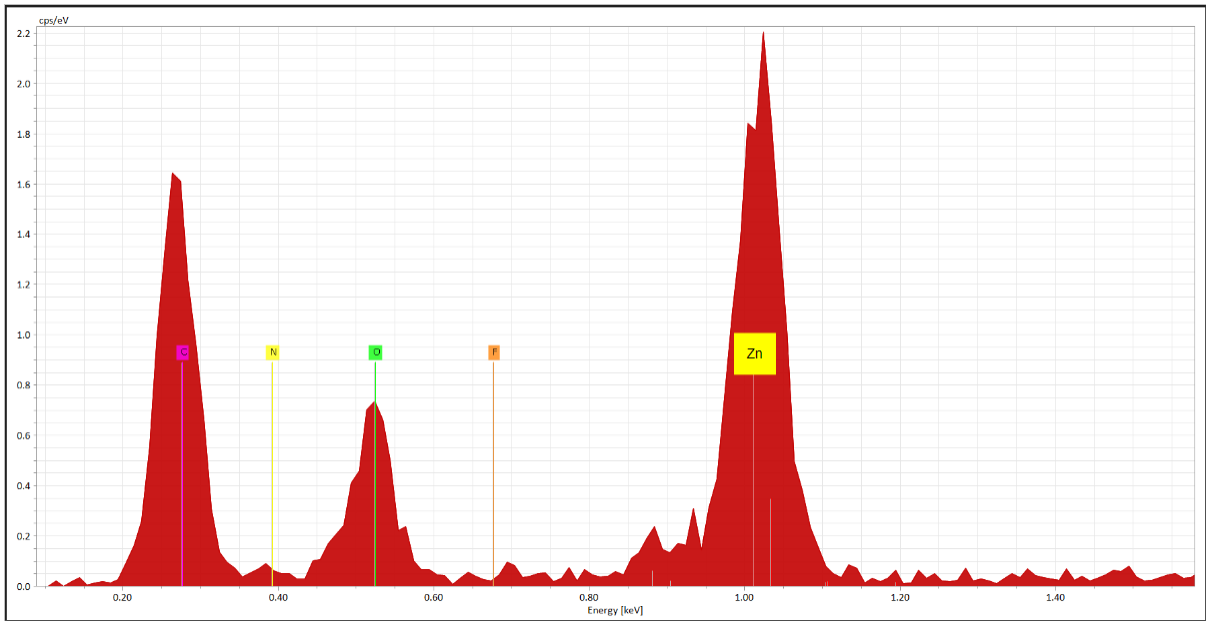

Figure 15: EDX Spectrum for the nylon piece coated by Polyol 30 g/L - Single coat. Without any previous surface activation of the textile.

3.5. Composition of Surface Groups Present on Pretreated, Un-Coated Samples.

Considering that the measurements of the post-coating and post-washing weights exhibited seemingly significant increases during the experiments involving chemical and physical activation of the nylon surfaces (those from experimental **Sets F, G** and **H** (paragraphs **2.2.6, 2.2.7** and **2.2.8**) with respect to those obtained in previous experimental sets, an additional step was taken to characterize these samples. The objective was to identify potential explanations for the observed behavior of the ZnO NPs coats achieved on the modified nylon textiles.

FTIR characterizations were conducted on a set of surface activated, yet un-coated, samples of nylon textile, in order to identify any significant changes in its chemical structure that might give some explanation for the behavior of the ZnO NPs added coating in each instance. The following are the nylon samples that were characterized using FTIR:

Table 6: List of the surface activated, un-coated nylon textile samples.

Nylon Textile Samples Characterized using FTIR
Blank (Nylon textile with no surface activation/pretreatment)
Nylon pretreated with NaOH 1% (0.25 M)
Nylon pretreated with acetic acid (0.5 M)

Nylon pretreated with HCl (0.25 M)
Nylon surface activated by UVC (20 min exposure)

The purpose of these characterizations was to identify any significant differences between the measured absorbance spectrum of the blank nylon textile and the nylon textiles pretreated/activated by the different chemical and physical processes presented in the methodology. The differences in the absorbance spectra might indicate a change in the chemical structure of the nylon caused by the surface pretreatment/activation techniques which in turn might have affected, either in a positive or a negative way, the ZnO NPs coating process on the substrate.

The following graphs **(Figure 16-Figure 19)** show the absorbance spectra measured via FTIR of each of the treated/activated samples compared against the spectrum of the blank nylon sample (which is shown in blue in each of the graphs).

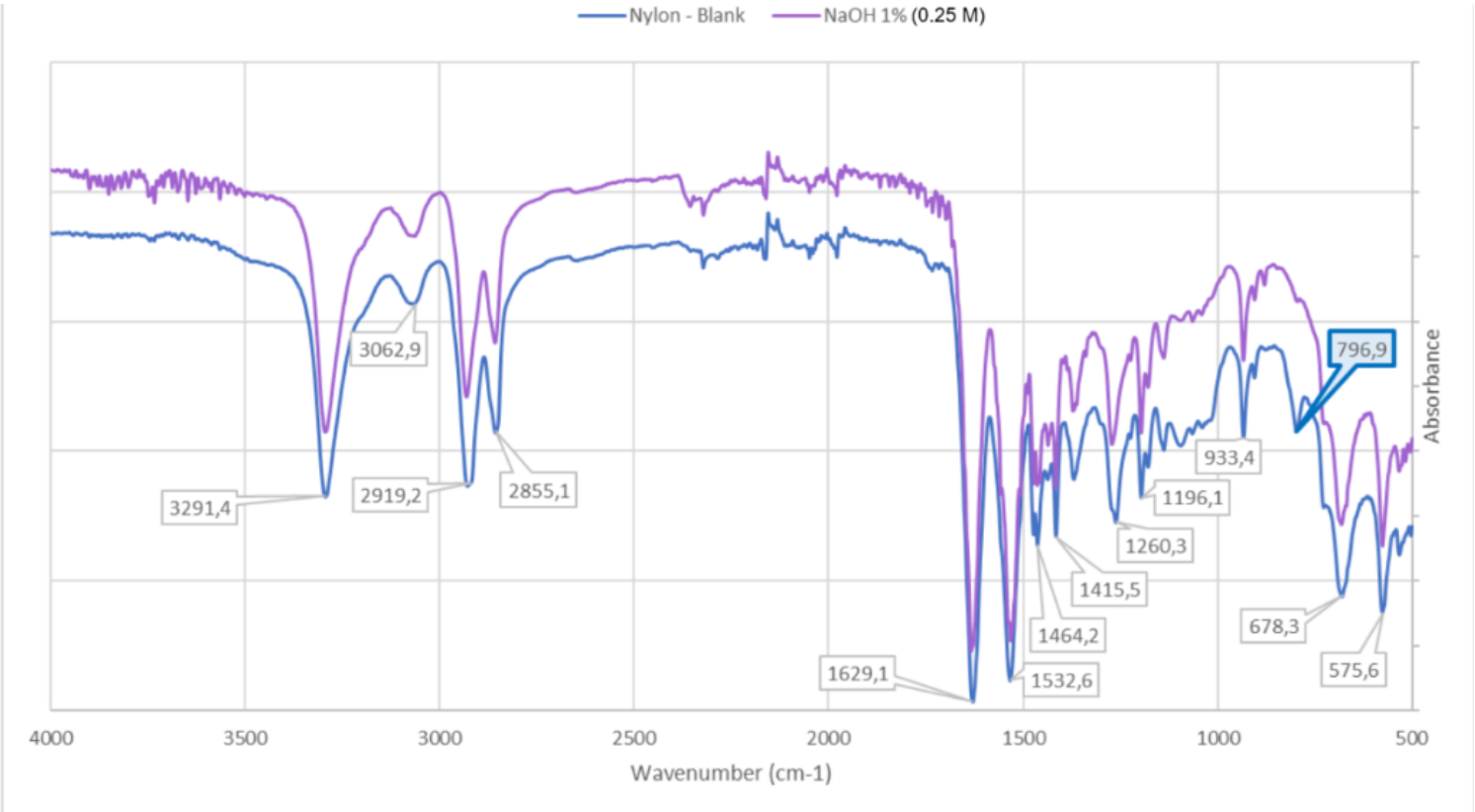

Figure 16: FTIR spectrum of the NaOH (0.25 M) pretreated nylon vs the blank.

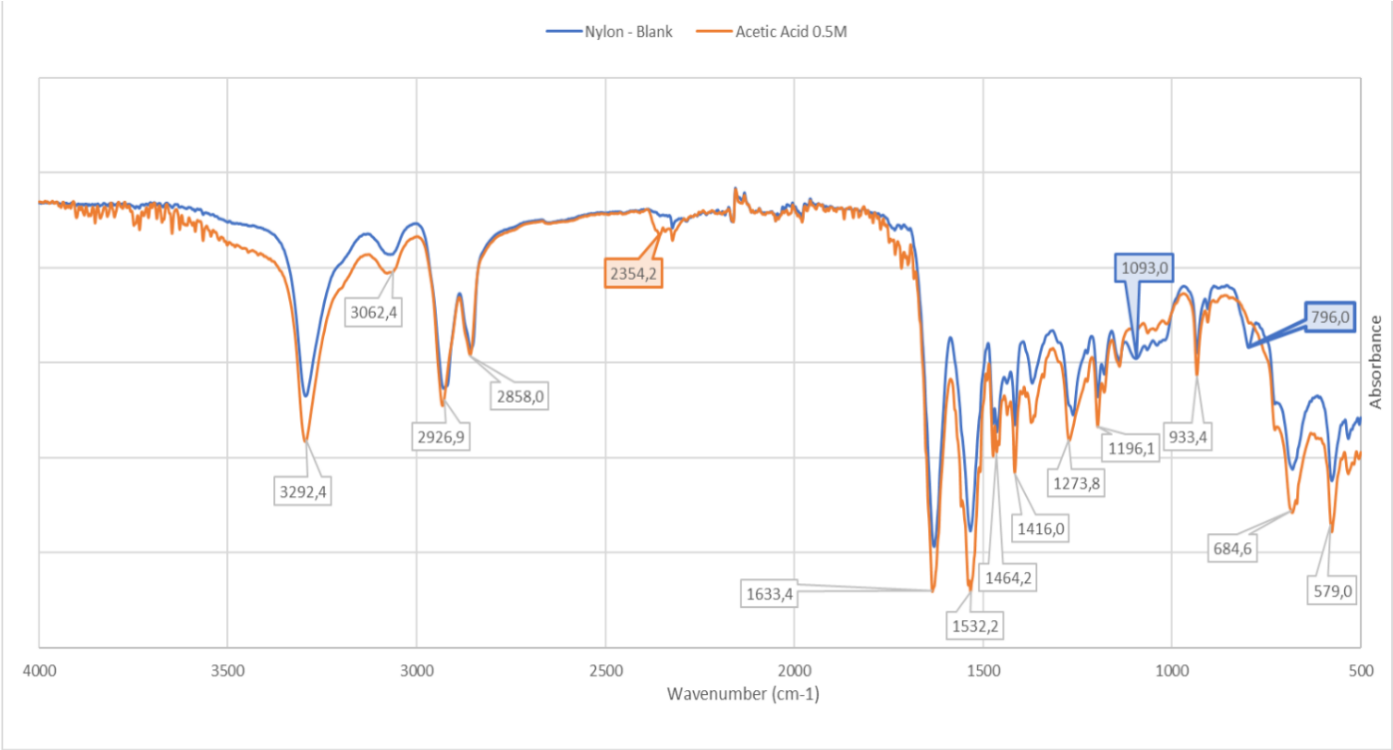

Figure 17: FTIR Spectrum of the Acetic Acid 0.5 M Pretreated Nylon vs the Blank.

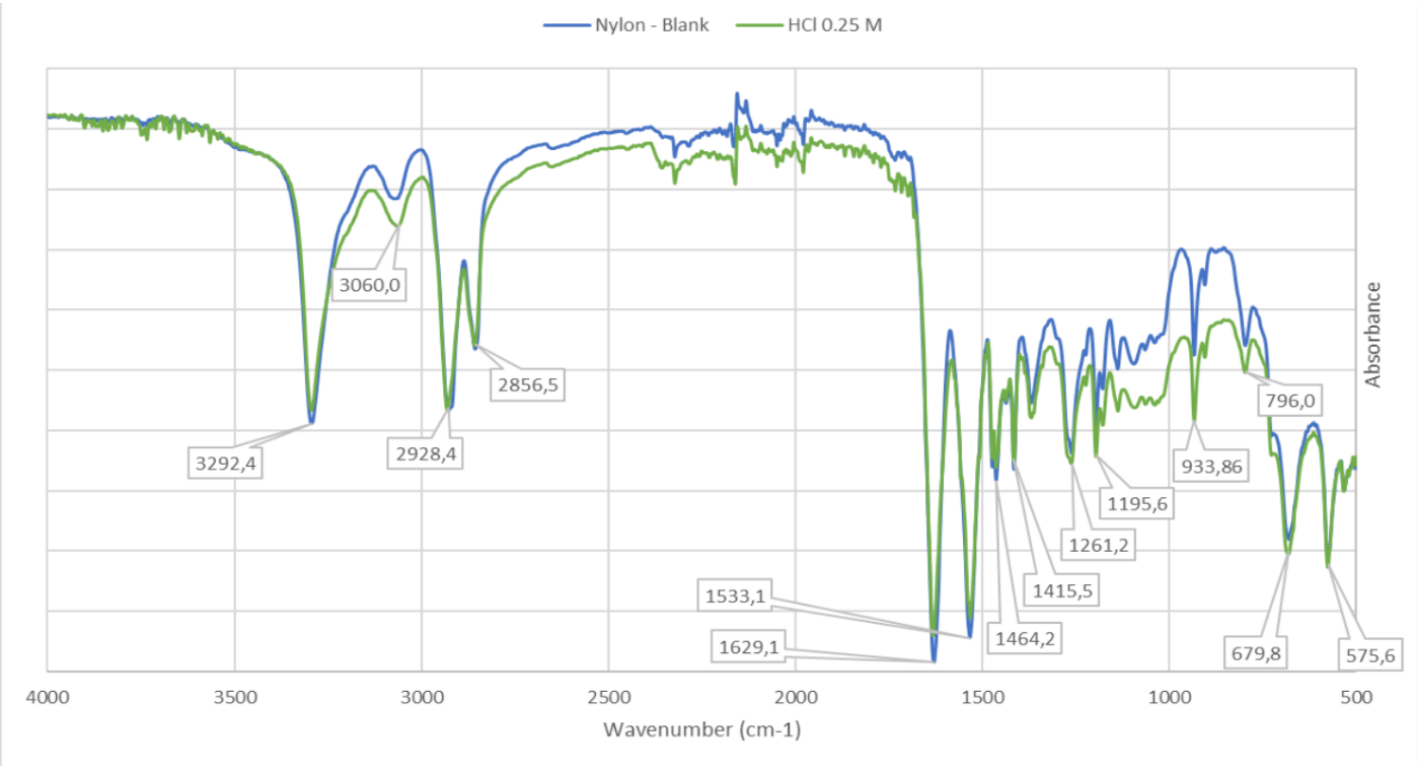

Figure 18: FTIR Spectrum of the HCl 0.25 M Pretreated Nylon vs the Blank.

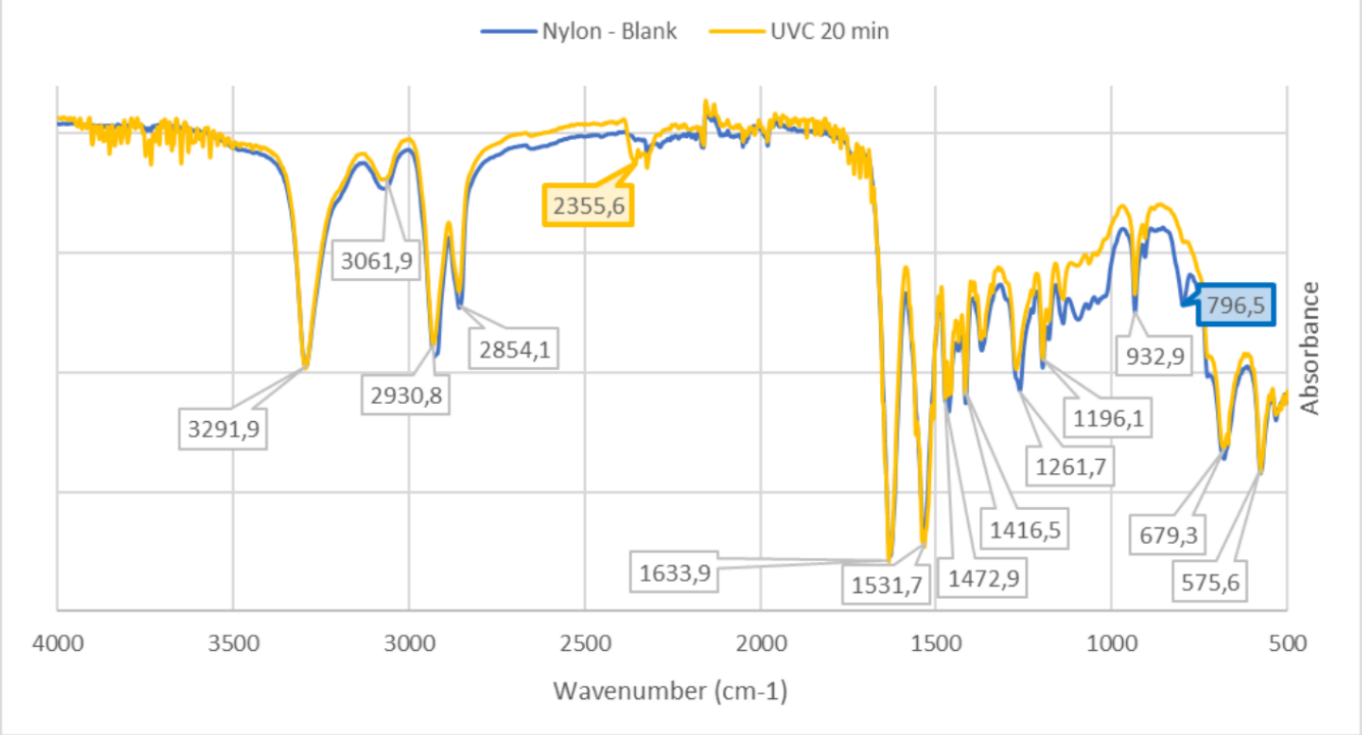

Figure 19: FTIR Spectrum of the UVC Activated (20 min exposure) Nylon vs the Blank.

For analysis purposes, **Figure 20** below is taken as a reference for an FTIR spectrum for nylon, unaltered by any chemical or physical processes and **Table 7** outlines the characteristic bond vibrations attributed to the nylon 6 (polyamide 6) molecule, with their respective wavenumbers at which the peaks of the spectrum appear.

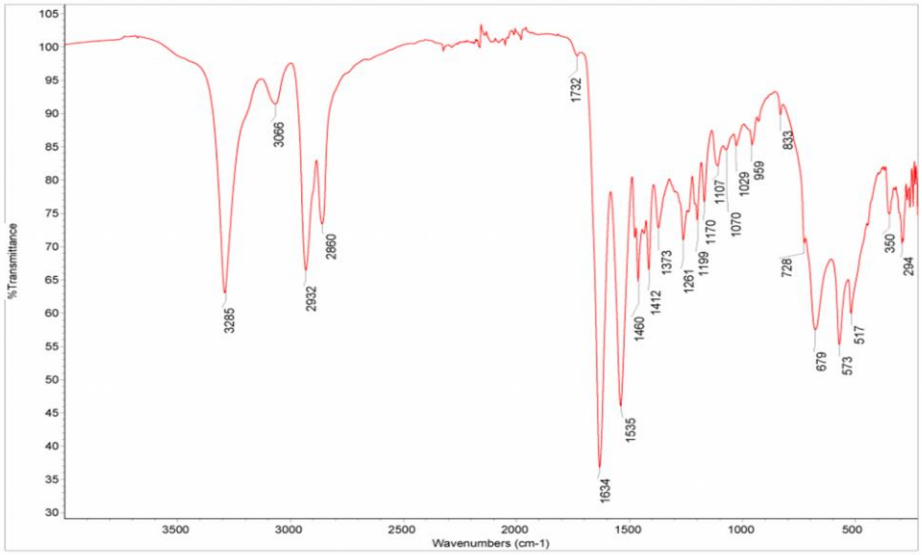

Figure 20: Reference FTIR Spectrum of nylon (Database of ATR-FT-IR Spectra of Various Materials, 2023).

Table 7: Characteristic FTIR Spectrum Peaks for Nylon and the corresponding bonds (Veerasingam et al., 2020).

Wavenumber (cm^{-1})	Bond Assignment
3298	N - H Stretching
2932	CH Stretching
2858	CH Stretching
1634	C = O Stretching
1538	NH bending, C - N Stretching
1464	CH Bending
1372	CH Bending
1274	NH bending, C - N Stretching
1199	CH Bending
687	NH Bending, C = O Bending

3.6. NBT Degradation Activity of Samples, in the Dark.

As described in the methodology section (section **2.4**), the NBT degradation test was carried out by measuring the absorbance of NBT solutions after being in contact with each of the coated nylon samples for 48 h, under dark conditions. The NBT solution was made at a concentration of 0.05 mMol and the amount of solution added to each test tube was sufficient to ensure a concentration of 10 g/L of ZnO, in relation to the NBT solution. The test was done for samples of coating done with the pepti synthesized ZnO NPs as well as the polyol synthesized NPs. The results are shown below in **Table 8a** and **Table 8b:**

Table 8a-b: Description of the samples, **a)** Pepti 10 g/L and **b)** Polyol 30 g/L, for the NBT degradation test with their corresponding values for added weight achieved and relative decrease in measured absorbance (%).

Pepti 10 g/L		
Description	**Added Weight Measured (mg)**	**Relative Decrease in Measured Absorbance (%)**
Triple Coat (5 g/L)	15,6	10%

Acetic Acid 0.5M Single Coat	9,71	25%
HCl 0.25 M Single Coat	16,64	25%
UVC 60 min	6,49	29%

Polyol 30 g/L		
Description	**Added Weight Measured (mg)**	**Relative Decrease in Measured Absorbance (%)**
Single Coat	8	1%
Acetic Acid 1%	15,81	26%
HCl 0.1M	18,64	24%
UVC 60 min	16,02	27%

4. DISCUSSION

Given that the objective of this project is the development of functionalized antibacterial filters for industrial water treatments using a specific nylon fabric as the substrate and coating it with pepti and polyol synthesized ZnO NPs via dip-coating, the measurements and tests carried out during the development of the experiments were geared towards determining:

1. The specific set of experimental conditions and techniques that result in the larger amount of ZnO NPs adhering to the substrate.

2. Whether the resulting nylon textiles coated with ZnO exhibit the formation of ROS in the dark and thus, are able to display antibacterial activity in the dark.

This section will be dedicated to analyzing all of the relevant data and results obtained from the series of experiments and characterizations that were carried out during the development of this thesis, to ultimately conclude on the nature of the synthesized ZnO NPs, the effectiveness of the coating processes and the antibacterial functionalization of the textile.

4.1. Characterization and crystallite size of the synthesized NPs.

The first set of data and results that will be analyzed and discussed is the characterization and analysis of the ZnO NPs powders that had been synthesized through the pepti and polyol pathways. The results for the synthesis processes of the ZnO set the basis for the development of the rest of the experiments and thus, the subsequent results.This is due to the fact that, as was mentioned in the introduction section, the particle size, dispersion and NP morphology are all factors that have an influence over the desired properties of the nanomaterial.

The XRD analyses were performed on the NPs powders (as explained in **Section 3.1** and shown in **Figure 4**) with the aim of validating that the NPs that were synthesized through the pepti and polyol methods and which were being seen through the TEM imaging (shown in **Figure 5a and 5b**) were in fact ZnO NPs. In order to validate this, a known XRD pattern for this material was taken from the literature as a reference (**Figure 21b** shown below). Since the XRD pattern is particular to each specific substance and can in fact be considered as a fingerprint for that substance, the comparison between the obtained XRD results and the reference will confirm the nature of the substance being analyzed (Henry & Mogk, 2023). According to Rajan *et al* (2023), the authors of the study from which the XRD pattern for ZnO was referenced, their results match satisfactorily with the XRD data from

JCPDS (the Joint Committee on Powder Diffraction Standards) File number 36-1451 for ZnO. This gives a good indication that the XRD pattern being referenced is reliable.

When observing side by side the diffractograms obtained for this work and the diffractogram referenced from Rajan *et al's* work (2023), (**Figure 21a**), it can be seen that in fact, the materials synthesized through both the pepti and the polyol pathways, present characteristic peaks at the angles corresponding to the ZnO fingerprint, specifically at around 31º (100), 35º (002) and 36º (101). This indicates that the NPs that have been synthesized through both methods are in fact ZnO.

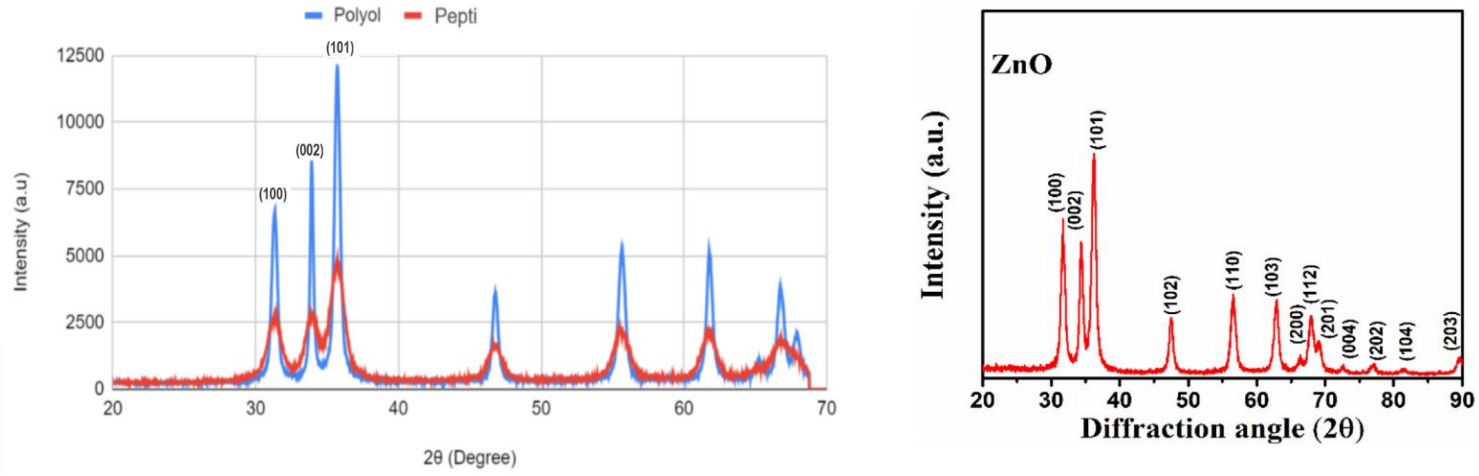

Figure 21: Comparison between the **(a)** diffractograms of the synthesized NPs and **(b)** the ZnO reference XRD diffractogram (Rajan et al., 2023).

On the other hand, it is observed that the peaks that were measured for the polyol synthesized NPs (shown in blue in **Figure 21a**) were notably higher than those obtained for the pepti synthesized NPs (shown in red in **Figure 21a**). This could be due to a larger quantity of sample being measured or due to a better dispersion of the crystallites across the polyol sample, which leads to more X-rays being reflected (Speakmen, 2020). Both of these explanations can be qualitatively supported by what is observed in the TEM images shown in **Figure 5.**

The Scherrer equation, shown in the equation (9) (Monshi *et al*., 2022) was applied using the XRD data in order to calculate the crystallite size for the pepti and the polyol synthesized ZnO NPs.

$$D = \frac{K\lambda}{\beta cos\theta} \qquad (9)$$

where:

- D is the diameter of the crystallite in nm
- K is the Scherrer constant, taken as 0.9

- $\boldsymbol{\lambda}$ is the X-ray wavelength (0.15405 nm)
- $\boldsymbol{\beta}$ is the full width at half maximum (FWHM) of the XRD spectrum peaks (rad)
- $\boldsymbol{\theta}$ is the angles at which the peaks are located in the spectrum ($\frac{2\theta}{2}$)

The diameters were calculated for each peak obtained in each of the spectrums and an average was obtained: 6.25 nm for the pepti ZnO NP crystallites and 17.33 nm for the polyol ZnO NP crystallites. This means that the polyol synthesized NPs formed on average crystallites up to 3 times larger than those formed by the pepti synthesized ZnO NPs. Based on what was described in **section 1.2.1** of the introduction, this difference in average crystallite size might have an effect on the antibacterial performance of these NPs, since, it has been found that antibacterial activity is inversely related to particle size. However, it is worth keeping in mind the findings of Adams *et al* (2006) which state that between ZnO NPs suspensions with small particle size and suspensions that presented aggregation of the nanoparticles, which had the same concentrations, similar antibacterial activity was observed.

From the TEM images (**Figure 5a**) it is observed that the morphology of the pepti ZnO NPs appears to be spherical, though the particles present a significant level of agglomeration. An image processing tool (ImageJ, 2012) was used to make approximate conclusions with regards to the NPs morphology and particle size. From the observations done using this program, it could be confirmed that the general morphology of the pepti ZnO NPs was in fact spherical, and an estimate of the average particle was calculated to be around 5 nm. However, no detailed calculations on the particle size distribution were carried out.

Similarly, when analyzing the TEM image (**Figure 5b**) for the polyol synthesized ZnO NPs, it is obsverved that the morphology is either spherical or of oblong nanorods. These NPs however, seem to present a much more homogeneous particle dispersion from what can be observed in the TEM image, with notably less agglomeration taking place. When using the ImageJ tool, it could be estimated that the average particle size for these polyol NPs was larger, at around 15 nm. These values, though less accurate, reflect the values calculated previously through the Scherrer equation.

The results for the estimated particle sizes of both types of ZnO NPs that were synthesized coincide with what is reported by Shamhari *et al* (2018) and Alves *et al* (2018). The fact that the polyol NPs present a higher and more homogenous dispersion also coincides with what is reported by Alves *et al* (2018) with respect to DEG being a good stabilizing agent. The fact that the morphology of the NPs is seen to be spherical and rod-like can be considered advantageous for the purposes of this project, given that it has been noted in the literature that these morphologies are favorable for

achieved effective antibacterial properties in the ZnO NPs (Verbic *et al*., 2019), (Da Silva *et al.,* 2023).

In their study, Rajan *et al* (2023), who synthesized their ZnO NPs through a precipitation method, using $ZnCl_2$ as a precursor, calculated the ZnO NPs particle sizes from their XRD data and reported an average particle size of 13 nm. This is in line with the general scale of sizes that has been discussed throughout the report, specifically those obtained for the polyol synthesized ZnO NPs, including the approximate sizes obtained through the ImageJ processing of the TEM images and the average size calculated from the XRD data using the Scherrer equation.

With regards to the qualitative observations made on the precipitation times of the pepti 10g/L and the polyol 30 g/L ZnO NPs suspensions (shown in **Figure 6**) it was observed that between the two, the polyol synthesized NPs lasted suspension homogeneously for longer than the pepti synthesized NPs before precipitating. While the polyol suspension could remain dispersed for almost 24 h after it was first made, the pepti suspension started precipitating within 6 h. This is another observation that aligns with what is observed in the TEM images and presents more evidence to support the claim that the pepti ZnO NPs present a higher level of agglomeration than the polyol synthesized ones, which have a high and relatively homogeneous dispersion. However, it is important to note that since the suspensions that are being used do not have the same concentrations, conclusions on their particle dispersion stability as well as comparisons in their coating performance will not be fully reliable.

Ultimately, the synthesized NPs using both the pepti and the polyol pathways were concluded to in fact be ZnO, the particle sizes calculated for each type of NPs fall within the expected orders of magnitude and ranges. It is possible to speculate that, due to the spherical and rod-like morphologies of the crystallites, these ZnO NPs will be effective in achieving the intended antibacterial functionalization of the textiles, based on what has been stated in previous literature.

4.2. Achieved coatings based on the added weight results.

The next set of results that were presented were those pertaining to the added weight measurements for the dip-coating experiments. As was mentioned in **section 3.2**, the results from these measurements are the main focus of the objectives of this thesis, since the ultimate goal is to achieve the highest amount of ZnO NP coating on the nylon substrate. The reason for this is because having the highest amount of ZnO NPs possible adhered to the nylon textile will help increase efficiency of the functionalized property and the lifespan of the functionalized textile.

The diagram below (**Figure 22**) is a representation of the general principle of the dip-coating process that was done for every experiment that was carried out, as described in the methodology **Section 2.2** and listed in **Table A - 1:** Complete List of the Dip-Coating Experiments.

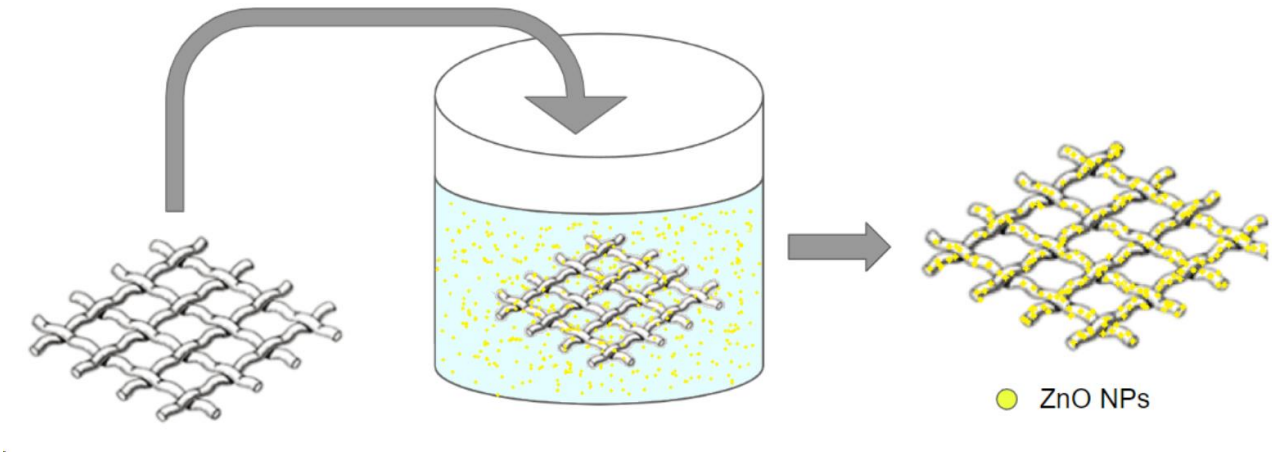

Figure 22: Schematic representation of the general principle applied during the dip-coating processes.

As was described in **section 3.2**, the values from the added weight measurements were normalized to a unit of mg of ZnO / g of nylon to make them comparable, and a statistical significance analysis performed in order to have a solid basis as to whether the different added weights achieved were significantly different and be able to conclude as to whether the different variables being evaluated in the experiments had a direct, significant effect on these results.

From the results obtained for experimental **Sets A-E** (paragraphs **2.2.1 - 2.2.5**)**,** meaning the experimental sets in which the nylon textiles did not undergo any additional chemical pretreatment or physical surface activate, the average added weights post wash achieved ranged from 2.48 - 8.53 mg (14.03 - 106 mg of ZnO / g of nylon). Comparatively, Fiedot-Tobola *et al* (2018) achieved an added weight of 6.3 ± 0.2 mg on nylon pieces with an area of 100 cm^2 (which comes up to around 8.75 mg of ZnO / g of nylon). This could be considered as a good indication that the dip-coating method is an effective technique for achieving a significant coating of the textile, given that while Fiedot-Tobola *et al* used hydrothermal deposition for their coating experiments, similar results were achieved in this thesis using the dip-coating technique. As far as could be seen, Fiedot-Tobola's study is the only study that could be used as a reference for these results since their study is the only one that was found to be attempting to coat a nylon 6 textile with ZnO NPs and reporting the added weight.

Experimental **Sets A – E** (paragraphs **2.2.1 - 2.2.5**) mainly dealt with the operating parameters of the dip-coater itself and with other variables that did not have a direct influence on the substrate's molecular structure, such as the washing agent used to clean the nylon before coating, the type of

ZnO NPs (based on the synthesis pathways) and the concentration of the suspensions. From the data obtained through the statistical analyses (***Table A - 12***) it is observed that most of the variables that were considered during the development of these sets of experiments, did not have a significant effect on the differences of the added weight measurements. Meaning that across the variables that were considered in those initial experiments, (the duration of the dipping time, the nature of the washing agents, the speed-up setting on the dip-coater and the comparison of the performance between the different types and concentrations of the ZnO NPs suspensions and the number of coats applied); most of these variables did not affect the coating performance in a statistically significant way (based on the t-student evaluation).

In the observation of the results obtained across experimental **Sets A – E** (paragraphs **2.2.1 - 2.2.5**), there were only two instances in which a difference in the weights achieved presented a statistical significance, these were firstly in the comparison between the added weights achieved using the pepti 10 g/L suspension vs the polyol 30 g/L suspension and secondly, the comparison between the total added weight achieved when applying a triple coat using the pepti 5 g/L vs the added weights achieved for the double coats applied using the pepti 10 g/L and the polyol 30 g/L suspensions.

These observations would indicate that, on the first hand, none of the general process and operating parameters, such as the exit speed of the substrate from the suspension, the time the substrate remains submerged in the suspension, or the washing agent used to clean the substrate, had any notable effect on the outcome of the added weights. Considering that the objective of adding a washing step to the general dip-coating process was to eliminate any impurities, to prevent them from altering the process in any way, this lack of statistical significance of the effect of the washing agents on the achieved added weights could be seen as a positive result. This is because it would mean that when considering the scaling up of this process, the washing agent used can be chosen under criteria such as affordability or safety, rather than its effect on the coating process itself.

On the other hand, the type of suspension and the concentration of the suspension did make a significant difference. The results for the average added weights achieved using the polyol suspension resulted in more than 1.5 or even 2 times the added weights achieved when using the pepti 10 g/L ZnO NPs suspension. A possible explanation for this is the particle dispersion of the suspensions; the polyol synthesized ZnO NPs clearly present a higher dispersion and more homogeneous suspension while the pepti synthesized NPs present a notable agglomeration of the particles, as seen in the TEM images of the powders (**Figure 5**) and the qualitative observations of the suspensions, previously described (**Figure 6**). This proposed explanation for the difference in the added weights achieved using the different types of ZnO NPs suspensions implies that, the more highly dispersed the NPs are in the suspension, the more easily they will be able to make contact

with the nylon surface and create a bond and the more NPs will adhere to the surface. The SEM images obtained for these experiments (**Figure 10** and **Figure 11**) could support this hypothesis, given that there is a distinct difference that can be observed between the coats from the pepti suspensions and the polyol suspensions. While the pepti NPs coated nylon pieces appeared to be covered in flakes, the polyol covered nylon appears to be covered by a homogeneous coat, like what would be observed with a paint coat.

The difference in the concentrations of the suspensions was tested between the pepti 10 g/L and the pepti 5 g/L suspensions, during experimental **Set D** (paragraph **2.2.4**). The added weight achieved when using the 10 g/L suspension (60.96 mg of ZnO / g of nylon) was almost twice as much as the added weight achieved when using the 5 g/L suspension (32.86 mg of ZnO / g of nylon). However, the added weight value achieved with the application of the first coat using the pepti 5 g/L suspension in experimental **Set E** (paragraph **2.2.5**) (Double and Triple coats) was 74.8 mg of ZnO/g of nylon, which would negate the results for experimental **Set D**. Considering this, it could be concluded that with regards to the suspension's effect on the efficiency of the coating process, a high particle dispersion would appear to increase the chances of creating a successful coat. The importance of concentration can be supported by the fact that the polyol suspension has a concentration 3 and 6 times higher than the other two suspensions (pepti 5 g/L and pepti 10 g/L). This last conclusion however, cannot be considered decisive, since there is not enough evidence to support the hypothesis that concentration is a determining factor in achieving a high amount of adhered coat due to the results of added weights achieved by the pepti 10 g/L vs the pepti 5 g/L suspensions.

It is important to note that no experiments were carried out comparing both types of synthesized NPs (pepti and polyol) in suspensions that had the same concentrations. Meaning that even though the hypothesis of the effect of the particle dispersion from the polyol suspension leading to a significantly higher achieved coating can be plausible, there is no guarantee that the decisive factor in this difference is the type of ZnO NPs. It would be relevant to conduct further work in the future, in which the performance of the pepti suspension and the polyol suspension with regards to the added weight measurements be compared across several experiments in which both suspensions have the same concentrations.

The final analysis that can be made with respect to the added weight results for these initial experimental sets is with regards to the results obtained for experimental **Set E**. The first piece of data that is immediately noticeable is the fact that the total added weight achieved from the three coats of pepti 5 g/L suspension was 16.46 mg (192.8 mg of ZnO / g of nylon) which is by far the highest weight achieved out of all of the experiments considered so far. When looking at the SEM

image of this triple coated nylon (**Figure 10e**), it can be seen that the particles have adhered on top of each other, in similar flakes as those observed for the single (**Figure 10c**) and double (**Figure 10d**) coats, even to the point of covering holes of the nylon mesh. This would indicate that the ZnO NPs of the latter coats are not in fact bonded to the nylon's surface but to each other. This is a plausible explanation given the fact that ZnO molecules are polar, and hence, are able to create dipole-dipole bonds between the oxygen and the zinc atoms of each molecule.

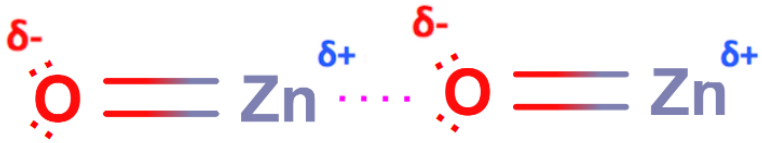

Figure 23: Molecular representation of the dipole-dipole bond between ZnO NPs[1].

In a sense, this could prove detrimental to the ultimate application of the functionalized textile, given that for the application it is necessary that the water of the industrial process be able to flow through the filters without obstruction. Inversely, the addition of a second coat proved to be insignificant in the experiments using the pepti 10 g/L and the polyol 30 g/L suspensions. It was calculated that around 80% of the second coat for the pepti 10 g/L suspension and around 90% of the second coat for the polyol 30 g/L suspension were washed away during the washing step of the coating process. Once again, looking at the TEM images in **Figure 5** and the SEM images in **Figure 10** and **Figure 11**, it is possible that this can be attributed to particle agglomeration and dispersion respectively.

In the first case, it is possible that the agglomeration of the ZnO NPs is such that it affects the ability of the ZnO NPs to make sufficient contact with the nylon surface or with other ZnO NPs, for them to successfully adhere to the textile. This difficulty for forming successful bonds would probably increase for the second coat given that a lot of the surface of the nylon available, would no longer be able to be adhered to, since the space was already taken by previous ZnO NPs.

This last part could prove true tor the polyol case as well, given what is seen in **Figure 10f**, there appears to be an evenly distributed coat on the nylon's surface after one round of dip-coating, taking up almost all the space on the nylon's surface and leaving limited options for dipole-dipole bonds between the ZnO NPs. Additionally, the high dispersion of the particles in the polyol ZnO NPs compared to those of the pepti NPs could be an indication that somehow the polyol NPs have a lower capacity of forming these dipole-dipole bonds (be it due to their morphology or another factor).

[1] All of the molecular structure diagrams presented in the discussion were made by the thesis author using the Molview program (Bergwerf, 2023) unless otherwise specified.

Experimental **Set F** (paragraph **2.2.6)** (Basic and Acid Pre-Treatment) delivered the most interesting added weight results across all three types of suspensions. On the one hand, the acid pretreatment of the nylon textile led to the highest added weights achieved, while the basic pretreatment of the nylon led to the lowest added weights achieved, across the board. All of the statistical significance calculations done, comparing the performance of the acid pretreatment vs the basic pretreatment indicate that there is a greatly significant difference when comparing the added weights achieved. This would indicate that the acid pretreatment of the nylon might have an important role in achieving an effective coating of the ZnO NPs on the textile, while the basic pretreatment has a significantly detrimental effect on the desired goal. This conclusion gives a clue as to what might be happening with the textile when exposed to acid or basic solvents, in order to affect the adherence of the ZnO NPs in such ways. Taking this into account, as well as certain observations from the literature, such as the fact that Sudrajat and Babel (2016) their polyester textile with NaOH before coating it, while Damle *et al* pretreated their nylon 6,6 textile with HCl in order to achieve enzyme immobilization, possible adherence mechanisms were proposed to explain these results. These will be presented below in **Section 4.4.**

Another interesting aspect of the added weight measurements obtained from experimental **Set F** (**2.2.6)** is the fact that there is a clear pattern in which the acid pretreatment of the textile yielded lower results, as the concentration of the acid used increased. This was true both for the HCl and for the Acetic Acid. When looking at the results for the statistical significance analyses, it is observed that the higher concentrated acids proved to be significantly detrimental to the coating process. The difference in the added weight achieved in the experiments in which the nylon was pretreated with each of the acids at the lowest concentrations, compared to the added weights achieved in the experiments that used the acids at the highest concentrations, was statistically significant. Meaning that the concentration of the acid used on the nylon textile affects the outcome of the coating process directly, in an inversely proportional relation. On the other hand, when measuring the statistical significance of the difference in the weights achieved using HCl vs Acetic Acid at the lowest concentrations, there was no significant difference between the two.

Experimental **Set G** (paragraph **2.2.7**) consisted of the combination of the acid-catalyzed hydrolysis treatment on the nylon textile and the application of a triple coat using the pepti 5 g/L suspension. In these experiments a higher added weight value was achieved (using the HCl 0.25M) than what was achieved with the triple coat with no surface activation (in terms of mg of ZnO / g of nylon). Still, it is important to consider what was mentioned earlier with regards to the possible blockage of the water in the filter due to the presence of ZnO NPs on the textile's mesh holes. When comparing what is seen in **Figure 10c** (which depicts the nylon textile double coated with the pepti 5 g/L suspension) and **Figure 10e** (which depicts the nylon textile triple coated with the 5 g/L suspension) there is a

notable increase in the presence of NPs in the textile's mesh holes. Thus, it would be pertinent to carry out further tests in order to determine whether this obstruction of the textile mesh holes affects the regular flow of the water or not.

Even though in experimental **Set G** (paragraph **2.2.7**) there seems to be a big difference between the added weight achieved when using the acetic acid at 0.5M and the HCl at 0.25M, the statistical significance calculations indicated that the difference is not in fact significant, however, further work would be recommended in testing this triple coat + acid pretreatment methodology using a wider variety of acid concentrations.

The last set of dip-coating experiments that was carried out were those of experimental **Set H** (paragraph **2.2.8**) - UVC surface pretreatment. In general, it could be seen that the added weights achieved during this experimental set, both for the pepti 10 g/L and the polyol 30 g/L suspensions, were on the middle ground between the results achieved with no textile pretreatment (which were among the lowest) and the ones achieved with the low concentration acid pretreatment (which were the highest). This gives an indication of the fact that the exposure of the nylon textile to UVC light does have a positive effect in achieving a more efficient coat, however, it is not as effective as the low concentration acids. Still, this might prove favourable in terms of scalability, the use of UVC light vs acid solvents has advantages in terms of safety and ease of implementation. When looking at the results for each of the exposure times evaluated, the same pattern emerges for both types of suspensions, in which the 1 min exposure yields a relatively high added weight, the 20 min exposure yields the highest among the three times, even to the point of being close to the highest added weight achieved with the acid pretreatment, and the 60 min exposure yields the lowest among the three. This would suggest that there are more exposure times, possibly between 1 min and 20 min, or between 20 min and 60 min, that might yield even better results. This is yet another avenue worth exploring in future work.

Finally, when looking at the calculations for the percentage of ZnO coats that were lost in the wash, there are no apparent patterns that can be drawn from the data. In general, the percentages of weight lost in the wash, meaning the difference between the post coating weight and the post wash weight, ranged from around 5% to around 33%. There were specific exceptions to this calculated range, for example for the double and triple coat experiments (**2.2.5**) and the NaOH chemical pretreatment experiments (**2.2.6**), in which the calculated percentages of weight lost after the wash were significantly higher, between 50% and 90%. The samples that consistently showed the lower percentage of weight lost after the wash were the acid pretreated nylon textiles coated with the polyol 30 g/L suspension and the UVC surface activated nylon textiles coated with the polyol 30 g/L suspension. This would suggest there might be a link between the adherence mechanism of the ZnO

NPs to the nylon, the effect of the acid pretreatment or the UVC surface activation on this adherence mechanism and the nature of the polyol NPs, that yields a stronger adhesion with higher resistance to flowing water.

It is important to note that the washing process that was done on the nylon textiles after having been coated, did not follow any specific protocol or standardized procedure. Standardized protocols for washing tests, such as the *ISO 6330:2021: "Textiles — Domestic washing and drying procedures for textile testing"* apply specifically to laundry of textiles that are intended to be used in clothes manufacturing (International Organization for Standardization (ISO), 2021), still, it might be worth looking into or developing a standardized functionalized textile washing protocol that may serve for the purpose of testing the ability of a functionalized textile of withstanding flowing water and maintaining its functionalization for the purposes of industrial water treatment. This was not possible however, within the scope of this thesis since the actual process water flow that the filter is intended to withstand in the industrial partner's process is unknown and this was not the focus of the project at this stage. For this reason, it is recommended that more thorough and standardized washing tests be done to evaluate the loss of the ZnO NPs coat from the nylon, when exposed to flowing water, in future work, considering this operating parameter from the intended process application.

Another notable observation to make with regards to the calculated percentages of weight lost post wash, is that the values obtained for these calculations, specifically for the experiments for the acid pretreatment and the UVC surface activation, using the polyol 30 g/L suspension, were all in the lower end of the range presented above (5% to 33%). These experiments also presented some of the lowest relative standard deviations. Both of these observations could be once again related to the particle dispersion of the polyol synthesized NPs. Once again, having a better dispersion would allow for a more uniform contact of the ZnO NPs to the nylon surface (as evidenced in the SEM image in **Figure 10f**), allowing them to adhere more thoroughly to the surface. Additionally, it is possible that a more homogeneous dispersion in a suspension , rather than a suspension with a highly agglomerated group of particles, would have a higher probability of achieving similar results more often, increasing the reliability of the reproduction of the experiments.

4.3. Discussion on ZnO NPs' Characterization

In addition to the added weight measurements, characterization techniques (SEM, BSE, EDX) were applied to confirm that the results of the measurements of the added weight of the nylon pieces in fact corresponded to the adhesion of ZnO NPs. From the SEM images (**Figure 10** and **Figure 11**) it can be seen that there is clearly a layer of material that is coating the nylon. In the case of the nylon that was coated using the pepti suspensions, this coat has an appearance similar to adhered flakes,

while the nylon pieces coated with the polyol suspension, appear to have a relatively smooth and homogeneous layer of coating, similar to a layer of paint. From the BSE images (**Figure 12**) it can be seen that there is a clear contrast between the material of the substrate (the nylon) and the material out of which the coats are made, indicating that these are in fact, two distinct materials. Additionally, there does not appear to be a distinct third intensity of the light that is being reflected, suggesting that there are only two distinct materials making up the sample that is being characterized (the nylon substrate and the coat). Finally, from the EDX spectra (shown in **Figure 13, Figure 14** and **Figure 15**) it can be seen that i) there is little presence of oxygen and zinc on the spectrum measure for the uncoated nylon, and there is a high presence of carbon, as is expected for a polyamide, some oxygen is also expected because of the polyamide ii) the spectrum for both the pepti and the polyol coated nylon pieces display a presence of both oxygen and zinc, confirming that the added materials in the coated samples, which can be seen in the SEM and BSE images, in fact ZnO NPs.

4.4. Proposed Mechanisms for the Interaction between the ZnO NPs and the Nylon Substrate.

As was mentioned in **Section 1.4,** a great variety of studies exist with regards to the functionalization of textiles using ZnO NPs. There are a wide range of parameters in all these studies which vary greatly, including the intended functionalization, the textile to be functionalized, the technique employed for the coating of the textile, the ZnO NPs synthesis methods, among others (Verbic *et al*., 2019), (Fiedot-Tobola *et al*., 2018). After conducting the literature review regarding this topic, it became apparent that there seem to be limited resources that can be used as references for the ZnO NP dip-coating experiments carried out for this thesis, given the fact that none of the studies found match the specific set of parameters pertinent to this thesis completely. This set of parameters are:

- Textile substrate: polyamide 6 (nylon 6)
- ZnO NPs synthesis methods: pepti and polyol
- Coating method: dip-coating
- Desired functionality: antibacterial activity **in the dark.**

Table 9 shows a comparison between the parameters of some of the works analyzed, previously exposed in **Table 1**, and the parameters used for the development of this thesis. In **Table 9**, the parameters that match this work completely are highlighted in green and those that match partially are highlighted in yellow. As can be seen in the table, there is no study that is a complete match.

Table 9: Comparison between the factors involved in textile functionalization with ZnO coating in this thesis and some examples from the literature.

Textile Substrate	ZnO NPs Synthesis	Coating Methods	Additional Treatment	Intended Functionalization	Authors
Polyamide 6 (Nylon 6)	Pepti and Polyol	Dip coating	Acetic acid / HCl NaOH UVC irradiation	Antibacterial activity in the **dark**	This work
Polyamide 6	Unspecified	Hydrothermal deposition	Hexamethylenetetramine	Antibacterial Activity	Fiedot-Tobola et al (2018)
Polyamide 6	Unspecified	Spray coating	Modified siloxane (APESP)	Enhancing washing durability	Song et al (2022)
Polyester	Solvothermal (NaOH + Urea as reactants)	Dip coating	N/A	Antibacterial activity	Amani et al. (2018)
Polyester	Sol-gel	Dip coating + shaking	NaOH UVC irradiation	Photocatalytic activity	Sudrajat and Babel (2016)
Polyester	Purchased (Sigma-Aldrich)	Dip coating	NaOH	Antibacterial and self-cleaning activities	Nourbakhsh et al., (2018)
Polyamide 6,6	N/A	Enzyme Immobilization	HCl	Self-cleaning properties	Damle et al., (2018)

Amani *et al*. (2018) reported the antibacterial functionalization of a polymer textile through dip-coating, using ZnO NPs synthesized via a sol-gel method (solvothermal). However, the textile used as substrate in this instance was polyester and the solvothermal method synthesis used NaOH and urea as reactants with zinc acetate, unlike the ethanol and diethylene glycol used in the pepti and polyol methods from this thesis. Sudrajat and Babel (2016) developed a functionalized polyester for photocatalytic activity employing a pretreatment of the fabric of NaOH and UVC irradiation. Later, Sudrajat (2017) reported achieving superior photocatalytic degradation by developing functionalized polyester using sol-gel synthesized ZnO NPs, by dip-coating and shaking, with no additional treatment. Still, neither of these meet the requirement of needing antibacterial activity to happen in the dark, and it does not meet the requirement for the nylon substrate. Nourbakhsh *et al.* (2018) developed antibacterial and self-cleaning functionalized polyester by dip-coating it with ZnO; they used additional pretreatment of the textile involving NaOH. Once again, the substrate used is polyester rather than nylon, and in this case, the synthesis method for the ZnO NPs is not specified given that they were directly acquired as ZnO NPs from Sigma Aldrich (Nourbakhsh *et al*., 2018).

On the other hand, Fiedot-Tobola *et al.* (2018) and Song *et al*. (2022) both report the development of antibacterial functionalized textiles using nylon 6 or polyamide 6 as the textile substrate. However, Fiedot-Tobola *et al.* (2018) employed hydrothermal deposition as the coating method, while Song *et al.* (2022) spray coated the ZnO. Additionally, the ZnO synthesis method is not specified in either of these cases.

As can be seen from the examples above, there are instances in which the polymeric textile that is being functionalized is pre-treated with NaOH and/or UVC irradiation. Additionally, other examples can be found in the literature where HCl is used as treatment of nylon 6 and nylon 6,6 textiles with the aim of increasing the immobilization of enzymes on the textile (Damle *et al.*, 2018) or improving the adhesion of coating on the substrate (Tanahashi *et al*., 1995).

The studies carried out by Fiedot-Tobola *et al* (2018) seem to be the most relevant reference given that they use the same textile substrate and are seeking to achieve the antibacterial functionalization of the textile. The purpose of their study is to assess the performance and efficiency of the ZnO NP coating on different polymeric textiles. Similarly to this thesis, Fiedot-Tobola *et al* measure the amount of ZnO NPs adhere to the textiles through the calculation of the added weight measured. In their study, they compared the amount of ZnO coating achieved between polyamide 6 (PA), polypropylene (PP) and polyethylene terephthalate (PET) textiles, and concluded that the highest coating achieved was on the PA textile. They suggest several factors that may have had an influence on this result, including a high level of wettability and a relatively low roughness. However, they fail to suggest a possible mechanism to explain the adherence of the ZnO NPs to any of the substrates, including the nylon. As far as could be seen in the literature review, Zhang *et al* (2018) and Song *et al* (2022) have carried out the only two other studies involving ZnO NP coating specifically on nylon textile so far, however, neither of them provide a proposed explanation for the adherence mechanism of the ZnO NPs to the substrate.

An possible explanation for the adherence mechanism between the ZnO NPs and the nylon 6 textile during the dip-coating process will be provided in this work, based on chemical principles and the observations done across the different experimental sets that were carried out during the development of this work, including variations to the mechanism based on the results for the experiments that involved chemical or physical pre-treatment and activation of the textile surface.

When considering all the experiments, it can be said that the experimental **Sets A-E** (paragraphs **2.2.1 - 2.2.5**) can be grouped together by the fact that the nylon substrate has not been altered through either chemical or physical means in any of these experiments. Meaning that the main proposed mechanisms responsible for the adherence of the ZnO NPs to the nylon textile applies to all these experiments, without any alterations.

Nylon 6 is a polyamide formed by a single monomer composed of 6 carbon atoms and an amide group (which contains an oxygen and a nitrogen), because of this, the nylon molecule is polar and

has the capacity to form hydrogen bonds (DeMello, 2019). **Figure 24** depicts the structure of nylon 6 and how the hydrogen bonds are formed.

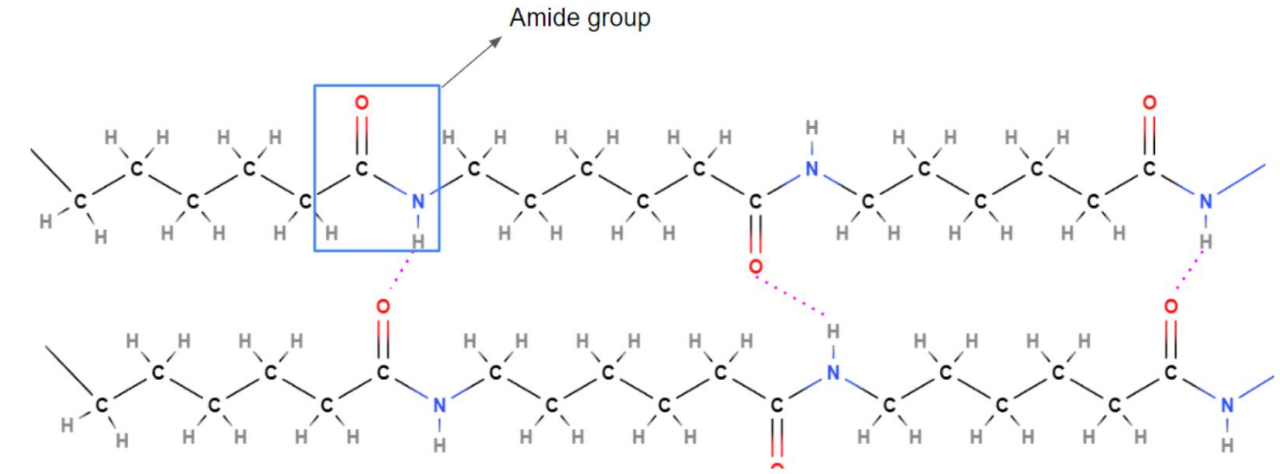

Figure 24: Molecular Structure of Nylon 6 with hydrogen bonds.

Similarly, ZnO is also a polar molecule which contains oxygen, meaning it too has the capacity to create hydrogen bonds. Considering the hydrogen bonds as well as the polarity of the molecules of the nylon and the ZnO, it is probable that the explanation for the adherence of the ZnO NPs to the nylon is the formation of both hydrogen and dipole-dipole bonds between the ZnO molecules and the amide group's oxygens and hydrogens available on the surface of the textile. **Figure *25*** is a representation of this proposed explanation.

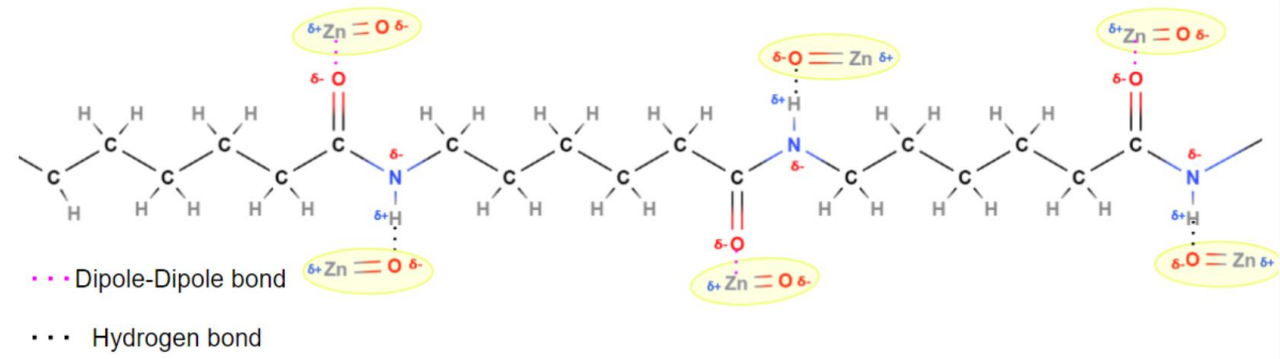

Figure 25: Representation of the proposed intermolecular interactions happening between the ZnO NPs and the nylon 6 textile during dip-coating, causing the adherence of the coating.

It is also probable that the ZnO NPs are forming dipole-dipole bonds amongst themselves, causing the layer of adhered NPs to increase. This is also a possible explanation for the agglomeration and precipitation observed in the suspensions, as shown in **Figure 5** and **Figure 6.**

Considering that according to the monofilament nylon filter bags datasheet from Eaton, the thickness of the monofilaments is <125 µm (EATON, 2016) and that the size of the ZnO NPs was estimated to be between 6 - 17 nm (for the pepti and the polyol ZnO NPs respectively), it can be inferred that

there are thousands of amide groups available on the surface of the substrate for the ZnO NPs to adhere to it.

The next group of experimental **Sets F-G** (**2.2.6** and **2.2.7**) dealt with experiments based on the chemical pretreatment of the nylon textile. These experiments consisted in the use of either basic or acidic chemicals in order to alter the superficial interactions between the ZnO NPs and the nylon substrate. The chemicals used were NaOH, HCl and Acetic Acid at different concentrations.

There are several instances in which studies have reported the use of basic pretreatment, specifically NaOH, when working on textile functionalization with ZnO NPs. Pandimurugan and Thambidurai (2017) and El-Naggar *et al* (2018), reported using NaOH as a post-treatment and a pretreatment respectively, in the functionalization of cotton textiles for antibacterial activity using ZnO. Nourbakhsh *et al* (2018) and Sudrajat and Babel (2016) reported using NaOH as a pretreatment for the functionalization process of polyester in order to achieve antibacterial activity and photocatalytic degradation functionalization of the textiles respectively. Finally, Amani *et al* (2018) used a NaOH/Urea solution for the synthesis of a corn silk/ZnO hydrogel nanocomposite to be added to polyester fabric. On the other hand, there have been studied such as the one conducted by Damle *et al* (2018) in which they applied acid hydrolysis to a nylon 6,6 textile, using HCl, claiming that they did so in order to split some of the amide bonds and create carboxylic acid (-COOH) and amine ($-NH_2$) functional groups on the textile surface; this with the intention of creating more opportunities for bonding sites that would allow for the immobilization of pectinase of the textile. The chemical mechanism suggested by Damle *et al* (2018) supports the hypothesis of the mechanism proposed earlier; the formation of hydrogen and dipole-dipole bonds between the ZnO NPs and the nylon's molecules.

Essentially, what was done during the experimental **Sets F-G** (**2.2.6** and **2.2.7**) by treating the nylon textile with these chemicals, were base-catalyzed and acid-catalyzed amide hydrolysis reactions. The mechanisms of which are shown in the schematics below:

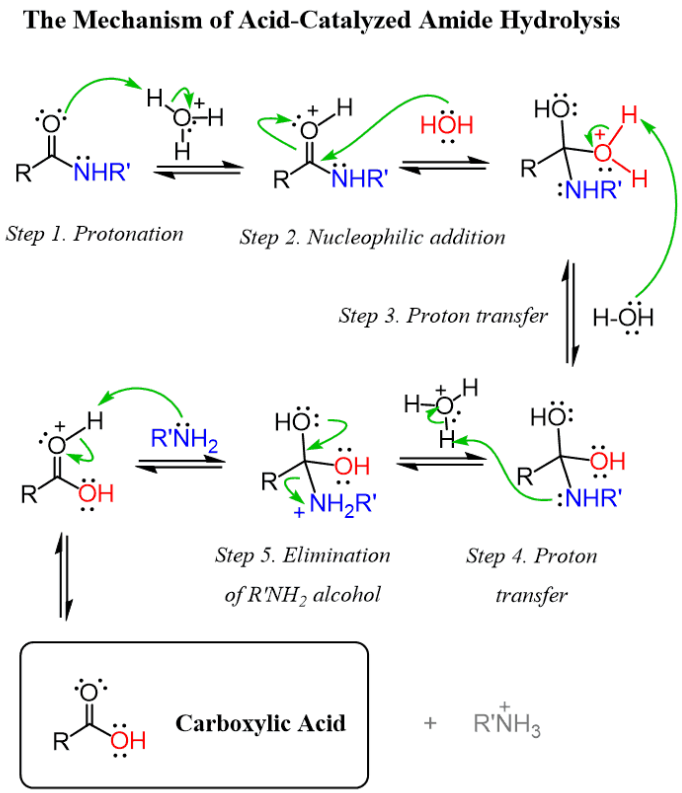

Figure 26: Mechanism of Acid-Catalyzed Hydrolysis of the Amide Functional Group (Gevorg, 2022)

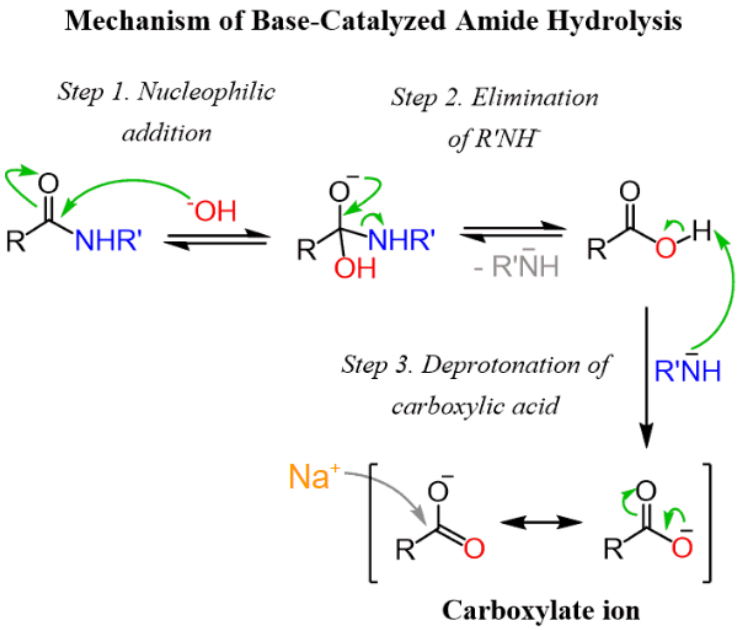

Figure 27: Mechanism of Base-Catalyzed Hydrolysis of the Amide Functional Group (Gevorg, 2022).

As can be seen from the process shown in **Figure 26**, the process of acid-catalyzed hydrolysis of the amide functional group ultimately results in the formation of a carboxylic acid functional group (R-OOH) as well as the presence of an amine functional group (R-N¨H_2), which falls in line with the statement of Damle *et al* (2018) in their study. The new free pairs of electrons available in the new

oxygen atom of the carboxylic acid, plus the already present free pairs of electrons in the oxygen and nitrogen atoms of the previous amide group, turn carboxylic acid and amine, provide even more polarity to the molecules, which in turn increase the chances for polar bonds. Additionally, the new presence of peripheral hydrogen atoms, both in the carboxylic acid and the amine group, provide more opportunities for hydrogen bonds. On the other hand, when looking at the mechanism displayed in **Figure 27**, the resulting functional group that comes from the base-catalyzed hydrolysis of an amide group is a carboxylate anion, that can easily react with a cation, making it possible for a Na^+ cation available from the NaOH to take up the space that would otherwise serve as a possible bonding site for the ZnO NPs.

Based on these mechanisms, the following molecular models were drawn to represent the effects of these hydrolysis processes and the resulting possibilities for hydrogen and dipole-dipole bond formations. Given that the acid pretreatment experiments yielded the highest added weight measurements, the proposed models corresponding to these experiments will be shown and discussed first.

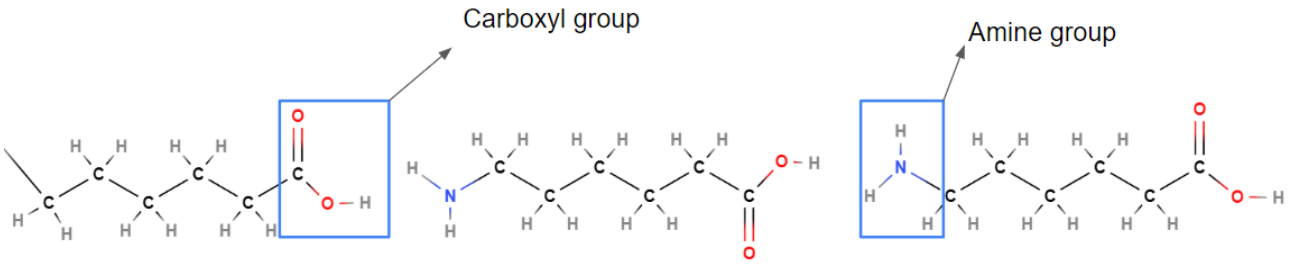

Figure 28: Molecular structure of the hydrolyzed nylon 6 monomers with acid.

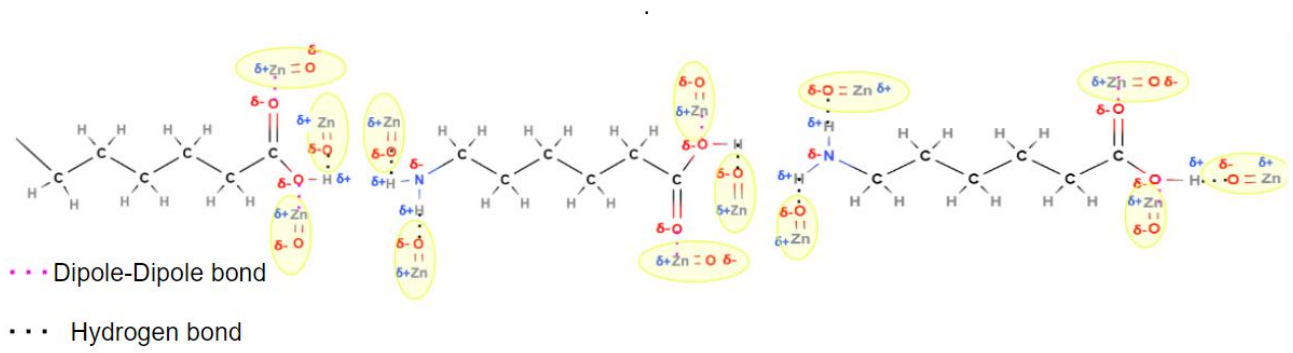

Figure 29: Representation of the possible intermolecular interactions happening between the ZnO NPs and the acid hydrolyzed nylon 6 textile causing the adherence of the coating.

As can be seen from the representation in **Figure 29,** due to the acid hydrolysis of the amide groups of the nylon 6 molecule that has taken place, the possible bonding sites between the ZnO NPs and the textile have multiplied. This thanks to the presence of the new carboxylic acid and amine functional groups. The fact that the added weight measurements achieved by the experiments involving the treatment of acid on the nylon surface were the highest amongst all the experiments

and across all three suspensions, supports the hypothesis that the hydrolysis reaction is creating more potential bonding sites on the nylon's surface. It is worth mentioning that both the carboxylic acid and the amine functional are less polar than the amide group (Moore *et al*., 2023), which could lead to having the dipole-dipole interactions weakened, this however seems not to have a significant impact considering the added weights achieved. It could be said that the increase in potential bonding sites trumps over the loss in polarity of the molecule.

There are two important factors to note in this process. The first one being that the reactions of the hydrolysis of amide groups are usually assisted by heat as well as the strength of the acid or base being used (Clark, 2023). Given that the process of chemical surface activation of the nylon during the experiments was done at room temperature which was raised only slightly through the use of the ultrasonic bath and given that the nylon was submerged in the acids and base for a few minutes, it could be hypothesized that the hydrolysis process was limited and slow, therefore maintaining most of the integrity of the textile. It was observed however, that in the case of the nylon pieces that were treated with acids of higher concentrations (1M), there was visible deterioration of the surface, indicating a more advanced and complete hydrolysis in these instances. Photographic evidence of this deterioration can be seen in the images in **Figure 30.**

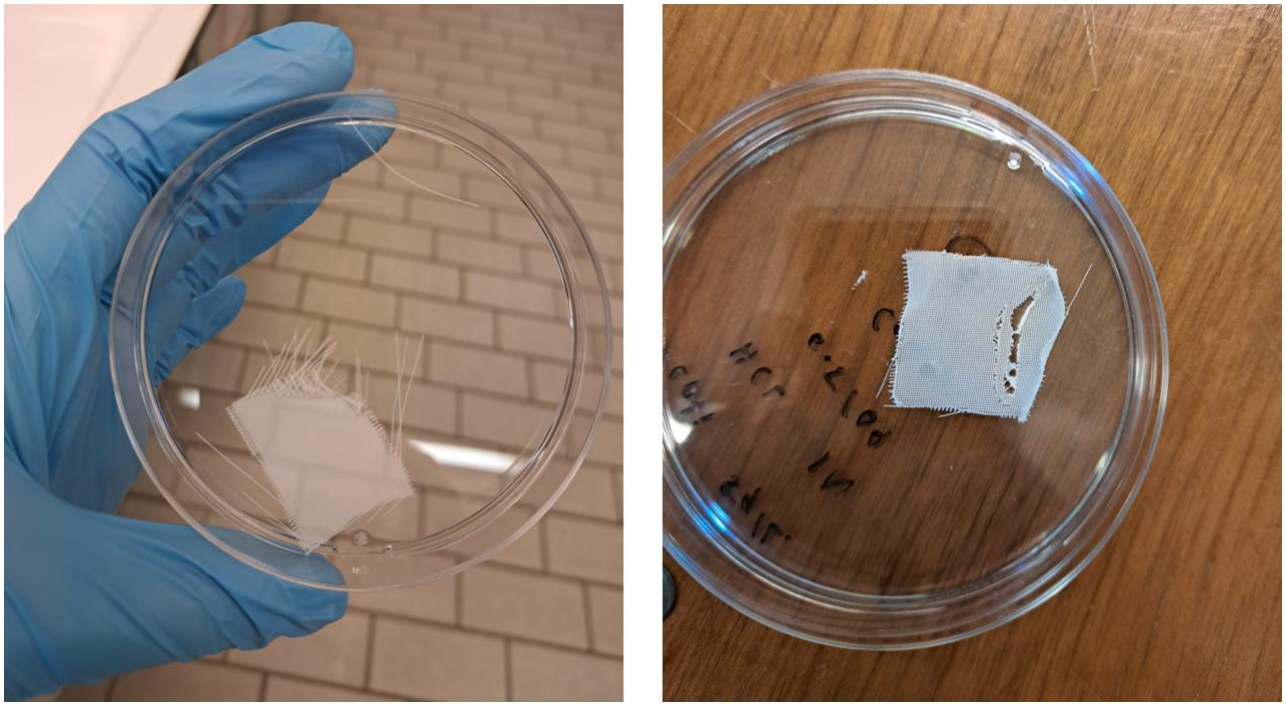

Figure 30: a) Physical appearance of the nylon textile after being submerged in Acetic Acid 1M for 15 min. **b)** Physical appearance of the nylon textile after being submerged in HCl 1M for 15 min.

When looking at the added weight results for the experimental **Sets E** and **G** (paragraphs **2.2.5** and **2.2.7)**, it could be seen that the dip-coating performed in conjunction with the acid hydrolysis that was done with the lowest concentration of the acids used (acetic acid 1% (0.17M), acetic acid 0.5M, and HCl 0.25M) yielded the highest added weight results across all three types of ZnO NPs

suspensions (not including the pepti 5 g/L triple coat), as can be seen in **Figure 7, Figure 8** and **Figure 9.** However, as the concentration of the acids was increased, the added weight results decreased. A possible explanation for this phenomenon is the fact that as the concentration increases the more rapidly the hydrolysis process progresses, negatively affecting the integrity of the textile, creating the holes and unweaving the textile, as seen in **Figure 30.**

On the other hand, the statistical significance analysis done comparing the results for the experiment with lowest concentration of acetic acid vs those for the experiment with the lowest concentration of HCl would indicate that there is no significant difference between them. Meaning that the effects that a weak acid (acetic acid) has on the nylon molecule are comparable to the effects that the strong acid (HCl) has. This falls in line with the conclusions found by Hocker *et al* (2014) in their study "Polyamide Hydrolysis Accelerated by Small Weak Organic Acids" which indicated that the weaker acids were capable of hydrolysing polyamides at even as much as twice the rate that the HCl presented. These findings are advantageous from the perspective of the scalability of the process given that it would allow for the use of weaker, less concentrated, and therefore less dangerous, acid that could yield the most favorable coating process found in this thesis. The lower concentrations of the acid are also a favorable factor from a budgetary perspective.

In contrast to the acid hydrolysis, the basic hydrolysis (using NaOH 0.25M) had the opposite effect on the amount of coating achieved, yielding the lowest added weight results of all the experiments across all two types of ZnO NPs suspensions used. Two possible explanations are proposed for this behavior. The first is the fact that during the base-catalyzed hydrolysis process of the amide groups of the nylon, the Na^+ cation that gets dissociated from the NaOH molecule is left free in the solution to react with the carboxylate ion rather than it reacting with a proton to form a carboxylic acid group (as is shown in **Figure 32**).This means that instead of having the additional hydrogen of the carboxylic acid group for additional hydrogen bonds, as could be seen in the acid hydrolysis, there is a sodium atom.

This explanation is shown in the figures below:

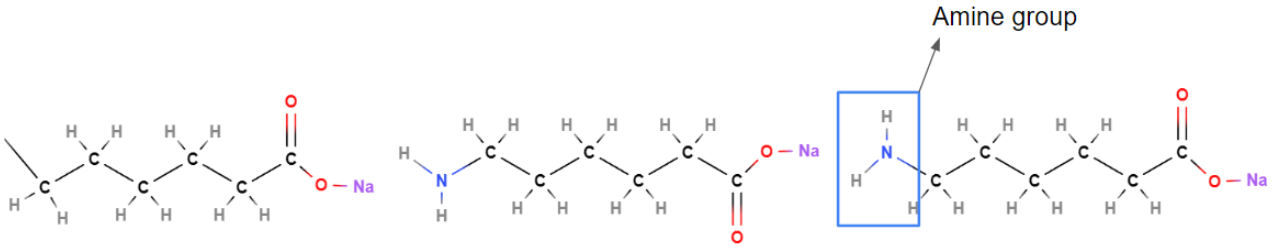

Figure 31: Molecular structure of the nylon 6 monomers once the basic hydrolysis takes place.

.

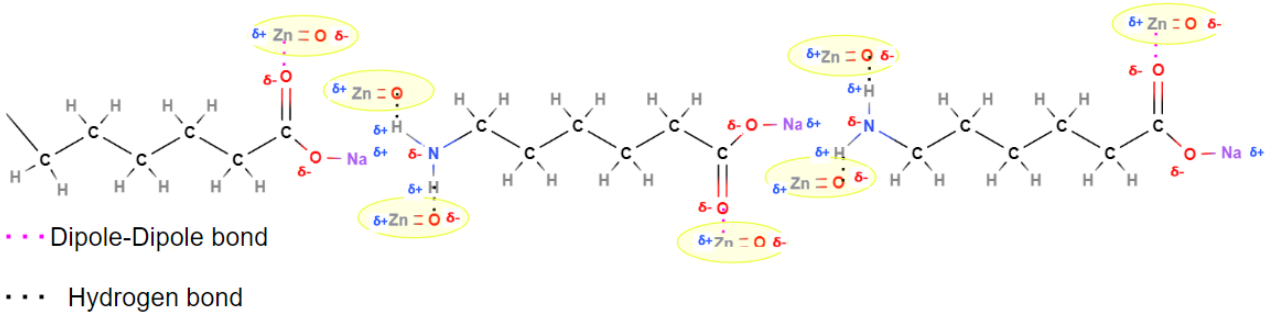

Figure 32: Representation of the possible intermolecular interactions happening between the ZnO NPs and the base hydrolyzed nylon 6 textile causing the adherence of the coating.

Another possible factor that might be contributing to the lowered efficiency in the coating presented in the base hydrolyzed nylon might be related to the atomic sizes of the elements involved. The fact that the sodium ions not only could be taking the place of the protons meant to create the carboxylic acid group, but also the fact that the sodium atom is significantly bigger than the hydrogen atom. It may be possible that simply due to the space that the new sodium atoms are taking up by being attached to the nylon, the ZnO NPs are not even able to reach the nylon molecules at a close enough distance to form a secure bond, be it hydrogen or dipole-dipole bonds. The bigger size of the sodium atom also has the effect of lowering the electronegativity of the O - Na bond vs the O - H bond, which could also lead to decreasing the ability of the atoms involved in those bonds to form a dipole-dipole bond with the ZnO NPs.

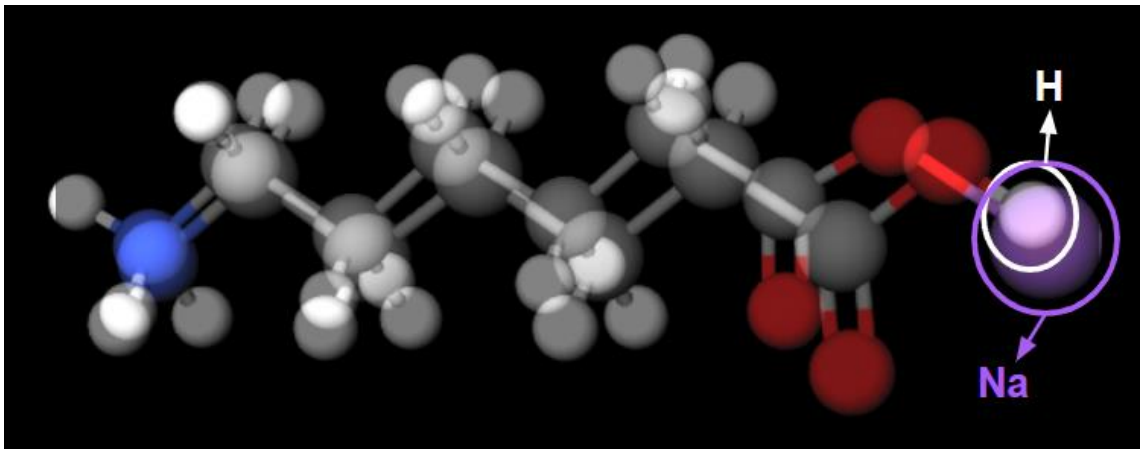

Figure 33: Molecular model of the acid hydrolyzed nylon monomer overimposed on the base hydrolyzed nylon monomer to evidence the difference in size of the Na and the H atoms.

The fact that, as was mentioned earlier, the calculated percentage of weight loss of the substrates after the washing step was significantly higher for the experiments involving NaOH pretreatment, could also be taken as evidence to support the proposed hydrolysis mechanism taking place. Since it is possible that the presence of the Na atoms bonded to the carboxylate ions from the nylon's structure causes the polar bonds between the ZnO NPs to be even weaker.

The final experimental set (**Set H - 2.2.8**) consisted of testing the possibility of physical surface activation of the nylon textile through its exposure to UVC light. These experiments were carried out using the pepti 10 g/L and the polyol 30 g/L suspensions, and establishing the exposure of the nylon textile to the UVC light at 1 min, 20 min and 60 min. The highest achieved results from this specific experimental set were slightly lower than the highest achieved through the acid hydrolysis of the nylon and significantly higher than those achieved in experiments that did not involve any alteration of the nylon surface. This can be explained due to the fact that, similarly to the hydrolysis process, UV light has the capacity of breaking the C - N bond present in the amide functional group of the nylon molecule, allowing for the formation of carboxylic acid and amine groups (Johnson *et al*., 2011), (Holyavka *et al*., 2019), except in this instance, the ethanol present in the ZnO NPs suspensions acts as the hydroxyl donor that forms the carboxylic acid group, rather than the water present in the usual hydrolysis process.

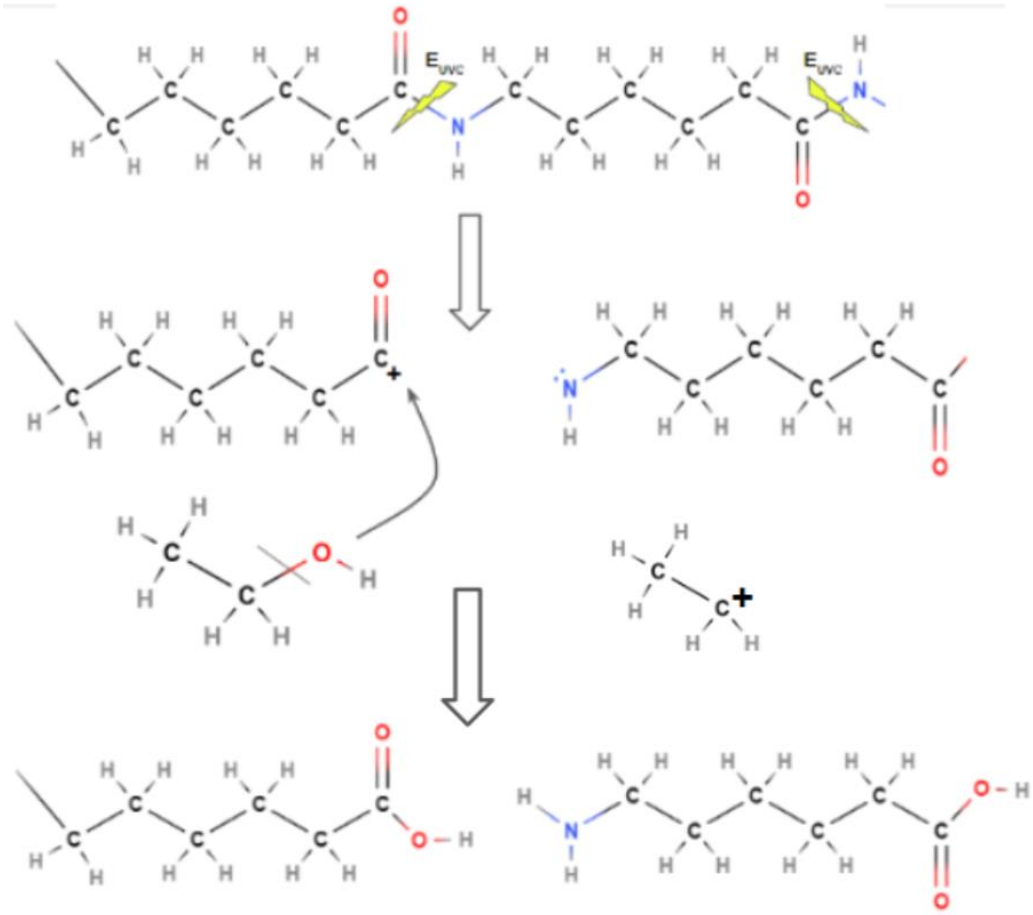

Figure 34: Proposed mechanism for the reaction between ethanol and the broken C-N amide bond to form carboxylic acid and amine groups.

It should be considered that for the proposed mechanism to work, there would need to be a viable source of protons available to react with the freed, and now negatively charged nitrogen from the previous amide bond, otherwise the remaining ethyl group could react with this atom.

Considering once again the added weight results for experimental **Set H** (**2.2.8**), it could be seen that the exposure of the nylon after 20 mins yielded the results that were slightly lower than those achieved with the acid hydrolysis, while the exposure for only 1 min and for 60 min yielded lower results. Assuming that the proposed mechanism shown in **Figure 34** is correct it could be proposed that, similarly to the acid hydrolysis experiments, an exposure of 60 min to the UVC could lead to too many amide bond breakages, leading to bigger damage to the nylon' surface than needed, while an exposure of just 1 min and even 20 mins lead to not enough breakages happening to match a similar amount of carboxylic acid and amine groups to be created as are created with the acid reactions.

As was mentioned earlier, resources like those of Fiedot-Tobola *et al* (2018) and Song *et al* (2022) did not mention proposed mechanisms to explain the adherence of the ZnO NPs on the nylon substrate, however they did mention (in both studies) the fact that the wettability of the substrate is a factor that affects the level of adherence. As they claim, the higher the wettability of the substrate the better the results achieved on the coating of the ZnO NPs. Specifically, Fiedot-Tobola's study compares the performance of the ZnO NPs coating process on polyamide 6 (PA 6 - nylon), polypropylene (PP) and polyester (PET), and claim that the PA 6 yielded the highest added weight because it presents the highest wettability measurement among the three polymeric textiles. Additionally, they claim that the roughness of the surface also contributes to the adhesion of the ZnO NPs, meaning that the rougher the surface the more ZnO NPs are able to adhere to the surface. Assuming that the mechanisms that have been proposed in this thesis are correct, the claim that roughness improves adhesion is consistent, given that the roughness of the surface would mean that more atoms available to form the hydrogen bonds would be exposed.

This might also be a factor that could be contributing to the significant increase of results in added weight in the acid and UVC activation experiments since, as observed from the SEM images in **Figure 10d, e and f,** the surface of the nylon appears to be rougher and presents more defects than the surface seen in **Figure 10a**, which is the SEM image of the blank, unaltered nylon textile surface. This change in the roughness of the nylon surface can be attributed to the breakage of the bonds due to the hydrolysis reactions.

The final set of characterization analyses that were performed were the FTIR analyses for the uncoated nylon samples, which had been pretreated with the NaOH, HCl, Acetic Acid and the UVC exposure. This was done with the purpose of finding indications in the FTIR spectra of what might be happening to the nylon's structure due to the pretreatments. This could help draw more founded conclusions with regards to how the different types of pretreatments were affecting the added weight measurements obtained previously. At first look, all of the obtained FTIR spectra match the reference

FTIR spectrum for (blank) nylon very closely, and they present peaks in all of the expected wavenumbers (listed in **Table 10**). Still, considering the proposed mechanisms and the peaks at which the bond vibrations of the resulting functional groups present in the FTIR spectrum, it might be possible that this characterization technique is insufficient to validate these mechanisms, given that many of the functional groups involved present the same wavenumbers.

Table 10: Comparison of the bond vibrations for the proposed functional groups and the nylon FTIR spectrum, with their respective wavenumber (Merck, 2022)

Wavenumber (cm^{-1})	**Nylon 6 (amide)**	**Carboxyl group**	**Primary Amine group**
3500	-	-	N - H
3298	N - H	O - H (usually at 3000 cm^{-1})	-
2932	CH		-
2858	CH		-
1760	-	C = O	-
1720 - 1706	-	C = O	-
1634	C = O	-	N - H
1538	NH, C - N	-	-
1464	CH	O - H	-
1372	CH		-
1274	NH, C - N		C - N
1199	CH	-	-
687	NH, C = O	-	-

The similarity of the FTIR spectra for each of the analyzed pretreated nylon samples against the blank and the reference spectrum, is clear, and what is shown in **Table 10**, illustrates that many of the spectrum's wavenumbers in which peaks appear are shared among different bond vibrations of the considered functional groups. Considering this, and the fact that some of the types of bond

vibrations that present at a certain wavenumber for a specific functional group are already present at a different wavenumber for the nylon, it cannot be said that the FTIR characterizations present conclusive evidence as to whether the proposed mechanisms for the adherence of the ZnO NPs to the nylon are correct. Even the free ethyl group from the proposed mechanism for the UVC surface activation (as seen in **Figure 34**) has a C-H bond at 1465 cm^{-1}(Merck, 2022) the same as the nylon.

In addition to this, an important consideration to have in mind is the fact that, as was mentioned before, the hydrolysis processes that were done on the nylon were limited because they were carried out at room temperature, the concentrations used for the acids were relatively low and the time of exposure of the nylon to the acids or bases was relatively short. This might possibly result in the formation of the carboxylic acid and amine groups being significantly lower than the amount of amide groups that were preserved. It is possible that this difference in quantities of functional groups present in the material could lead to the intact nylon monomer bonds to obstruct and overshadow the manifestation of the carboxylic acid and amine bonds in the FTIR spectra. Because of this, it would be recommended that future work be done with regards to validating the proposed adherence and bond mechanisms between the ZnO NPs and the nylon, and the effects of the different types of pretreatments and surface activations.

Assuming that the proposed mechanisms are correct, and considering the information that has been analyzed earlier with regard to the decline on ZnO NPs as the concentration of the acids used in the pretreatment of the nylon increased, due to the resulting damage on the integrity of the textile, it would be pertinent to carry out more tests, to determine whether the damage (as observed in **Figure 30**) is due to hydrolysis. These experiments would lead to finding the optimum concentration which could result in the highest possible amount of carboxylic acid and amine groups formation, before the integrity of the nylon is compromised and the efficiency of the coating is negatively affected.

There are a few peaks at certain wavenumbers, seen across all the measured FTIR spectra, that do not align with those taken from the reference as presented in **Table 10** and **Figure 20.** These peaks are present in all the measured FTIR spectra, including the blank and they are the following: at 796 cm^{-1}, at 933 cm^{-1}, and at 2355 cm^{-1}. While the first two were not found to correspond to any specific bond vibration, the last one (at 2355 cm^{-1}) corresponds to CO_2 (Merck, 2022), which can be attributed to the detection of CO_2 in the room at the time of the measurements.

4.5. Pollutant Degradation Efficiency of the Coated Nylon Samples in the Dark.

Lastly, the NBT degradation tests were conducted, using functionalized nylon samples from experimental **Sets G** and **H** (**2.2.7** and **2.2.8**), specifically for the pepti 10 g/L and the polyol 30 g/L

suspensions. It was observed that in fact, there was degradation of the NBT compound within 48 h, based on the reduction in the measured absorbance. The percentage of the NBT degradation obtained between all the samples that had been pretreated with acid were very similar, between 24% and 26%, regardless of the type of ZnO NPs suspension used. Considering this, and piecing it together to what was observed from the TEM and XRD characterizations, it is possible to pose the hypothesis that crystallite size is not an influential factor in achieving ROS formation from the ZnO NPs, during a period of 48 h. However, this be considered conclusive evidence that size does not affect the efficiency of the NPs' antibacterial activity in the dark overall, since the NBT degradation process is only testing the formation of ROS but, as was explained in the methodology section (**Section 2.4**), there are other proposed mechanisms that are attributed to being responsible for the ZnO NPs' antibacterial activity. Still, this last conclusion falls in line with what was reported by Adams *et al* (2006) who stated that the same antibacterial activity was observed in specific antibacterial tests for ZnO NPs suspensions that presented agglomeration and those that had smaller particle sizes.

On the other hand, the percentage of reduction in the measured absorbance for the coated nylon samples with no pretreatment was significantly lower than all the other ones measured (10% for the pepti coated sample, with a coating of 15.6 mg and 1% for the polyol coated sample, with a coating of 8 mg). This would suggest that there is something about the acid pretreatment and the UVC surface activation of the nylon textile that has an influence over the performance of the coated ZnO NPs with regards to the formation of ROS. Given the fact that all of the coated nylon pieces were submerged in the NBT solution in such a way as to ensure a concentration of 10 g of ZnO per liter of NBT solution, the amount of added weight measured for each of the tested samples should not be a factor. Which is why positing that the pretreatments (both physical and chemical) must have had an effect on the generation of ROS, is a plausible hypothesis.

As was mentioned in **Section 1.2**, while explaining the proposed antibacterial mechanisms of ZnO NPs, Prasanna and Vijayaraghavan (2015) have claimed that the antibacterial activity of ZnO NPs in the dark can be attributed to the formation of ROS, not from a photocatalytic process, but from superoxide ions ($\cdot O_2^-$) that are available due to ZnO NPs' surface defects. Considering this, it would be possible to suggest that the formation of the carboxylic acid and the amine functional groups on the nylon's surface, from the chemical and physical mechanisms described above (**Section 4.4)**, and their subsequent interactions with the ZnO NPs in the coating process, might have an effect over the ease with which these superoxide ions from the ZnO NPs' surface become available to interact with the NBT solution. However, this is only a hypothesis and further work should be conducted in the future to determine its validity.

The fact that there is almost a 30% reduction in the absorbance measurements of the test indicates that the degradation of the NBT is in fact taking place, this in turn gives confirmation that ROS are being generated in the dark, specifically, superoxide ions as described in **Figure 3**, and as is suggested by Prassana and Vijayaraghana (2015) and Hirota *et al* (2009). Even though only a maximum of around 30% of degradation of the NBT was achieved over a period of 48 h, it is important to have in mind that the filter will be continuously in contact with the flowing process water which, by being in a closed loop will be disinfected several times. Additionally, the other proposed mechanisms for the antibacterial property of ZnO need to be considered, since the NBT degradation test is only directed at testing for the generation of ROS, the possible antibacterial activity attributed to the Zn^{2+} ions and the internalization of ZnO NPs into the cells (as described in **Sections 1.2.1** and **1.2.2**) have not been tested and considered in the development of this thesis. Further work should include the application of a variety of antibacterial activity tests that are able to identify and possibly measure these other mechanisms. It is possible that in fact all of these proposed mechanisms contribute to the ZnO's antibacterial activity, and ultimately enhance the overall antibacterial activity of the functionalized textile under dark conditions.

5. CONCLUSIONS AND PERSPECTIVES

The general objective of this thesis is to develop an antibacterial functionalized nylon 6 textile by coating it with ZnO NPs, in order to develop filters for process water disinfection, with the specific requirement that the antibacterial function is able to work under dark conditions. It has been established that ZnO NPs are an attractive material in the field of antibacterial treatment due to its multiple proposed mechanisms for antibacterial activity as well as the fact that ZnO can be synthesized in various ways, which are relatively simple and affordable processes, and that it has been deemed safe in terms of bio-compatibility for humans. Thus, the aim is to use the nylon 6 textile from the filters that are already being used by the project's industrial partner as a medium on which to fix the ZnO NPs, to provide the industrial partner with an applicable water disinfection solution for their process.

The specific objectives of this these were to:

- Identify a specific set of conditions that yields the highest amount possible of ZnO NPs coating on the textile through the dip-coating technique

- To test whether the coatings done on the textiles remain adhered even after exposure of the textile to running water,

- To validate via characterization techniques that the substance that is being coated onto the nylon is actually ZnO

- To confirm through an NBT degradation test that the antibacterial property of ROS generation by ZnO NPs coated onto the nylon textile, can in fact take place in the dark.

It was found that both the pepti and the polyol synthesis pathways yield ZnO NPs with crystallite sizes of around 6 nm and 17 nm respectively, as evidenced by the XRD and TEM characterizations. The polyol synthesized NPs presented a spherical/rod-like morphology and a notably higher dispersion of the particles, which is an advantage for the coating process, as it results in a more uniform coating on the nylon's surface. The pepti ZnO NPs have a smaller crystallite size and a spherical morphology but present significant agglomeration of the particles. It was suggested that the reason for the higher particle dispersion of the polyol synthesized particles could be because the DEG used in the synthesis process may be a better stabilizing agent than the ethanol used in the pepti synthesis process.

In terms of the dip-coating experiments, it was proposed that the mechanisms responsible for the adherence of the ZnO NPs to the nylon textile was the formation of hydrogen bonds and dipole bonds between the ZnO NPs and the oxygen and hydrogen atoms from the amide groups of the nylon molecule, that were available for interaction on the textile's surface.

It was found that changes in the operation parameters, such as speeds and dipping times, did not present a significant effect on the quantity achieved for the coat. On the other hand, the synthesis pathway with which the ZnO NPs used for the coating were created has a direct effect on the amount of ZnO NPs that adhered to the textile, with the polyol synthesized ZnO NPs proving more successful. As mentioned, this was attributed to the notably higher particle dispersion observed in the polyol synthesized NPs. Additionally, it was found that a significantly higher quantity of ZnO NPs adhered to the nylon textile, when this textile has been previously treated with acid at mild conditions (room temperature and low concentrations). It was proposed that the acid treatment of the nylon lead to a small fraction of the amide groups of the nylon hydrolyze. The acid hydrolysis of the amide groups lead to the formation of carboxylic acid and amine groups which increase the amount of potential bonding sites.

The highest amount of ZnO NPs coating achieved for each of the types of suspensions used in the experiments was:

- Pepti 5 g/L: 14.37 mg (201.69 mg of ZnO/g of nylon ± 27.79)
- Pepti 10 g/L: 6.29 mg (119.85 mg of ZnO/g of nylon ± 11.93)
- Polyol 30 g/L: 17.1 mg (225.32 mg of ZnO/g of nylon ± 16.76)

The polyol synthesized NPs proved to be the most effective for the coating process in all regards: the highest total amount of coating achieved, the lowest percentage of coating lost after the washing process and the lowest proportional standard deviations for the measured added weights. From the washing experiments, it was found that no more than 30% of the added weight achieved post coating was lost after the nylon samples were exposed to running water, this was attributed to the strength of the hydrogen bonds that would've been formed according to the proposed adherence mechanisms. However, it was proposed that more thorough and standardized washing tests be conducted to reach conclusive results on the resistance of the coating when exposed to flowing water.

Results and observations for the SEM, BSE and EDX characterizations confirmed that the added weights that were measured corresponded to the coatings that were achieved and that in turn, these coatings were in fact made from ZnO NPs.

FTIR characterizations were conducted on blank nylon samples which had been treated with NaOH, HCl, Acetic Acid and UVC exposure. The results however, were inconclusive with respect to the proposed theory that the acid and the UVC treatment were responsible for the hydrolysis of amide groups present in the nylon's surface into carboxylic acid and amine groups. It was therefore suggested that further work be conducted to find an optimal point in terms of the concentration of the acids or the exposure time of the nylon to UVC in which the most carboxylic acids and amine bonds are formed, before compromising the structure of the textile, and monitor these results through FTIR. In other words, carry out tests to confirm that the proposed hypothesized mechanisms are correct.

With regards to the antibacterial functionalization of the textile being effective in the dark, the results for the NBT degradation tests evidence the presence of ROs in the interaction between NBT solution and the ZnO coating nylon textiles, specifically the superoxide ion ($\cdot O_2^-$), based on the formula for NBT degradation, shown in **Figure 3**. This is in turn evidence that the ZnO coated nylon textile can exhibit antibacterial properties in the dark through the generation of ROS. It was found that there was no difference on the efficiency of NBT degradation between the pepti and the polyol synthesized ZnO NPs, indicating that their difference in size was not a decisive factor in their efficiency for generating ROS in the dark during a period of 48 h.

There are several suggestions that can be made for further future work on this project, including the performance of other tests to evaluate the antibacterial property of the ZnO functionalized nylon in the dark through other possible mechanisms, further analysis on the effects of the acid and UVC treatment of the nylon surface to validate whether the proposed adherence mechanisms in this thesis are in fact correct, the application of more thorough and standardized washing tests to determining the stability of the ZnO coating adherence to the textile and the research on other forms of surface activation, such as plasma, that can be applied to improve further the efficiency of the coating process.

Ultimately, it can be concluded that from the results obtained through the development of this thesis, there are some clear factors that might lead to the desired properties in the antibacterial functionalized textile from industrial waste water treatment, using a nylon 6 textile. On the one hand, acid pretreatment of the textile using soft acids at low concentrations significantly increases the amount of ZnO NPs that adhere to the textile. The use of polyol synthesized NPs also has a positive effect on the amount of ZnO NPs that adhere to the textile and leads to a good performance with regards to resistance against coating loss when exposed to running water. The surface activation of the textile using UVC light showed some promising results which should be explored further, since

both the acid pretreated coated textiles and the UVC surface activated coated textiles had presented evidence of ROS formation under dark conditions.

Another suggestion that can be made in terms of future experiments, with regards to evaluating the performance of the different factors that were evaluated when coating the nylon substrate, involves comparing different concentrations of the ZnO NPs suspensions. Some observations were made on the efficiency of both the pepti and the polyol suspensions, however, a more reliable comparison could be made by evaluating the performance of both suspensions at the same concentration i.e. both the polyol and the pepti suspensions at 5 g/L or both at 10 g/L. This would allow the results to give more reliable information with regards to the effect that the type of synthesis process has on the efficiency of the coating.

References

1. ACE Films. (2023). *ACE Films a Pioneer of Embossed Films for Hygiene and Medical*. ace-films.be. Retrieved June 4, 2023, from https://ace-films.be/about/
2. Adams, L. K., Lyon, D. Y., & Alvarez, P. J.J. (2006, September 29). Comparative Eco-Toxicity of Nanoscale TiO2, SiO2 and ZnO Water Suspensions. *Water Research*, *40*(19), 3527 - 3532. https://doi.org/10.1016/j.watres.2006.08.004
3. Alves, T.E.P., Kolodziej, C., Burda, C., & Franco Jr, A. (2018, March 6). Effect of particle shape and size on the morphology and optical properties of zinc oxide synthesized by the polyol method. *Materials and Design*, *146*, 125-133. https://doi.org/10.1016/j.matdes.2018.03.013
4. Amani, A., Montazer, M., & Mahmoudirad, M. (2018, November 14). Synthesis of applicable hydrogel corn silk/ZnO nanocomposites on polyester fabric with antimicrobial properties and low cytotoxicity. *International Journal of Biological Macromolecules*, *123*, 1079 - 1090. https://doi.org/10.1016/j.ijbiomac.2018.11.093
5. Ameta, R., Solanki, M. S., Benjamin, S., & Ameta, S. C. (2018). Chapter 6 - Photocatalysis. In S. C. Ameta & R. Ameta (Eds.), *Advanced Oxidation Processes for Wastewater Treatment: Emerging Green Chemical Technology* (pp. 135 - 175). Elsevier Science. https://www.sciencedirect.com/science/article/abs/pii/B9780128104996000061
6. Ameta, S. C. (2018). Chapter 1 - Introduction. In R. Ameta (Ed.), *Advanced Oxidation Processes for Wastewater Treatment: Emerging Green Chemical Technology* (pp. 1 - 12). Elsevier Science. https://www.sciencedirect.com/book/9780128104996/advanced-oxidation-processes-for-waste-water-treatment#book-info
7. Ameta, S. C., & Ameta, R. (Eds.). (2018). *Advanced Oxidation Processes for Wastewater Treatment: Emerging Green Chemical Technology*. Elsevier Science.
8. Arshi, N., Koo, B. H., Kumar, S., Ahmed, F., & Anwar, M. S. (2011, March 1). Growth and characterization of ZnO nanorods by microwave-assisted route: green chemistry approach. *Advanced Materials Letters*, *2*(3), 183 - 187. 10.5185/amlett.2011.1213
9. Babayevska, N., Przysiecka, L., Iatsunskyi, I., Nowaczyk, G., Jarek, M., Janiszewska, E., & Jurga, S. (2022, May 17). ZnO Size and Shape Effect on Antibacterial Activity and Cytotoxicity Profile. *Scientific Report*, *12*(8148). https://doi.org/10.1038/s41598-022-12134-3
10. Bai, X., Li, L., Tan, L., Liu, T., & Meng, X. (2014, December 24). Solvothermal Synthesis of ZnO Nanoparticles and Anti-Infection Application in Vivo. *Applied Materials and Interfaces*, *7*(2), 1308-1317. https://doi.org/10.1021/am507532p
11. Baig, N., Kammakakam, I., & Falath, W. (2021, February 23). Nanomaterials: A review of synthesis methods, properties, recent progress, and challenges. *Materials Advances*, *2*, 1821 - 1871. 10.1039/d0ma00807a
12. Bakr, A. R., & Rahaman, M. S. (2016, June). Electrochemical Efficacy of a Carboxylated Multiwalled Carbon Nanotube Filter for the Removal of Ibuprofen from Aqueous Solutions under Acidic Conditions. *Chemosphere*, *153*, 508 - 520. 10.1016/j.chemosphere.2016.03.078
13. Beers, B. (2023, March 28). *P-Value: What It Is, How to Calculate It, and Why It Matters*. Investopedia. Retrieved July 26, 2023, from https://www.investopedia.com/terms/p/p-value.asp
14. Bergwerf, H. (2023). *Molview*. MolView. Retrieved August 19, 2023, from https://molview.org/
15. Bielski, B. H., Shiue, G. G., & Bajuk, S. (1980, April 1). Reduction of nitro blue tetrazolium by CO2- and O2- radicals. *Journal of Physical Chemistry*, *84*(8), 830 - 833. https://doi.org/10.1021/j100445a006
16. Brayner, R., Ferrari-Iliou, R., Brivois, N., Djediat, S., Benedetti, M. F., & Fiévet, F. (2006, Marzo 11). Toxicological Impact Studies Based on Escherichia coli Bacteria in Ultrafine ZnO Nanoparticles Colloidal Medium. *Nano Letters*, *6*(4), 866-870. https://doi.org/10.1021/nl052326h

17. Center for Disease Control. (2016, October 11). *Industrial Water | Other Uses of Water | Healthy Water*. CDC. Retrieved October 25, 2023, from https://www.cdc.gov/healthywater/other/industrial/index.html
18. Clark, J. (2023, January 22). *The Hydrolysis of Amides*. Chemistry LibreTexts. Retrieved August 20, 2023, from https://chem.libretexts.org/Bookshelves/Organic_Chemistry/Supplemental_Modules_(Organic_Chemistry)/Amides/Reactivity_of_Amides/The_Hydrolysis_of_Amides
19. Collivignarelli, M. C., Abbà, A., Benigna, I., Sorlini, S., & Torretta, V. (2017, December 31). Overview of the Main Disinfection Processes for Wastewater and Drinking Water Treatment Plants. *Sustainability*, *18*(1). https://doi.org/10.3390/su10010086
20. Damle, M., Badhe, P., Mahajan, G., & RV, A. (2018, April 09). Immobilisation of Marine Pectinase on Nylon 6,6. *Journal of Textile Engineering and Fashion Technologies*, *4*(2), 181-187. 10.15406/jteft.2018.04.00138
21. Da Silva, B. L., Abuçafy, M. P., Manaia, E. B., Oshiro Junior, J. A., Chiari-Andreó, B. G., Pietro, R. C. R., & Chiavacci, L. A. (2023, January 2). Relationship Between Structure and Antimicrobial Activity of Zinc Oxide Nanoparticles: An Overview. *International Journal of Nanomedicine*, *14*(2019), 9395 - 9410. http://doi.org/10.2147/IJN.S216204
22. Database of ATR-FT-IR Spectra of Various Materials. (2023). *Polyamide (Nylon 6) – Database of ATR-FT-IR spectra of various materials*. Database of ATR-FT-IR spectra of various materials. Retrieved July 30, 2023, from https://spectra.chem.ut.ee/textile-fibres/polyamide/
23. Debbarma, M., Das, S., & Saha, M. (2013, April 28). Effect of Reducing Agents on the Structure of Zinc Oxide under Microwave Irradiation. *Advances in Manufacturing*, *1*, 183 - 186. DOI 10.1007/s40436-013-0020-7
24. DeMello, N. (2019, July 1). *12.6: Intermolecular Forces: Dispersion, Dipole–Dipole, Hydrogen Bonding, and Ion-Dipole*. Chemistry LibreTexts. Retrieved August 19, 2023, from https://chem.libretexts.org/Courses/can/intro/12%3A_Liquids_Solids_and_Intermolecular_Forces/12.6%3A_Intermolecular_Forces%3A_Dispersion_DipoleDipole_Hydrogen_Bonding_and_Ion-Dipole
25. Deng, Y., & Zhao, R. (2015, September 18). Advanced Oxidation Processes (AOPs) in Wastewater Treatment. *Water Pollution*, *1*, 167 - 176. 10.1007/s40726-015-0015-z
26. Dong, C., Fang, W., Yi, Q., & Zhang, J. (2022, August 29). A comprehensive review on reactive oxygen species (ROS) in advanced oxidation processes (AOPs). *Chemosphere*, *308*. https://doi.org/10.1016/j.chemosphere.2022.136205
27. Droepenu, E. K., Wee, B. S., Chin, S. F., Kok, K. Y., & Maligan, M. F. (2021, August 14). Zinc Oxide Nanoparticles Synthesis Methods and its Effect on Morphology: A Review. *Biointerface Research in Applied Chemistry*, *12*(3), 4261 - 4292. https://doi.org/10.33263/BRIAC123.42614292
28. EATON. (2016, June). *SENTINEL® and SNAP-RING® monofilament filter bags for surface filtration*. Eaton - FILTER BAGS Monofilament. https://www.eaton.com/nl/nl-nl/catalog/filtration/monofilament-filter-bags.html
29. Essentra Components. (2022, March 22). *Nylon 6 vs. nylon 6/6*. Essentra Components. Retrieved August 7, 2023, from https://www.essentracomponents.com/en-us/news/solutions/fastening-components/the-differences-between-nylon-6-and-nylon-6-6
30. European Institute of Innovation and Technology. (2022). *EIT at a glance | EIT*. European Institute of Innovation and Technology. Retrieved August 3, 2023, from https://eit.europa.eu/about-us/eit-glance
31. Farcy, A., Lambert, S., & Heinrichs, B. (2023). *Development of antibacterial functionalized textiles by 3D printing (DAF3D): development of zinc oxide catalysts* [Nanomaterials, Catalysis, Electrochemistry (NCE) Department of Chemical Engineering]. University of Liège, Belgium.
32. Farcy, A., Lambert, S. D., Heinrichs, B., & Mahy, J. G. (2022). *Development of Antibacterial Functionalized Textiles by 3D Printing: Development of Zinc Oxide Catalysts*.
33. Fiedot-Tobola, M., Ciesielska, M., Maliszewska, I., Rac-Rumijowska, O., Suchorska-Wozniak, P., Teterycz, H., & Bryjak, M. (2018, April 30). Deposition of Zinc Oxide on

Different Polymer Textiles and Their Antibacterial Properties. *Materials*, *11*(5), 707. 10.3390/ma11050707
34. Fields, D. (2019, January 25). *What is Transmission Electron Microscopy?* News Medical. Retrieved August 18, 2023, from https://www.news-medical.net/life-sciences/What-is-Transmission-Electron-Microscopy.aspx
35. Gaston, B., & Protter, C. (2022, August 21). *Energy-Dispersive X-ray Spectroscopy (EDS)*. Chemistry LibreTexts. Retrieved August 18, 2023, from https://chem.libretexts.org/Courses/Franklin_and_Marshall_College/Introduction_to_Materials_Characterization__CHM_412_Collaborative_Text/Spectroscopy/Energy-Dispersive_X-ray_Spectroscopy_(EDS)
36. Gevorg, S. (2022). *Amide Hydrolysis: Acid and Base-Catalyzed Mechanism*. Chemistry Steps. Retrieved August 20, 2023, from https://www.chemistrysteps.com/amides-hydrolysis-acid-and-base-catalyzed-mechanism/
37. Goutam, S. P., Saxena, G., Roy, D., Yadav, A. K., & Bharagava, R. N. (2019). Green Synthesis of Nanoparticles and Their Application in Water and Wastewater Treatment. In *Bioremediation of Industrial Waste for Environmental Safety: Industrial Waste and Its Management* (1st ed., Vol. 16, pp. 349-379). Springer Nature Singapore. 10.1007/978-981-13-1891-7_16
38. Henry, D., & Mogk, D. (2023, October 18). *BraggsLaw*. SERC (Carleton). Retrieved November 26, 2023, from https://serc.carleton.edu/research_education/geochemsheets/BraggsLaw.html
39. Hirota, K., Sugimoto, M., Kato, M., Tsukagoshi, K., Tanigawa, T., & Sugimoto, H. (2009, October 12). Preparation of zinc oxide ceramics with a sustainable antibacterial activity under dark conditions. *Ceramics International*, *36*(2), 497 - 506. https://doi.org/10.1016/j.ceramint.2009.09.026
40. Hocker, S., Rhudy, A. K., Ginsburg, G., & Kranbuehl, D. E. (2014, September 26). Polyamide hydrolysis accelerated by small weak organic acids. *Polymer*, *55*(20), 5057 - 5064. https://doi.org/10.1016/j.polymer.2014.08.010
41. Holyavka, M., Pankova, S., Koroleva, V., Vyshkvorkina, Y., Lukin, A., Kondratyev, M., & Artyukhov, V. (2019, December). Influence of UV radiation on molecular structure and catalytic activity of free and immobilized bromelain, ficin and papain. *Journal of Photochemistry and Photobiology B: Bioligy*, *201*. https://doi.org/10.1016/j.jphotobiol.2019.111681
42. ImageJ. (2012). *ImageJ: Image Processing and Analysis in Java*. ImageJ. Retrieved November 27, 2023, from https://imagej.net/ij/
43. International Organization for Standardization (ISO). (2021). *ISO 9001:2015(en), Quality management systems — Requirements*. ISO. Retrieved December 6, 2023, from https://www.iso.org/obp/ui#iso:std:iso:6330:ed-4:v1:en
44. Joe, A., Park, S.-H., Shim, K.-D., Kim, D.-J., Jhee, K.-H., Lee, H.-W., Heo, C.-H., Kim, H.-M., & Jang, E.-S. (2016, October 15). Antibacterial Mechanism of ZnO Nanoparticles under Dark Conditions. *Industrial and Engineering Chemistry*, *45*(25), 430 - 439. https://doi.org/10.1016/j.jiec.2016.10.013
45. Johnson, P. S., Cook, P. L., Liu, X., Yang, W., Bai, Y., Abbott, N. L., & Himpsel, F. J. (2011, July 28). Universal mechanism for breaking amide bonds by ionizing radiation. *Journal of Chemical Physics*, *135*(4). 10.1063/1.3613638.
46. Jun, B.-M., Kim, S. H., Kwak, S. K., & Kwon, Y.-N. (2018, March 10). Effect of Acidic Aqueous Solution on Chemical and Physical Properties of Polyamide NF Membranes. *Applied Surface Science*, *444*, 387-398. https://doi.org/10.1016/j.apsusc.2018.03.078
47. Justia Patents. (1994, October 7). *Process for preparing antimicrobial polymeric materials using irradiation*. Justia Patents. Retrieved August 7, 2023, from https://patents.justia.com/patent/5428078
48. Kadam, A. R., Parauha, Y. R., Michalska-Domanska, M., & Dhoble, N. S. (2022). Chapter 10 - Nanosphors for radiation dosimetry. In *Radiation Dosimetry Phosphors* (pp. 215-277). Woodhead Publishing. https://doi.org/10.1016/B978-0-323-85471-9.00011-7

49. Kasemets, K., Ivask, A., Dubourguier, H.-C., & Kahru, A. (2009, May 30). Toxicity of nanoparticles of ZnO, CuO and TiO2 to yeast Saccharomyces cerevisiae. *Toxicology in Vitro*, *23*(6), 1116 - 1122. https://doi.org/10.1016/j.tiv.2009.05.015
50. Kolská, Z., Polanský, R., Prosr, P., Zemanová, M., Rysánek, P., Slepicka, P., & Svorcík, V. (2017, December 8). Properties of Polyamide Nanofibers Treated by UV-A Radiation. *Materials Letters*, *214*, 264-267. https://doi.org/10.1016/j.matlet.2017.12.029
51. Krosel, A. (2022, August 8). *How To Calculate Statistical Significance (And Its Importance)*. Indeed. Retrieved July 26, 2023, from https://www.indeed.com/career-advice/career-development/how-to-calculate-statistical-significance
52. Kurian, M. (2021, March 21). Advanced Oxidation Processes and Nanomaterials - A Review. *Cleaner Engineering and Technology*, *2*. https://doi.org/10.1016/j.clet.2021.100090
53. Kvilhaug, S. (2021, October 6). *Statistical Significance Definition, Types, and How It's Calculated*. Investopedia. Retrieved July 26, 2023, from https://www.investopedia.com/terms/s/statistical-significance.asp
54. Malis, D., Jeršek, B., Tomšič, B., Štular, D., Golja, B., Kapun, G., & Simončič, B. (2019, October 17). Antibacterial Activity and Biodegradation of Cellulose Fiber Blends with Incorporated ZnO. *Materials*, *12*(20). https://doi.org/10.3390/ma12203399
55. Matei, A., Tucureanu, V., & Dumitrescu, L. (2014). Aspects Regarding Synthesis and Applications of ZnO Nanomaterials. *Bulletin of the Transilvania University of Brasov*, *7*(56), 45-52. http://rs.unitbv.ro/BU2013/2014/BULETIN%20I/Matei%20A.pdf
56. Merck. (2022, October 2). *What is FTIR Spectroscopy?* Merck - Photometry and Reflectometry. Retrieved August 18, 2023, from https://www.sigmaaldrich.com/BE/en/technical-documents/technical-article/analytical-chemistry/photometry-and-reflectometry/ftir-spectroscopy
57. Montero, L. H., Paraguay-Delgado, F., & Mendoza, N. P. (2021, August 1). Structure and Morphology Changes of Zinc Oxide Nanoparticles. *Microscopy and Microanalysis*, *27*(S1), 2342-2343. https://doi.org/10.1017/S1431927621008424
58. Moore, J., Zhou, J., & Garand, E. (2023, August 3). *2.5: Day 13- Alcohols, Carboxylic Acids, Amines, Amides; Hydrogen Bonding*. Chemistry LibreTexts. Retrieved August 20, 2023, from https://chem.libretexts.org/Bookshelves/General_Chemistry/Interactive_Chemistry_(Moore_Zhou_and_Garand)/02%3A_Unit_Two/2.05%3A_Day_13-_Alcohols_Carboxylic_Acids_Amines_Amides_Hydrogen_Bonding
59. Nguyen, V. T., Vu, V. T., Nguyen, T. H., Nguyen, T. A., Tran, V. K., & Nguyen-Tri, P. (2019, June 17). Antibacterial Activity of TiO2- and ZnO Decorated with Silver Nanoparticles. *Journal of Composites Science*, *3*(2). https://doi.org/10.3390/jcs3020061
60. Noor, N., Mutalik, S., Younas, M. W., Chan, C. Y., Thakur, S., Wang, F., Yao, M. Z., Mou, Q., & Leung, P. H. (2019, December 3). Durable Antimicrobial Behaviour from Silver-Graphene Coated Medical Textile Composites. *Polymers*, *11*(12). https://doi.org/10.3390/polym11122000
61. Nourbakhsh, S., Montazer, M., & Khandaghabadi, Z. (2018, February). Zinc Oxide Nanoparticles Coating on Polyester Fabric Functionalized Through Alkali Treatment. *Journal of Industrial Textiles*, *47*(6). https://doi.org/10.1177/1528083716657819
62. Parihar, V., Raja, M., & Paulose, R. (2018, August 01). A Brief Review of Structural, Electrical and Electrochemical Properties of Zinc Oxide Nanoparticles. *Reviews on Advanced Materials Science*, *53*, 119-130. https://doi.org/10.1515/rams-2018-0009
63. Perkin Elmer. (2019). *MP, TG, and Structure of Common Polymers*. PerkinElmer. Retrieved May 30, 2023, from https://resources.perkinelmer.com/corporate/cmsresources/images/44-74863tch_mptgandstructureofcommonpolymers.pdf
64. Picraux, S. T. (2023, August 28). *Nanotechnology - Molecular, Assembly, Fabrication*. Britannica. Retrieved October 30, 2023, from https://www.britannica.com/technology/nanotechnology/Bottom-up-approach
65. Prasanna, L., & Rajagopalan, V. (2016, December 8). A New Synergetic Nanocomposite for Dye Degradation in Dark and Light. *Scientific Reports*, *6*. 10.1038/srep38606

66. Prasanna, V. L., & Vijayaraghavan, R. (2015, July 29). Insight into the Mechanism of Antibacterial Activity of ZnO: Surface Defects Mediated Reactive Oxygen Species Even in the Dark. *Langmuir*, *31*(33), 9155 - 9162. https://doi.org/10.1021/acs.langmuir.5b02266
67. Raghupathi, K. R., Koodali, R., & Manna, A. C. (2011, April 5). Size-dependent bacterial growth inhibition and mechanism of antibacterial activity of zinc oxide nanoparticles. *Langmuir*, *27*(7), 4020 - 4028. 10.1021/la104825u
68. Rajan, S., Venugopal, A., Kozhikkalathil, H., Valappil, S., Kale, M., Mann, M., Ahuja, P., & Munjal, S. (2023, June 9). Synthesis of ZnO nanoparticles by precipitation method: Characterizations and applications in decipherment of latent fingerprints. *Materials Today: Proceedings*. https://doi.org/10.1016/j.matpr.2023.05.680
69. Shahid, R., Soliman, H. M.A., Fathy, M., & Muhammed, M. (2012, December). Novel Low Temperature Route for Large Scale Synthesis of ZnO Quantum Dots. *International Journal of Sciences*, *1*, 153 - 161. https://papers.ssrn.com/sol3/papers.cfm?abstract_id=2572098
70. Shamhari, N. M., Wee, B. S., Chin, S. F., & Kok, K. Y. (2018, July). Synthesis and Characterization of Zinc Oxide Nanoparticles with Small Particle Size Distribution. *Acta Chimica Slovenica*, *65*(3), 578-585. DOI:10.17344/acsi.2018.4213
71. Sirelkhatim, A., Mahmud, S., Seeni, A., Haida, N., Kaus, M., Ann, L. C., Bakhori, S. K. M., Hasan, H., & Mohamad, D. (2015, April 19). *Review on Zinc Oxide Nanoparticles: Antibacterial Activity and Toxicity Mechanism*, *7*(3), 219-42. DOI 10.1007/s40820-015-0040-x
72. Social Science Statistics. (2023). *Social Science Statistics*. T-Test Calculator for 2 Independent Means. Retrieved July 28, 2023, from https://www.socscistatistics.com/tests/studentttest/default.aspx
73. Somkuwar, V. (2021). Textiles Functionalization - A Review of Materials, Processes, and Assessment. In M. K. Singh & B. Kumar (Eds.), *Textiles for Functional Applications*. IntechOpen. 10.5772/intechopen.96936
74. Song, T., Liu, L., Xu, F., Pan, Y., Qian, M., Li, D., & Yang, R. (2022, July 14). Multi-dimensional characterizations of washing durable ZnO/phosphazene-siloxane coated fabrics via ToF-SIMS and XPS. *Polymer Testing*, *114*. https://doi.org/10.1016/j.polymertesting.2022.107684
75. Speakman, S. A. (2020). *Introduction to X-Ray Powder Diffraction Data Analysis*. Applications of In situ X-Ray Diffraction. Retrieved August 19, 2023, from http://prism.mit.edu/xray/documents/2%20Introduction%20to%20XRPD%20Data%20Analysis.pdf
76. Stankovic, A., Dimitrijevic, S., & Uskokovic, D. (2013, February 1). Influence of size scale and morphology on antibacterial properties of ZnO powders hydrothermally synthesized using different surface stabilizing agents. *Colloids and Surfaces B: Biointerfaces*, *102*, 21-28. https://doi.org/10.1016/j.colsurfb.2012.07.033
77. Sudrajat, H. (2017, December 5). Superior photocatalytic activity of polyester fabrics coated with zinc oxide from waste hot dipping zinc. *Journal of Cleaner Production*, *172*, 1722 - 1729. https://doi.org/10.1016/j.jclepro.2017.12.024
78. Sudrajat, H., & Babel, S. (2016, November). A new, cost-effective solar photoactive system N-ZnO@polyester fabric for degradation of recalcitrant compound in a continuous flow reactor. *Materials Research Bulletin*, *83*, 369-378. https://doi.org/10.1016/j.materresbull.2016.06.025
79. Szyk, B., & Szczepanek, A. (2023, June 30). *p-value Calculator | Formula | Interpretation*. Omni Calculator. Retrieved July 26, 2023, from https://www.omnicalculator.com/statistics/p-value#what-is-p-value
80. Talukdar, K. (2023, May 5). *Moseley's law: Statement, Analysis, Derivation, Application and Periodic table*. CollegeSearch.in. Retrieved November 26, 2023, from https://www.collegesearch.in/articles/moseley-law
81. Tanahashi, M., Yao, T., Kokubo, T., Minoda, M., Miyamoto, T., & Yamamuro, T. (1995, June). Apatite coated on organic polymers by biomimetic process: improvement in adhesion to substrate by HCl treatment. *Journal of Materials Science: Materials in Medicine*, *6*, 319 - 326. https://doi.org/10.1007/BF00120299

82. ThermoFischer Scientific. (2022, October 2). *Electrons in SEM*. ThermoFischer Scientific - Materials Science Learning Center. Retrieved August 18, 2023, from https://www.thermofisher.com/be/en/home/materials-science/learning-center/applications/sem-electrons.html
83. Thompson, R., Austin, D., Wang, C., Neville, A., & Lin, L. (2021, April 1). Low-frequency plasma activation of nylon 6. *Applied Surface Science*, *544*. https://doi.org/10.1016/j.apsusc.2021.148929
84. Tojo, Y., Syou, R., Yoshida, M., Momose, J., Ginya, H., Takahashi, M., Tajima, H., & Yohda, M. (2006, August 17). Pretreatment of Polyamide Monofilament with Hydrochloric Acid Improves Sensitivity of Three-Dimensional Microarray, Bio-Strand. *Journal OF Bioscience and Bioengineering*, *102*(5), 474-477. 10.1263/jbb.102.474
85. Turney, S. (2022, April 29). *Student's t Table (Free Download) | Guide & Examples*. Scribbr. Retrieved July 26, 2023, from https://www.scribbr.com/statistics/students-t-table/
86. Tyuftin, A. A., & Kerry, J. P. (2020, January 27). Review of Surface Treatment Methods for Polyamide Films for Potential Application as Smart Packaging Materials: Surface Structure, Antimicrobial and Spectral Properties. *Food Packaging and Shelf Life*, *24*. https://doi.org/10.1016/j.fpsl.2020.100475
87. Ul-Hamid, A. (2018). *A Beginners' Guide to Scanning Electron Microscopy*. Springer International Publishing. https://doi.org/10.1007/978-3-319-98482-7
88. USGS. (2018, June 7). *Industrial Water Use | U.S. Geological Survey*. USGS.gov. Retrieved October 25, 2023, from https://www.usgs.gov/special-topics/water-science-school/science/industrial-water-use
89. Veerasingam, S., Ranjani, M., Venkatachalapathy, R., & Bagaev, A. (2020, August). Contributions of Fourier transform infrared spectroscopy in microplastic pollution research: A review. *Critical Reviews in Environmental Science and Technology*, *51*(1), 1 - 63. 10.1080/10643389.2020.1807450
90. Vendatu. (2023, August 11). *X-Ray Diffraction - Detailed Explanation and FAQs*. Vedantu. Retrieved August 18, 2023, from https://www.vedantu.com/physics/x-ray-diffraction
91. Verbic, A., Gorjanc, M., & Simoncic, B. (2019, August 27). Zinc Oxide for Functional Textile Coatings: Recent Advances. *Coatings*, *9*(9), 550. https://doi.org/10.3390/coatings9090550
92. Verma, M., & Haritash, A. K. (2020, March 25). Review of advanced oxidation processes (AOPs) for treatment of pharmaceutical wastewater. *Advances in Environmental Research*, *9*(1), 1-17. https://doi.org/10.12989/aer.2020.9.1.001
93. Wang, Z. L. (2004, June). Nanostructures of Zinc Oxide. *Materials Today*, *7*(6), 26-33. https://doi.org/10.1016/S1369-7021(04)00286-X
94. Wintzer, J., Walther, J., & Leuthaeusser, J. (2015). Studies on UVC Treatment of Polyamide Fibers for Improved Adhesion on TPU and TPA. *Journal of Chemistry and Chemical Engineering*, *9*, 38-44. doi: 10.17265/1934-7375/2015.01.005
95. Wolski, L., Walkowiak, A., & Ziolek, M. (2019, August 1). Formation of reactive oxygen species upon interaction of Au/ZnO with H2O2 and their activity in methylene blue degradation. *Catalysis Today*, *333*, 54 - 62. https://doi.org/10.1016/j.cattod.2018.04.004
96. Zhang, L., Jiang, Y., Ding, Y., Povey, M., & York, D. (2006, October 10). Investigation into the Antibacterial Behaviour of Suspensions of ZnO nanoparticles (ZnO nanofluids). *Journal of Nanoparticle Research*, *9*, 479 - 489. https://doi.org/10.1007/s11051-006-9150-1
97. Zhang, Z., Chen, Y., & Guo, J. (2018, September 11). ZnO nanorods patterned-textile using a novel hydrothermal method for sandwich structured-piezoelectric nanogenerator for human energy harvesting. *Physica E: Low-dimensional Systems and Nanostructures*, *15*, 212 - 218. https://doi.org/10.1016/j.physe.2018.09.007

ANNEXES

The following tables and graphs display the results of average added weight post-coating and average added weight post-wash, both in terms of the total added weight in mg and the normalized added weight calculations if mg of ZnO/g of nylon substrate, together with their corresponding standard deviations for each of the experimental sets described in **section 2.2**.

Table A - 1: Complete List of the Dip-Coating Experiments that were carried out. Organized by Experimental Set

Experimental Set	ZnO NPs Suspension	Experiment Parameters
Set A Optimization of Dipping Times	Pepti 10 g/L	3 x 3 x 3
		10 x 5 x 3
Set B Determination of the Washing Agent	Pepti 10 g/L	Ethanol
		Acetone
		RBS + Acetone
	Polyol 30 g/L	Ethanol
		Acetone
		RBS + Acetone
Set C Determination of Speed Up Setting	Pepti 10 g/L	300 mm/min
		2000 mm/min
		6000 mm/min
	Polyol 30 g/L	300 mm/min
		2000 mm/min
		6000 mm/min
Set D Different Concentrations of Pepti Suspensions	Pepti	10 g/L
		5 g/L
Set E Double and Triple Coats	Pepti 10 g/L	Single coat
		Double coat
	Polyol 30 g/L	Single coat

		Double coat
	Pepti 5 g/L	Single coat
		Double coat
		Triple coat
Set F Basic and Acid Pre-treatment	Pepti 5 g/L	NaOH 1%
		Acetic Acid 1%
		Acetic Acid 0.5M
		HCl 0.1M
		HCl 0.25M
		HCl 1M
	Pepti 10 g/L	Acetic Acid 0.5M
		Acetic Acid 1M
		HCl 0.25M
		HCl 0.5M
	Polyol 30 g/L	NaOH 1%
		Acetic Acid 1%
		Acetic Acid 0.5M
		Acetic Acid 1M
		HCl 0.1M
		HCl 0.25M
		HCl 0.5M
		HCl 1M
Set G	Pepti 5 g/L	Acetic Acid 0.5M

Triple Coat + Acid Surface Pretreatment		HCl 0.25M
Set H UVC Surface Activation	Sol - gel 10 g/L	1 min
		20 min
		60 min
	Polyol 30 g/L	1 min
		20 min
		60 min

Table A - 2: Added Weight Results for Experimental **Set A (2.2.1)**

Set A - Optimization of the Dipping Times (Pepti 10 g/L)		
	3 x 3 x 3*	**10 x 5 x 3***
Added Weight Post-Coating (mg)	7,55	8,78
Added Weight Post-Washing (mg)	6,43	7,22
Added Weight Post Wash (mg ZnO / g Nylon)	23,12	29,95

***** The format in which the parameters are being displayed corresponds to the following information: time dip x time up x number of iterations, in line with the descriptions presented in **Table 3**.

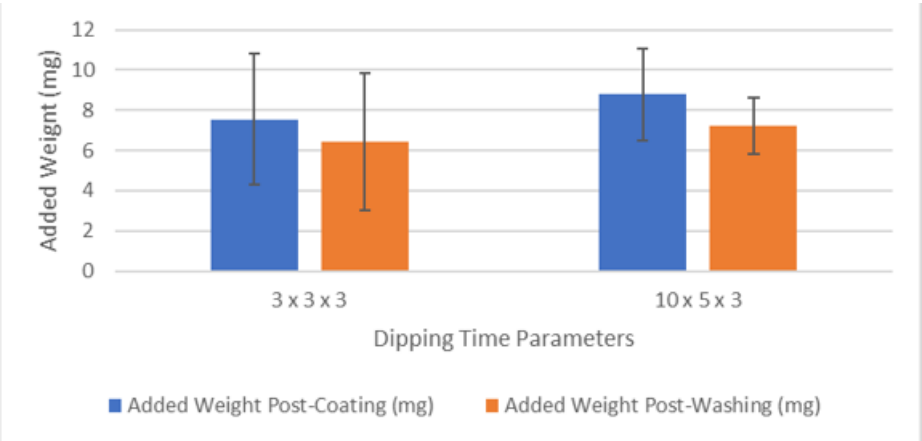

Figure A - 1: Added Weight Results for Experimental **Set A (2.2.1)** in terms of mg.

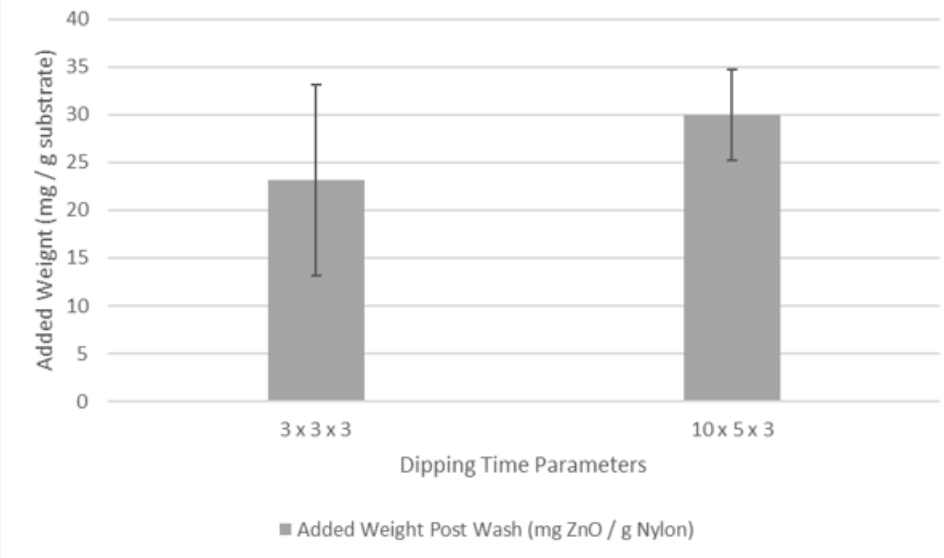

Figure A - 2: Added Weight Results for Experimental **Set A (2.2.1)** in terms of mg of ZnO / g of Nylon.

Table A - 3: Added Weight Results for Experimental **Set B (2.2.2)**

Set B - Determination of the Washing Agent						
	Pepti 10 g/L			**Polyol 30 g/L**		
	Ethanol	**Acetone**	**RBS + Acetone**	**Ethanol**	**Acetone**	**RBS + Acetone**
Added Weight Post-Coating (mg)	4.53	4.31	4.86	8.61	10.29	9.01
Added Weight Post-Washing (mg)	4	3.66	3.39	7.67	8.53	6.78
Added Weight Post-Washing (mg / g Substrate)	48.58	46.56	42.32	97.29	101.78	82.1

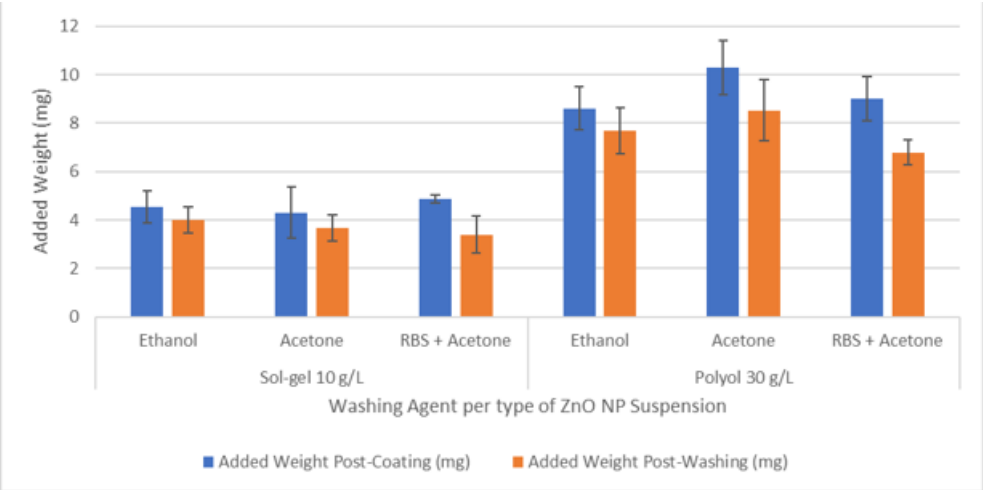

Figure A - 3: Added Weight Results for Experimental **Set B (2.2.2)** in terms of mg.

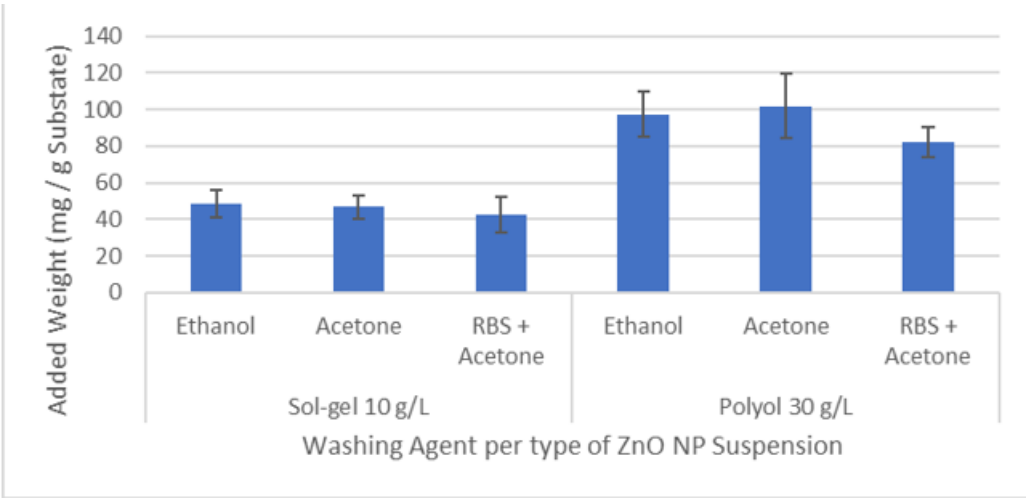

Figure A - 4: Added Weight Results for Experimental **Set B (2.2.2)** in terms of mg / g substrate

Table A - 4: Added Weight Results for Experimental **Set C (2.2.3)**

Set C - Determination of the Speed Up Setting						
	Pepti 10 g/L			**Polyol 30 g/L**		
Speed Up Setting (mm/min)	**300**	**2000**	**6000**	**300**	**2000**	**6000**
Added Weight Post-Coating (mg)	4.53	6.34	7.25	10.29	9.13	11.15
Added Weight Post-Washing (mg)	4	5.8	5.23	8.53	7.18	7.8

Added Weight Post-Washing (mg/g Substrate)	48.58	70.98	60.96	101.78	83.75	96.9

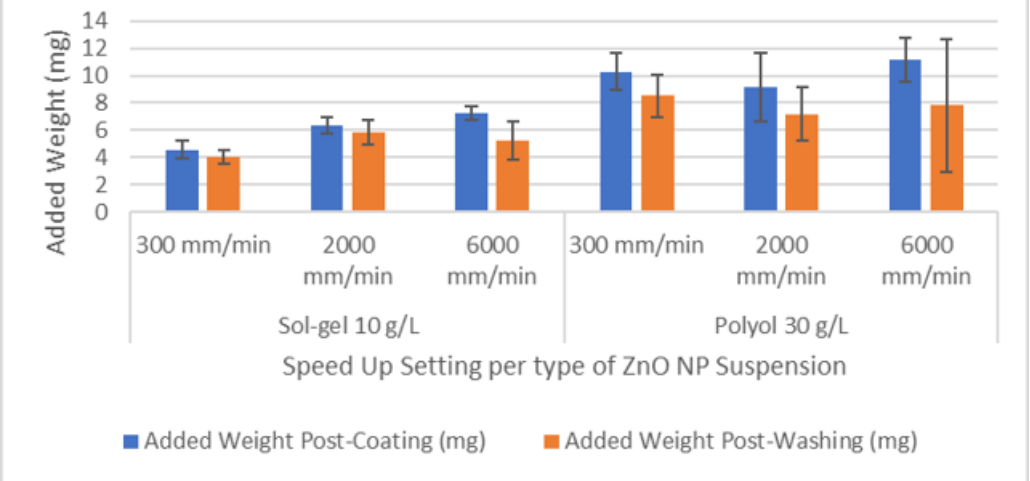

Figure A - 5: Added Weight Results for Experimental **Set C (2.2.3)** in terms of mg.

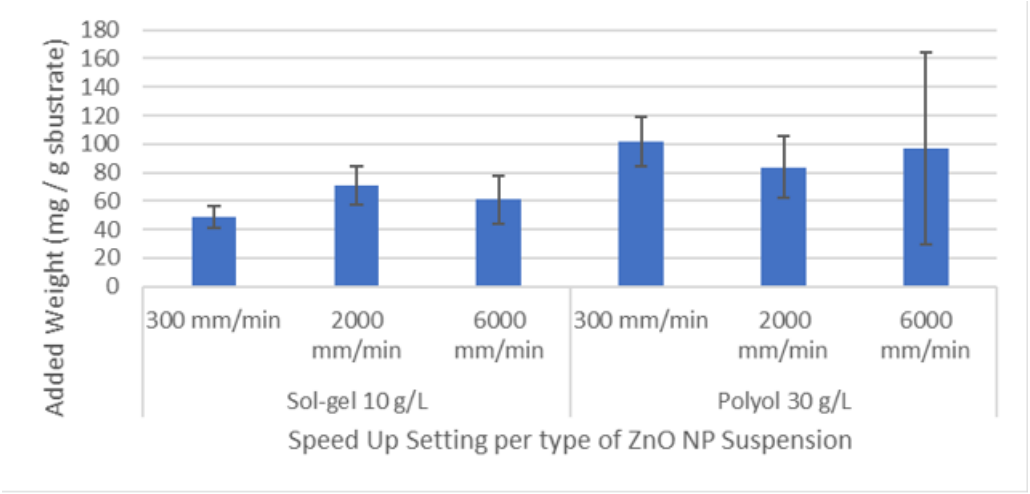

Figure A - 6: Added Weight Results for Experimental **Set C (2.2.3)** in terms of mg / g substrate

Table A - 5: Added Weight Results for Experimental **Set D (2.2.4)**

Set D - Different Concentrations of Pepti Suspensions			
	Added Weight Post-Coating (mg)	**Added Weight Post-Washing (mg)**	**Added Weight Post-Washing (mg/g Substrate)**
10 g/L	7.25	5.23	60.96
5 g/L	3.16	2.48	32.86

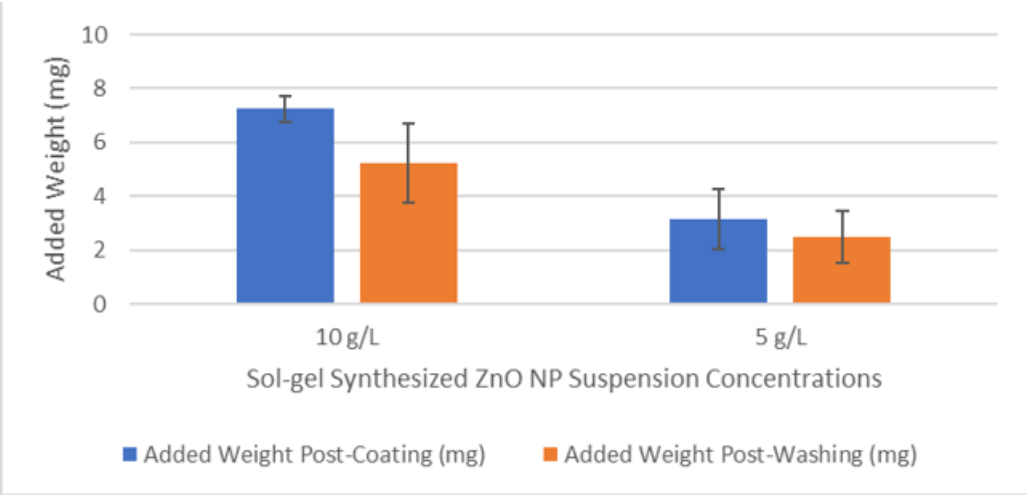

Figure A - 7: Added Weight Results for Experimental **Set D (2.2.4)** in terms of mg

Table A - 6: Added Weight Results for Experimental **Set E (2.2.5)**

Set E - Double and Triple Coating										
	Pepti 10 g/L			**Polyol 30 g/L**			**Pepti 5 g/L**			
	Coat 1	**Coat 2**	**Total Added Weight**	**Coat 1**	**Coat 2**	**Total Added Weight**	**Coat 1**	**Coat 2**	**Coat 3**	**Total Added Weight**
Added Weight Post-Coating (mg)	7.25	6.59	11.24	11.15	12.09	19.38	6.95	6.86	8.34	20.45
Added Weight Post-Washing (mg)	5.23	1.35	6.01	7.8	1.24	8.5	5.69	5.04	4.35	16.46
Added Weight Post-Washing (mg/g Substrate)	60.96	14.84	70	96.9	14.03	106	74.8	61.39	50.08	192.8

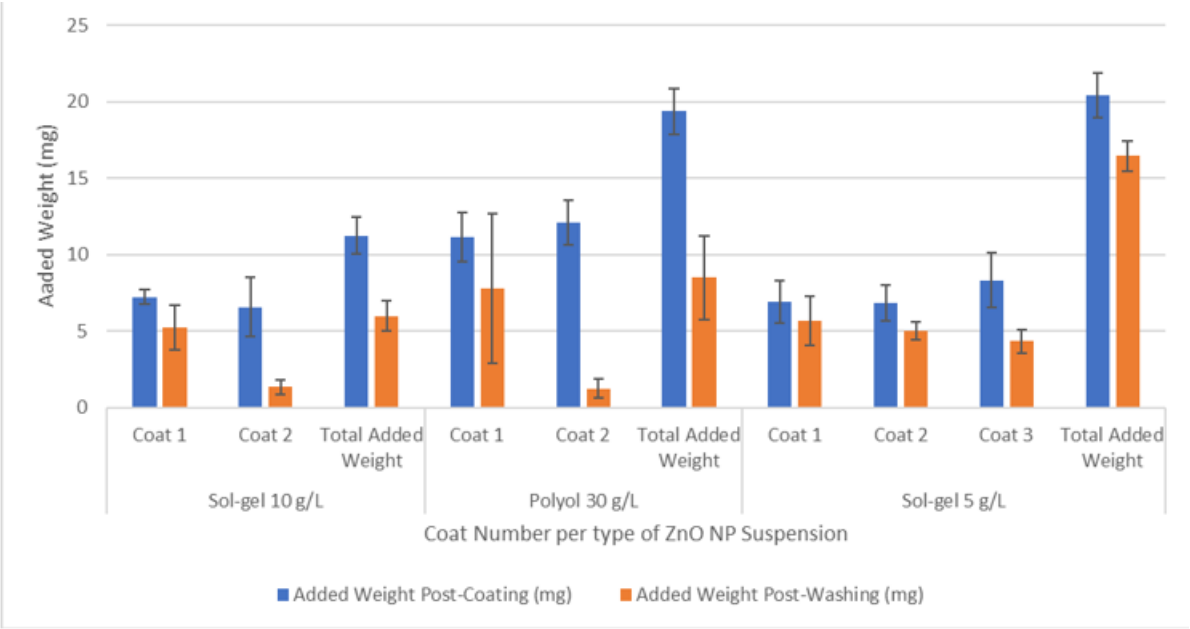

Figure A - 8: Added Weight Results for Experimental **Set E (2.2.5)** in terms of mg

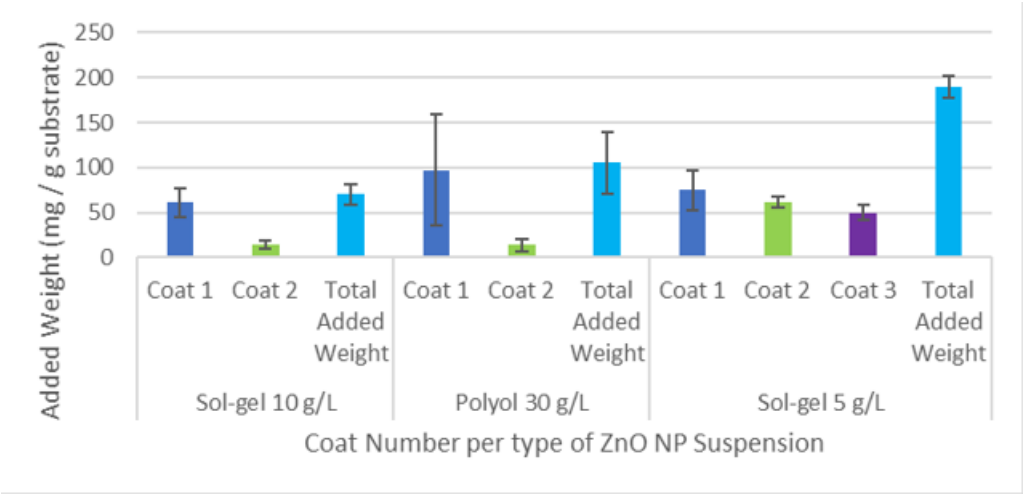

Figure A - 9: Added Weight Results for Experimental **Set E (2.2.5)** in terms of mg / g substrate.

Table A - 7: Added Weight Results for Experimental **Set F (2.2.6)** for ZnO NP suspension concentrations a) Pepti 5 g/L, b) Pepti 10 g/L, c) Polyol 30 g/L.

Set F - Basic and Acid Surface Pre-Treatment of the Nylon 6 - Pepti 5 g/L			
	Added Weight Post-Coating (mg)	**Added Weight Post-Washing (mg)**	**Added Weight Post-Washing (mg / g Substrate)**
NaOH 1%	6.42	2.77	35.33
Acetic Acid 1% (0.17M)	8.2	6.84	88.63
Acetic Acid 0.5M	6.94	5.62	79.83

HCl 0.1M	10.53	8.14	116.15
HCl 0.25M	8.54	6.19	88.29
HCl 1M	8.99	5.99	77.45
Set F - Basic and Acid Surface Pre-Treatment of the Nylon 6 - Pepti 10 g/L			
	Added Weight Post-Coating (mg)	**Added Weight Post-Washing (mg)**	**Added Weight Post-Washing (mg/g Substrate)**
Acetic Acid 0.5M	8,26	6,94	98,52
Acetic Acid 1M	5.19	3.76	54.81
HCl 0.25M	8.54	6.29	88.29
HCl 0.5M	6.06	4.44	56.99
Set F - Basic and Acid Surface Pre-Treatment of the Nylon 6 - Polyol 30 g/L			
	Added Weight Post-Coating (mg)	**Added Weight Post-Washing (mg)**	**Added Weight Post-Washing (mg/g Substrate)**
NaOH 1%	11.77	3.09	39.73
Acetic Acid 1% (0.17M)	17	14.64	204.63
Acetic Acid 0.5M	12.04	11.2	155.44
Acetic Acid 1M	9.4	8.75	124.95
HCl 0.1M	18.03	17.1	225.32
HCl 0.25M	15.62	13.8	185.92
HCl 0.5M	11.18	9.03	111.53
HCl 1M	16.01	6.95	90.61

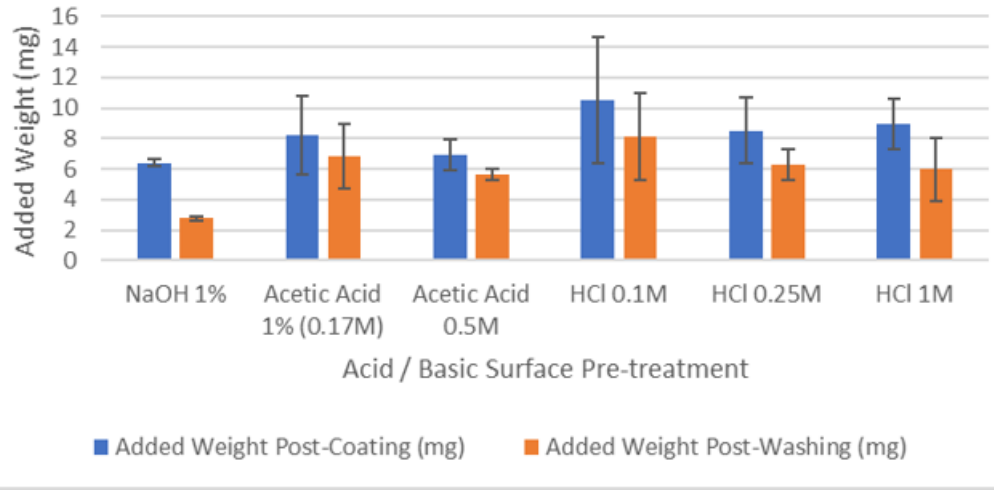

Figure A - 10: Added Weight Results for Experimental **Set F (2.2.6)** - ZnO NP Suspension Pepti 5 g/L

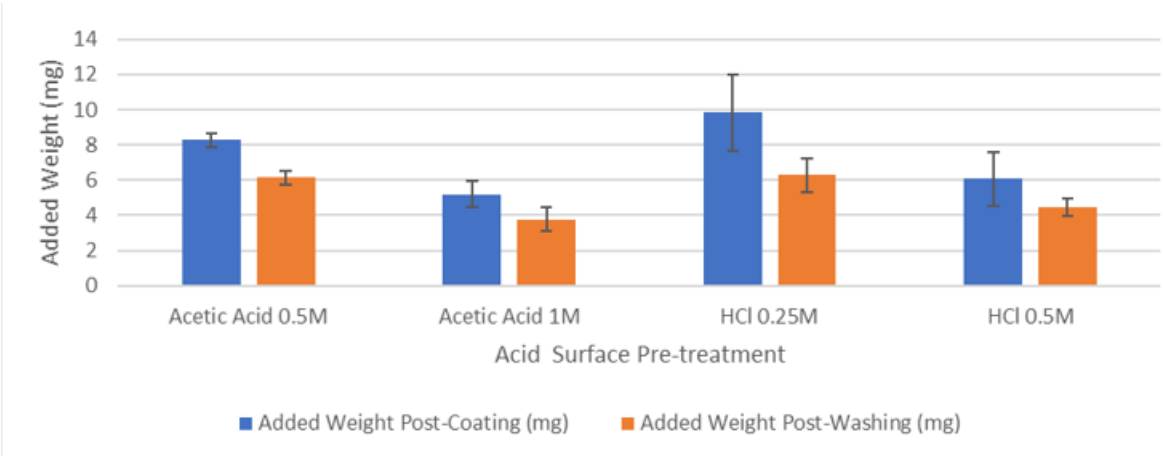

Figure A - 11: Added Weight Results for Experimental **Set F (2.2.6)** - ZnO NP Suspension Pepti 10 g/L

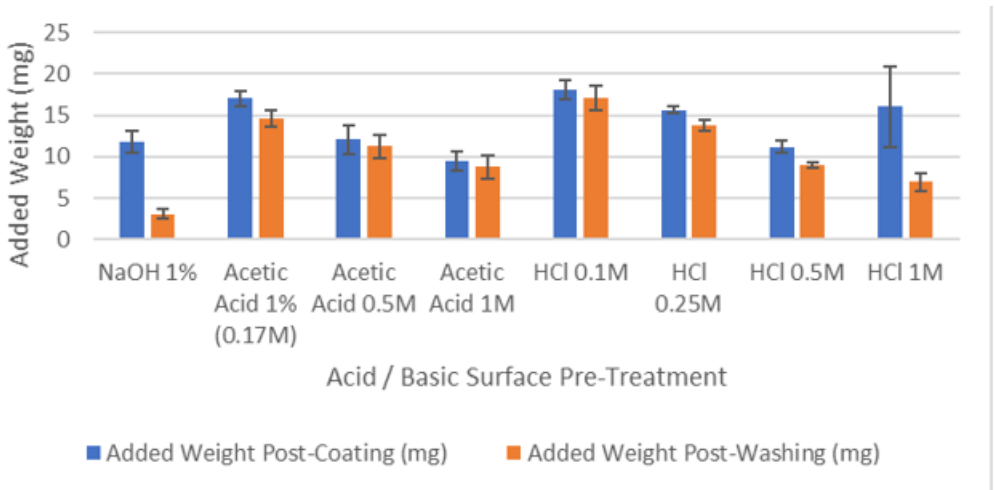

Figure A - 12: Added Weight Results for Experimental **Set F (2.2.6)** - ZnO NP Suspension Polyol 30 g/L

Table A - 8: Added Weight Results for Experimental **Set G (2.2.7)** for Zno NP suspension concentration Pepti 5 g/L

Set G - Double and Triple Coating with Acid Surface Pretreatment (Pepti 5 g/L)		
	Acetic Acid 0.5 M	**HCl 0.25 M**

	Coat 1	Coat 2	Coat 3	Total Added Weight	Coat 1	Coat 2	Coat 3	Total Added Weight
Added Weight Post-Coating (mg)	6.94	3.21	3.08	13.22	8.54	5.12	4.38	18.04
Added Weight Post-Washing (mg)	5.62	1.37	2.26	9.25	6.29	4.1	3.98	14.37
Added Weight Post-Washing (mg/g Substrate)	79.83	18.47	33.08	131.31	88.39	55.46	57.83	201.69

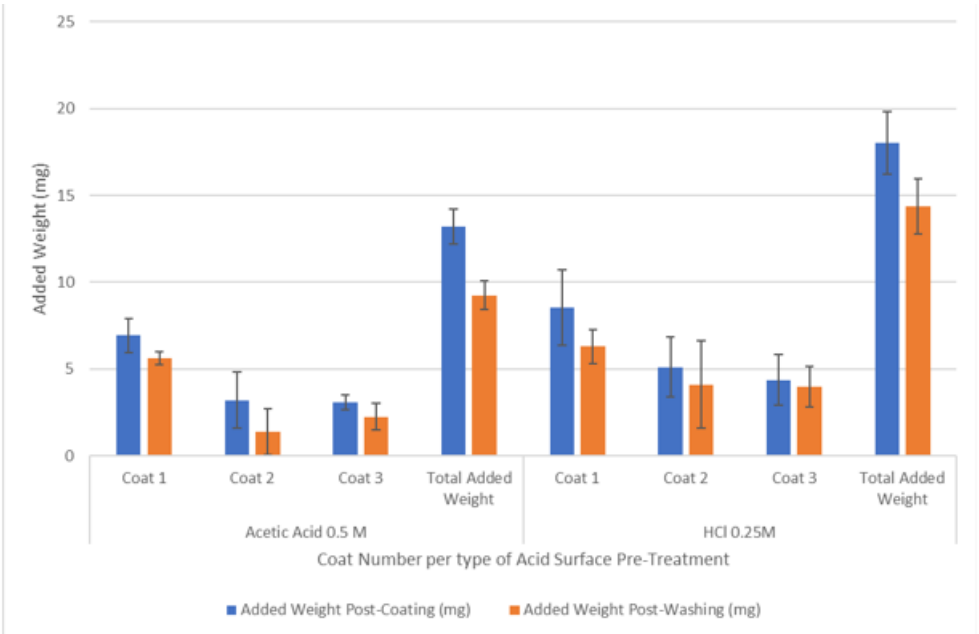

Figure A - 13: Added Weight Results for Experimental **Set G (2.2.7)** in terms of mg

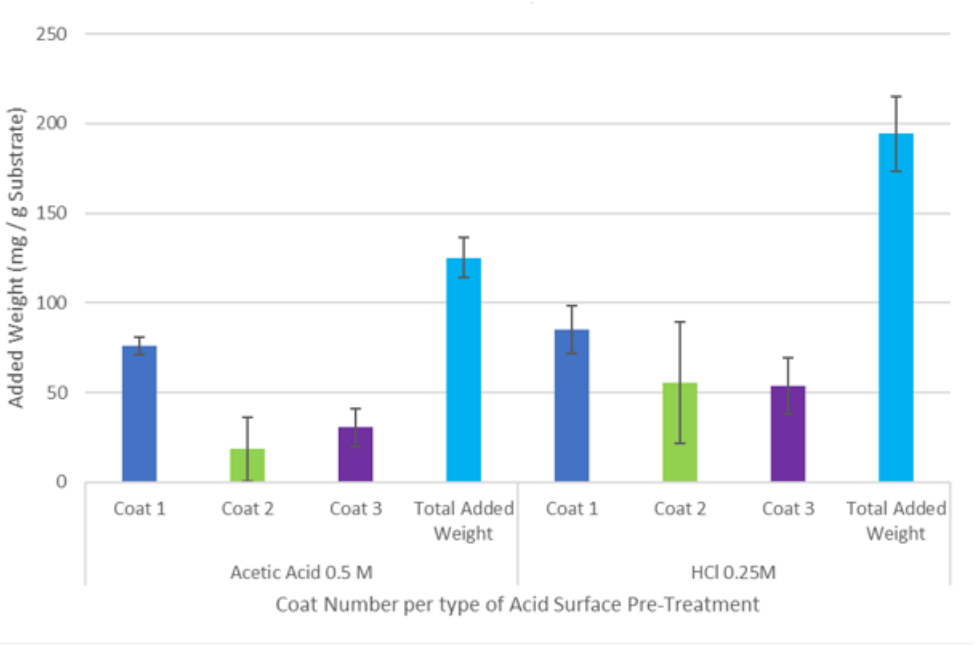

Figure A - 14: Added Weight Results for Experimental **Set G (2.2.7)** in terms of mg / g Substrate

Table A - 9: Added Weight Results for Experimental **Set H (2.2.8)**

Set H - UVC Activation						
	Pepti 10 g/L			**Polyol 30 g/L**		
	1 min	**20 min**	**60 min**	**1 min**	**20 min**	**60 min**
Added Weight Post-Coating (mg)	5.46	6.35	6.74	14.78	15.07	7.67
Added Weight Post-Washing (mg)	4.96	5.16	5.4	13.9	14.25	6.9
Added Weight Post-Washing (mg/g Substrate)	69.88	79.65	75.52	190.65	201.62	99.11

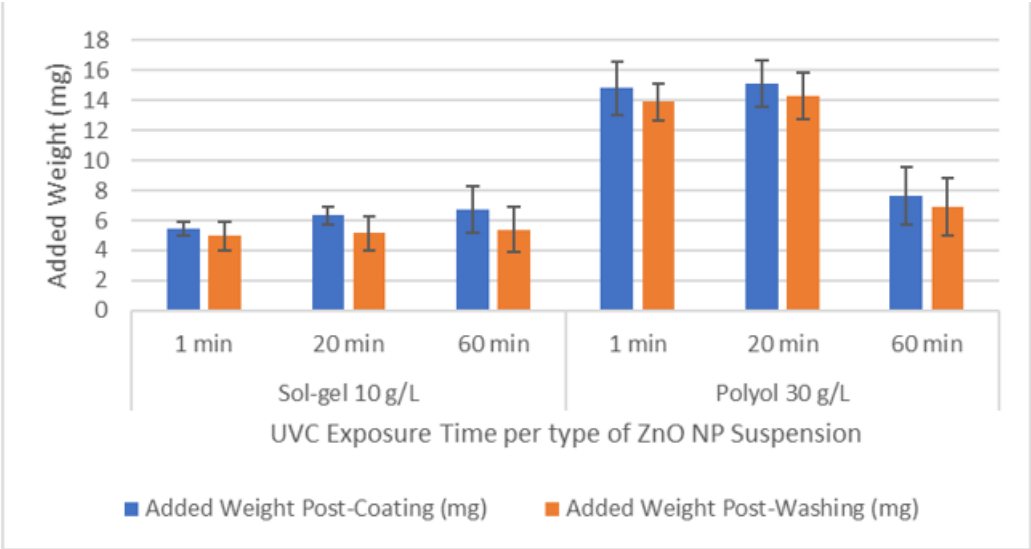

Figure A - 15: Added Weight Results for Experimental **Set H (2.2.8)** in terms of mg

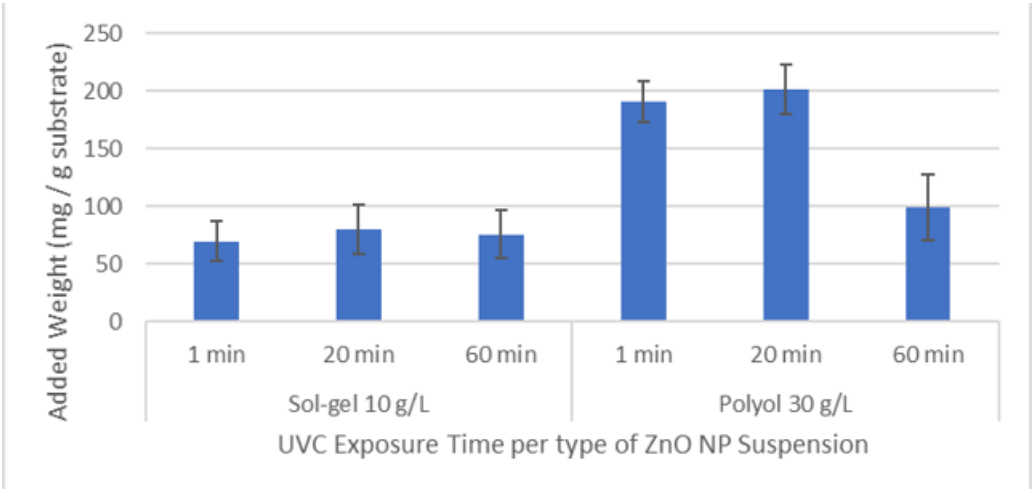

Figure A - 16: Added Weight Results for Experimental **Set H (2.2.8)** in terms of mg / g Substrate

Table A - 10: Compilation of the average added weight measurements post coating and post wash (in terms of mg) and the calculation of the % of weight of added coat lost after the washing process.

Experimental Set	ZnO NPs Suspension	Experiment Parameters	Added Weight Post Coat (mg)	Average Added Weight Post Wash (mg)	% of coat lost post wash
Set A Optimization of Dipping Times	Pepti 10 g/L	3 x 3 x 3	7,55	6,43	14,83%
		10 x 5 x 3	8,78	7,22	17,77%
Set B Determination of the Washing Agent	Pepti 10 g/L	Ethanol	4,53	4	11,70%
		Acetone	4,31	3,66	15,08%
		RBS + Acetone	4,86	3,39	30,25%
	Polyol 30 g/L	Ethanol	8,61	7,67	10,92%
		Acetone	10,29	8,53	17,10%
		RBS + Acetone	9,01	6,78	24,75%
Set C Determination of Speed Up Setting	Pepti 10 g/L	300 mm/min	4,53	4	11,70%
		2000 mm/min	6,34	5,8	8,52%
		6000 mm/min	7,25	5,23	27,86%
	Polyol 30 g/L	300 mm/min	10,29	8,53	17,10%
		2000 mm/min	9,13	7,18	21,36%
		6000 mm/min	11,15	7,8	30,04%
Set D Different Concentrations of Pepti Suspensions	Pepti	10 g/L	7,25	5,23	27,86%
		5 g/L	3,16	2,48	21,52%
Set E	Pepti 10 g/L	Single coat	7,25	5,23	27,86%

Double and Triple Coats		Double coat	6,59	1,35	79,51%
		Total	11,24	6,01	46,53%
	Polyol 30 g/L	Single coat	11,15	7,8	30,04%
		Double coat	12,09	1,24	89,74%
		Total	19,38	8,5	56,14%
	Pepti 5 g/L	Single coat	6,95	5,69	18,13%
		Double coat	6,86	5,04	26,53%
		Triple coat	8,34	4,35	47,84%
		Total	20,45	16,46	19,51%
Set F Basic and Acid Pre-treatment	Pepti 5 g/L	NaOH 1%	6,42	2,77	56,85%
		Acetic Acid 1%	8,2	6,84	16,59%
		Acetic Acid 0.5M	6,94	5,62	19,02%
		HCl 0.1M	10,53	8,14	22,70%
		HCl 0.25M	8,54	6,19	27,52%
		HCl 1M	8,99	5,99	33,37%
	Pepti 10 g/L	Acetic Acid 0.5M	8,26	6,13	25,79%
		Acetic Acid 1M	5,19	3,76	27,55%
		HCl 0.25M	8,54	6,29	26,35%
		HCl 0.5M	6,06	4,44	26,73%
	Polyol 30 g/L	NaOH 1%	11,77	3,09	73,75%
		Acetic Acid 1%	17	14,64	13,88%

		Acetic Acid 0.5M	12,04	11,2	6,98%
		Acetic Acid 1M	9,44	8,75	7,31%
		HCl 0.1M	18,03	17,1	5,16%
		HCl 0.25M	15,62	13,8	11,65%
		HCl 0.5M	11,18	9,03	19,23%
		HCl 1M	16,01	6,95	56,59%
Set G Triple Coat + Acid Surface Pretreatment	Pepti 5 g/L	Acetic Acid 0.5M	13,23	9,25	30,08%
		HCl 0.25M	18,04	14,37	20,34%
Set H UVC Surface Activation	Sol - gel 10 g/L	1 min	5,46	4,96	9,16%
		20 min	6,35	5,16	18,74%
		60 min	6,74	5,4	19,88%
	Polyol 30 g/L	1 min	14,78	13,9	5,95%
		20 min	15,07	14,25	5,44%
		60 min	7,67	6,9	10,04%

Table A - 11: Compilation of the average added weight measurements (post wash), in terms of mg, mg of ZnO/g of nylon and added percentage and the corresponding standard deviations results for each of the experiments.

Experimental Set	ZnO NPs Suspension	Experiment Parameters	Average Added Weight Post Wash (mg)	% increase in weight	Average Added Weight Post Wash (mg of ZnO / g of Nylon)	Standard Deviation (mg of ZnO / g of Nylon)	% of Stdev vs Added Weight
Set A Optimization of Dipping Times	Pepti 10 g/L	3 x 3 x 3	6,43	2,31%	23,12	9,98	43,17%
		10 x 5 x 3	7,22	2,99%	29,95	4,77	15,93%
Set B Determination of the Washing Agent	Pepti 10 g/L	Ethanol	4	4,86%	48,58	7,55	15,54%
		Acetone	3,66	4,66%	46,56	6,4	13,75%
		RBS + Acetone	3,39	4,23%	42,32	9,95	23,51%
	Polyol 30 g/L	Ethanol	7,67	9,73%	97,29	12,55	12,90%
		Acetone	8,53	10,18%	101,78	17,61	17,30%
		RBS + Acetone	6,78	8,21%	82,1	8,21	10,00%
Set C Determination of Speed Up Setting	Pepti 10 g/L	300 mm/min	4	4,86%	48,58	7,55	15,54%
		2000 mm/min	5,8	7,10%	70,98	13,35	18,81%
		6000 mm/min	5,23	6,10%	60,96	16,6	27,23%
	Polyol 30 g/L	300 mm/min	8,53	10,18%	101,78	17,61	17,30%

		2000 mm/min	7,18	8,38%	83,75	21,51	25,68%
		6000 mm/min	7,8	9,70%	96,9	61,57	63,54%
Set D Different Concentrations of Pepti Suspensions	Pepti	10 g/L	5,23	6,10%	60,96	16,6	27,23%
		5 g/L	2,48	3,29%	32,86	12,61	38,37%
Set E Double and Triple Coats	Pepti 10 g/L	Single coat	5,23	6,10%	60,96	16,6	27,23%
		Double coat	1,35	1,48%	14,84	4,82	32,48%
		Total	6,01	7,00%	70	10,71	15,30%
	Polyol 30 g/L	Single coat	7,8	9,70%	96,9	61,57	63,54%
		Double coat	1,24	1,40%	14,03	6,72	47,90%
		Total	8,5	10,60%	106	34,15	32,22%
	Pepti 5 g/L	Single coat	5,69	7,48%	74,8	22,46	30,03%
		Double coat	5,04	6,14%	61,4	5,78	9,41%
		Triple coat	4,35	5,01%	50,08	8,5	16,97%
		Total	16,46	19,28%	192,8	12,25	6,35%
Set F Basic and Acid Pre-treatment	Pepti 5 g/L	NaOH 1%	2,77	3,53%	35,33	3,12	8,83%
		Acetic Acid 1%	6,84	8,86%	88,63	28,83	32,53%
		Acetic Acid 0.5M	5,62	7,98%	79,83	5,36	6,71%
		HCl 0.1M	8,14	11,60%	116,15	28,25	24,32%
		HCl 0.25M	6,19	8,83%	88,29	13,55	15,35%

		HCl 1M	5,99	7,75%	77,45	39,03	50,39%
	Pepti 10 g/L	Acetic Acid 0.5M	6,13	8,7%	87,02	13,59	15,62%
		Acetic Acid 1M	3,76	5,48%	54,81	11,63	21,22%
		HCl 0.25M	6,29	11,98%	119,85	30,61	25,54%
		HCl 0.5M	4,44	5,70%	56,99	8,94	15,69%
	Polyol 30 g/L	NaOH 1%	3,09	3,97%	39,73	6,94	17,47%
		Acetic Acid 1%	14,64	20,46%	204,63	9,55	4,67%
		Acetic Acid 0.5M	11,2	15,54%	155,44	13,69	8,81%
		Acetic Acid 1M	8,75	12,50%	124,95	16,55	13,25%
		HCl 0.1M	17,1	22,53%	225,32	16,76	7,44%
		HCl 0.25M	13,8	18,60%	185,92	16,91	9,10%
		HCl 0.5M	9,03	11,15%	111,53	6,97	6,25%
		HCl 1M	6,95	9,06%	90,61	24,09	26,59%
Set G Triple Coat + Acid Surface Pretreatment	Pepti 5 g/L	Acetic Acid 0.5M	9,25	13,13%	131,31	9,64	7,34%
		HCl 0.25M	14,37	20,17%	201,69	27,79	13,78%
Set H UVC Surface Activation	Sol - gel 10 g/L	1 min	4,96	7,00%	69,88	17,46	24,99%
		20 min	5,16	7,97%	79,65	21,31	26,75%
		60 min	5,4	7,55%	75,52	20,84	27,60%
	Polyol 30 g/L	1 min	13,9	19,06%	190,65	17,67	9,27%

		20 min	14,25	20,16%	201,62	21,54	10,68%
		60 min	6,9	9,91%	99,11	28,75	29,01%

Table A - 12: Statistical significance analysis for selected pairs of experiment data sets within the experimental sets listed in **section** Error! Reference source not found..

Experimental Set	ZnO NPs Suspension	Experiment Data Set 1	Experiment Data Set 2	Average Added Weight (Post Wash) 1	Average Added Weight (Post Wash) 2	t-value	p-value
Set A Optimization of Dipping Times	Pepti 10 g/L	3 x 3 x 3	10 x 5 x 3	23,12	29,94	0,8725	0,4321
Set B Determination of the Washing Agent	Pepti 10 g/L	Ethanol	RBS + Acetone	48,58	42,32	0,8739	0,4315
	Polyol 30 g/L	Acetone	RBS + Acetone	101,78	82,1	1,7536	0,1543
	Pepti 10 g/L vs Polyol 30g/L	Pepti 10 g/L - Ethanol	Polyol 30 g/L - Acetone	48,58	101,78	4,81	0,0086
		Pepti 10 g/L - Ethanol	Polyol 30 g/L - RBS + Acetone	48,58	82,1	5,1946	0,0065
Set C Determination of Speed Up Setting	Pepti 10 g/L	300 mm/min	2000 mm/min	48,58	70,98	2,5242	0,065
	Polyol 30 g/L	300 mm/min	2000 mm/min	101,78	83,75	1,1218	0,3247
	Pepti 10 g/L vs Polyol 30g/L	Pepti 10 g/L - 2000 mm/min	Polyol 30 g/L - 300 mm/min	70,98	101,78	2,4141	0,7323
Set D Different Concentrations of Pepti Suspensions	Pepti 10 g/L vs 5 g/L	10 g/L	5 g/L	60,96	32,86	2,3346	0,0798

Set E Double and Triple Coats	Pepti 10 g/L vs Polyol 30 g/L	Pepti 10 g/L - Double Coat	Polyol 30 g/L - Double Coat	69,96	106	0,9307	0,4047
	Polyol 30 g/L vs Pepti 5 g/L	Polyol 30 g/L - Double Coat	Pepti 5 g/L - Triple Coat	106	192,8	2,3156	0,08152
	Pepti 10 g/L vs Pepti 5 g/L	Pepti 10 g/L - Double Coat	Pepti 5 g/L - Triple Coat	69,96	192,8	7,8536	0,00142
Set F Basic and Acid Pre-treatment	Pepti 5 g/L	HCl 0.1M	NaOH 1%	116,15	35,33	3,5595	0,0236
		Acetic Acid 1%	NaOH 1%	88,63	35,33	3,2005	0,0329
		HCl 0.1M	Acetic Acid 1%	116,15	88,63	0,9591	0,3918
	Pepti 10 g/L	HCl 0,25M	Acetic Acid 0,5M	88,29	87,02	0,777	0,4805
		HCl 0,25M	HCl 0,5M	88,29	56,99	3,5793	0,0232
		Acetic Acid 0,5M	Acetic Acid 1M	79,83	54,8	2,6137	0,0592
	Polyol 30 g/L	HCl 0,1M	NaOH 1%	225,32	39,73	17,7106	0,00006
		Acetic Acid 1%	NaOH 1%	204,63	39,73	24,1725	0,000017
		HCl 0.1M	Acetic Acid 1%	225,32	204,63	1,8549	0,1372
		HCl 0.1M	HCl 1M	225,32	90,61	7,8291	0,0014
		Acetic Acid 1%	Acetic Acid 1M	204,63	124,95	7,2005	0,00197

Set G Triple Coat + Acid Surface Pretreatment	Pepti 5 g/L	Acetic Acid 0.5M	HCl 0.25 M	131,32	201,69	4,144	0,0143
Set H UVC Surface Activation	Pepti 10 g/L	1 min	20 min	69,88	79,65	0,6143	0,5722
	Polyol 30 g/L	20 min	60 min	201,62	99,11	4,9426	0,0078
	Pepti 10 g/L vs Polyol 30 g/L	Pepti 10 g/L - 20 min	Polyol 30 g/L - 20 min	79,65	201,62	6,9713	0,0022